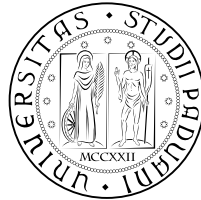# UNIVERSITÀ DEGLI STUDI DI PADOVA

DIPARTIMENTO DI FISICA E ASTRONOMIA "G. GALILEI"

STATISTICAL ANISOTROPY AND NON-GAUSSIANITY FROM THE EARLY UNIVERSE

Ph.D Candidate

Angelo Ricciardone

Thesis for the Degree of Doctor of Philosophy
Cycle XXVI

Supervisor   **Director of the Ph.D School**

Prof. Sabino Matarrese   Prof. Andrea Vitturi

Co-supervisor

Dr. Nicola Bartolo

Submitted: 31/01/2014

Assessment committee:

Prof. Jean–Philippe Uzan
Institut d'Astrophysique de Paris

Prof. Sabino Matarrese
Dipartimento di Fisica e Astronomia "G. Galilei", Università di Padova

Dr. Nicola Bartolo
Dipartimento di Fisica e Astronomia "G. Galilei", Università di Padova

Statistical Anisotropy and non-Gaussianity from the Early Universe

Short abstract:

The main objective of this thesis is to study primordial anisotropic models of universe that can account for the recent CMB anomalies observed by WMAP and (some of them) confirmed by *Planck* and construct consistency relations to constrain these models of the early universe where an anisotropic phase of expansion can be sustained. Basically, the thread of the thesis is the violation of symmetries in the early universe that reflects its effects on the cosmological observables giving statistical anisotropy, non-trivial angular dependence and parity violation in the correlation functions. These observational signatures put stringent limits on the physics and on the fields that have played an active role in the early universe and can help to discriminate among all the possible scenarios.

Keywords: Cosmology, Inflation, Statistical Anisotropy, non-Gaussianity, Parity Violation, Cosmic Microwave Background (CMB).

LIST OF PAPERS

I Bartolo, N., Matarrese, S., Peloso, M., Ricciardone, A.
   The anisotropic power spectrum and bispectrum in the $f(\phi)F^2$ mechanism.
   Phys.Rev. D87 (2013) 023504.

II Bartolo, N., Matarrese, S., Peloso, M., Ricciardone, A.
   Anisotropy in Solid Inflation.
   JCAP 1308 (2013) 022

III Shiraishi, M., Ricciardone, A., Shohei, S.
   Parity violation in the CMB bispectrum by a rolling pseudoscalar.
   JCAP 1311 (2013) 051

IV Shiraishi, M., Mota, D., Ricciardone, A., Arroja, F.
   CMB statistical anisotropy from noncommutative gravitational waves.
   Submitted to arXiv

CONTENTS

Abstract

Cosmological observations suggest that the universe is homogeneous and isotropic on large scales and that the temperature fluctuations are Gaussian. This has been confirmed by *Planck*, that measured a level of non-Gaussianity compatible with zero at 68% CL for the primordial local, equilateral and orthogonal bispectrum amplitude [1]. All these observational evidences seem to be in accordance with a scalar-driven inflation epoch in which a scalar field, the inflaton, drives a quasi de Sitter exponential phase of expansion. Nevertheless, *Planck* measures a *nearly* scale-invariant spectrum of fluctuations [2]. This *nearly* scale-invariance suggests that the time-traslational symmetry is slightly broken during inflation. So it becomes natural to ask if other symmetries are also broken and what are the observational consequences.

Furthermore, the evidence of some "anomalies", previously observed in the WMAP data [3], and now confirmed (at similar level of significance) by *Planck* [4], suggests a possible violation of some symmetries at some point in the evolution of the universe, possibly at very early times. Different anomalies have been observed: a quadrupole-octupole alignment, a dipolar power asymmetry and also an hemispherical asymmetry in power between the northern and southern hemisphere [4]. These features suggest a possible violation of statistical isotropy and/or of parity invariance. Invariance under spatial rotations and parity transformations remains unbroken in the usual inflation models based on scalar fields, so it is necessary to modify the matter content of primordial universe introducing new field(s) or assuming new configuration pattern for the background field that differs from the usual time-dependent background scalar field one.

Motivated by these observations, theoretical models that can sustain anisotropic phase of expansion can have an active role and generate statistical anisotropy in primordial fluctuations. This can be realized by introducing gauge field coupled with scalar [5] and/or pseudoscalar fields [6] or by considering three scalar fields in anisotropic background with an unusual breaking pattern of spacetime symmetries that does not involve breaking of time translations [7]. Breaking of rotational symmetry implies that the correlation functions exhibit a direction dependence and, in particular, the two-point correlation function in Fourier space (power spectrum) of primordial curvature perturbations defined by $\langle \zeta_{k_1} \zeta_{k_2} \rangle = (2\pi)^3 \, \delta^{(3)} \left(\mathbf{k}_1 + \mathbf{k}_2 \right) P_\zeta \left(\mathbf{k}_1 \right)$ is modified as

$$P_\zeta \left(\mathbf{k} \right) = P_{iso} \left(k \right) \left[1 + g_* \left(k \right) \left(\hat{\mathbf{k}} \cdot \hat{\mathbf{n}} \right) \right] \tag{1}$$

where $P_{iso} \left(k \right)$ is the isotropic power spectrum, $\hat{\mathbf{n}}$ is a space preferred direction and g_* is a parameter characterizing the amplitude of violation of rotational symmetry [8].

Within the context of primordial anisotropic models we have developed this Ph.D thesis and in particular we have analyzed a model in which a suitable coupling of the inflaton ϕ to a vector kinetic term F^2 generates an anisotropic power spectrum and a bispectrum with a non-trivial angular dependence in the squeezed limit. In particular we have found that an anisotropy amplitude g_* of order 1% (10%) is possible if inflation lasted

$\sim 5(\sim 50)$ e-folds more than the usual 60 required to produce the CMB modes. One of the most important results found in this analysis concerns the presence of infrared modes of the perturbations of the gauge field. These infrared modes determine a classical vector field that tends to raise the level of statistical anisotropy to levels very close to the observational limits. Peculiar predictions of this model are TB and EB mixing between temperature and polarizations modes in the CMB due to the anisotropy [9, 10] and a correlation between the anisotropy in power spectrum g_* and the amplitude of the bispectrum f_{NL} that can be considered a consistency relation for all these kind of models that break the rotational invariance.

Always in the aim of isotropy violation, but with a completely different approach that involves a scalar fields model, later we have shown, for the first time, how with standard gravity and scalar fields only, is possible to evades the conditions of the cosmic no-hair conjecture [11]. In this model, dubbed solid / elastic model, inflation is driven by a solid. A prolonged slow-roll period of acceleration is guaranteed by the extreme insensibility of the solid to the spatial expansion. We point out that, because of this property, the solid is also rather inefficient in erasing anisotropic deformations of the geometry. This allows for a prolonged inflationary anisotropic solution and for a generation of a non-negligible amount of anisotropy g_* in the power spectrum.

Finally we have investigated parity-violating signatures of temperature and polarization bispectra of the cosmic microwave background (CMB) in an inflationary model where a rolling pseudoscalar, coupled with a vector field, produces large equilateral tensor non-Gaussianity. We have shown that the possibility to use polarization information and the parity-even and parity-odd ℓ-space improves of many order of magnitude the detectability of such bispectra with respect to an analysis with only temperature. Considering the progressive improvements in accuracy of the next cosmological surveys it is useful to introduce and analyze particular tools, like statistical anisotropy, parity violation, new shapes of non-Gaussianity, that can help to discriminate between the plethora of primordial inflationary models.

Riassunto

Le osservazioni cosmologiche suggeriscono che l'universo è omogeneo e isotropo su grandi scale e che le fluttuazioni di temperatura sono Gaussiane. Questo è stato confermato da *Planck*, che ha misurato un livello di non-Gaussianità compatibile con zero con un livello di significatività del 68% per l'ampiezza del bispettro primordiale nelle configurazioni locale, equilatera e ortogonale. Tutte queste evidenze osservative sembrano essere in accordo con un'epoca inflazionaria guidata da un campo scalare dove questo campo, l'inflatone, guida una fase di espansione esponenziale quasi de Sitter. Tuttavia *Planck* misura uno spettro di potenza *quasi* invariante di scala. Questa *quasi* invarianza suggerisce che la simmetria per traslazioni temporali sia leggermente rotta durante l'inflazione. Quindi viene naturale chiedersi se altre simmetrie siano rotte e quali siano le conseguenze osservative.

Inoltre, l'evidenza di alcune anomalie, precedentemente osservate nei dati di WMAP, e ora confermate (con un simile livello di significatività) da *Planck*, suggerisce una possibile violazione di alcune simmetrie ad un certo punto durante l'evoluzione dell'universo, possibilmente a tempi molto primordiali. Diverse anomalie sono state osservate: un allineamento tra il quadrupolo e l'ottupolo, un'asimmetria dipolare in potenza e un'asimmetria emisferica in potenza tra l'emisfero galattico nord e l'emisfero galattico sud. Queste peculiarità suggeriscono una possibile violazione dell'isotropia statistica e/o dell'invarianza per parità. L'invarianza per rotazioni spaziali e trasformazioni di parità rimane conservata nei tipici modelli inflazionari basati su campi scalari, quindi è necessario modificare il contenuto della materia dell'universo primordiale introducendo nuovi campi o assumendo nuove configurazioni per il campo di background che differiscano dal background dipendente dal tempo che si ha nel caso dei tipici modelli scalari.

Motivati da queste osservazioni, modelli teorici che possono sostenere una fase di espansione anisotropa possono avere un ruolo attivo e generare anisotropia statistica nelle fluttuazioni primordiali. Questo può essere realizzato introducendo campi di gauge accoppiati con campi scalari e/o pseudoscalari o considerando tre campi scalari in un background anisotropo con una configurazione non-standard per le simmetrie spazio-temporali di background, che non sfrutta la rottura per traslazioni temporali. La rottura di simmetria per rotazione implica che le funzioni di correlazione esibiscono una dipendenza dalla direzione e, in particolare, la funzione di correlazione a due punti nello spazio di Fourier (spettro di potenza) delle perturbazioni primordiali di curvatura definita da $\langle \zeta_{k_1} \zeta_{k_2} \rangle = (2\pi)^3 \, \delta^{(3)} \left(\mathbf{k}_1 + \mathbf{k}_2 \right) P_\zeta \left(\mathbf{k}_1 \right)$ si modifichi in

$$P_\zeta \left(\mathbf{k} \right) = P_{iso} \left(k \right) \left[1 + g_* \left(k \right) \left(\hat{\mathbf{k}} \cdot \hat{\mathbf{n}} \right) \right] \tag{2}$$

dove $P_{iso} \left(k \right)$ rappresenta lo spettro di potenza isotropo, $\hat{\mathbf{n}}$ è una direzione spaziale privilegiata e g_* un parametro che caratterizza l'ampiezza della violazione di simmetria per rotazione.

Nel contesto di modelli primordiali anisotropi abbiamo sviluppato questo lavoro di tesi di dottorato e in particolare abbiamo analizzato un modello in cui un opportuno accoppiamento tra l'inflatone ϕ e il termine cinetico vettoriale F^2 genera uno spettro di potenza anisotropo e un bispettro con una dipendenza angolare non banale nella configurazione "squeezed". In particolare abbiamo trovato che un'ampiezza dell'anisotropia g_* dell'ordine del 1% (10%) è possibile se l'inflazione dura ~ 5 (~ 50) e-folds in più dei soliti 60 richiesti per generare i modi della radiazione di fondo cosmico di microonde. Uno dei risultati più importanti trovati in questa analisi riguarda la presenza di modi infrarossi delle perturbazioni del campo di gauge. Tali modi infrarossi determinano un campo vettoriale classico che in genere tende ad innalzare il livello di anisotropia statistica a livelli molto vicini ai limiti osservativi. Predizioni caratterizzanti per questo modello è il mixing tra i modi TB e EB, tra polarizzazione e temperatura, causati dall'anisotropia, e una correlazione tra l'anisotropia nello spettro di potenza g_* e l'ampiezza del bispettro f_{NL} che può essere considerata una relazione di consistenza per tutti i tipi di modelli che rompono l'invarianza per rotazione.

Sempre nell'ottica della violazione di isotropia, ma con un approccio completamente differente che coinvolge campi scalari, abbiamo poi mostrato, per la prima volta, come con gravità standard e campi scalari, è possibile violare le condizioni del teorema di Wald. In questo modello, chiamato modello solido/elastico, l'inflazione è guidata da un solido. Un prolungato periodo di accelerazione con lento rotolamento è garantito dall'estrema insensibilità del solido all'espansione spaziale. Noi abbiamo dimostrato che, a causa di questa proprietà, il solido è anche piuttosto inefficiente nel diluire deformazioni anisotrope della geometria. Questo permette una soluzione inflazionaria anisotropa prolungata e la generazione di un contributo anisotropo non trascurabile g_* allo spettro di potenza.

Infine abbiamo investigato i segnali di violazione di parità nel bispettro del fondo cosmico di microonde per temperatura e polarizzazione in un modello dove un campo pseudoscalare che rotola lentamente, accoppiato ad un campo vettoriale, produce elevata non-Gaussianità nella configurazione equilatera. Abbiamo mostrato che la possibilità di usare la polarizzazione con segnale non nullo sia nello spazio delle configurazioni delle ℓ pari che dispari accresce di diversi ordini di grandezza la rilevabilità di tali bispettri rispetto ad un'analisi con solo temperatura.

Considerando i progressivi miglioramenti in accuratezza delle prossime missioni spaziali è utile introdurre e analizzare mezzi particolari, come l'anisotropia statistica, la violazione di parità e nuove configurazioni per la non-Gaussianità, che possano essere utili per discriminare tra la pletora di modelli inflazionari primordiali.

THESIS OUTLINE

The outline of the thesis is the following: Chapter 1 is devoted to an overview of
the standard Big Bang model and of the problems that led to the inflationary
paradigm. In this Chapter we give also all the observational constraints given by
the *Planck* satellite about statistical anisotropy, non-Gaussianity and anomalies;
Chapter 2 is a review of anisotropic models, their problems about instability and
possible wayout. We briefly introduce homogeneous but anisotropic spacetime
(e.g. Bianchi I) that are usually considered in presence of anisotropic sources; in
Chapter 4 we describe the scalar-vector model in which the inflaton is coupled
to a $U(1)$ gauge field and we compute the two and three-point correlation
functions showing how the anisotropic source modifies the power spectrum and
the bispectrum; Chapter 5 focuses on the *Solid Inflation* model in a Bianchi
I space-time; we show, for the first time, how to obtain anisotropic features
with scalar fields and standard gravity; In Chapter 6 we analyze a model where
parity-violating features appear in the tensor bispectrum due to a coupling
between a pseudoscalar field and a vector field; finally, in the last chapter we
conclude the thesis and we give hints about possible future improvements.

INTRODUCTION

The six parameters standard cosmological model seems to describe with high accuracy our current universe. This model predicts that the universe is statistically isotropic (i.e. looks the same in all the directions) and homogeneous (i.e. the statistical properties are the same everywhere) on large scales. In this picture, the inflationary phase has become a corner-stone: at very early times a quasi de Sitter exponential expansion, driven by a scalar field, solves the open problems left by the Big Bang model and gives a natural explanations of the origin of both the Large Scale Structures (LSS) and the Cosmic Microwave Background (CMB).

Recently, also in cosmology, it has become clear that the role of symmetries is crucial to characterize the physics of the early universe and the observational signatures in the CMB [12, 13]. The de Sitter spacetime, that characterizes the inflation period, described by the metric $ds^2 = -dt^2 + e^{2Ht}d\vec{x}^2$, where the Hubble parameter H is constant, respects ten symmetries: three spatial translations, three spatial rotations, one time translation accompanied by spatial dilation ($t \to t - \frac{\lambda}{H}$ and $\vec{x} \to e^{\lambda}\vec{x}$) and three special conformal transformations. These symmetries give strong constraints on the nature of primordial fluctuations. For example, as the shift symmetry in field space suppress the level of interaction and so the amount of non-Gaussianity, the invariance under translations and rotations strongly constraint the form of the power spectrum and higher order correlation functions. In fact, in the two point correlation function in Fourier space, defined as $\langle \zeta_{k_1} \zeta_{k_2} \rangle = (2\pi)^3 \delta^{(3)}(\mathbf{k}_1 + \mathbf{k}_2) P_\zeta(\mathbf{k}_1)$, where $P(\mathbf{k})$ is the power spectrum, the translational invariance gives the delta function, while the rotational invariance would give $P(\mathbf{k}) \to P(k)$. The necessary time-dependence of the expansion rate H in order to stop inflation, which is the natural consequence that inflation happens in a quasi de Sitter space, breaks slightly the time dilation invariance. Hence also the spatial dilation symmetry is broken giving a two point correlation function that is nearly, but non exactly scale invariant[i], as confirmed by the CMB analysis where $k^3 P(k) \propto k^{-0.04}$ with more than 5σ significance [2]. So it becomes natural to ask whether there are other broken symmetries during the early universe.

Beside theoretical motivations there are observational evidences that point in the direction of violation of symmetry at some point in the evolution of the universe: the so-called "anomalies", previously observed in the WMAP data [3, 14], and now confirmed (at similar level of significance) by *Planck* [4]. Different anomalies have been observed, indication of a possible violation of statistical isotropy and/or of parity invariance: a quadrupole-octupole alignment, a dipolar power asymmetry and also an hemispherical asymmetry in power between the northern and southern hemispheres [4]. Of course, possible explanations for these anomalies have been suggested such as improper foreground substraction, statistical flukes, systematics, but the most exciting is the possibility of a non-negligible contribution of an anisotropic source in the (early

---

[i]The deviation from de Sitter is quantified by the slow roll parameter ε, and this is of the same order of the tilt of the power spectrum

stage of the) universe. If this is the case, the correlation functions assume a direction dependence and in particular the power spectrum becomes:

$$P_\zeta \left(\mathbf{k}\right) = P_{iso}\left(k\right)\left[1 + g_*\left(k\right)(\hat{\mathbf{k}} \cdot \hat{\mathbf{n}})^2\right]$$

where$P_{iso}\left(k\right)$ is the isotropic power spectrum, $\hat{\mathbf{n}}$ is a space preferred direction and g_* is a parameter characterizing the amplitude of violation of rotational symmetry [8].

In [15], after removing the effects of *Planck*'s asymmetric beams and the Galactic foreground emission, it is found $g_* = 0.002 \pm 0.016$ (68% CL) from the temperature data of *Planck*. The 95% CL limit is $-0.030 < g_* < 0.034$. Meanwhile in [16], using the last WMAP and *Planck* data, the alignment of the largest structures observed in the CMB, the quadrupole and the octupole, is still confirmed in good agreement with results from the previous WMAP data release. Moreover, in the *Planck* paper [4] the deficit in power shown by one of the hemisphere with respect to the opposite, that contains oscillations between odd and even mode,s may be related to a parity violation.

Although these anomalies are under debate and more informations will come from the *Planck* full mission and polarization data, a cosmological origin would be more intriguing; but up to today physically motivated models that can give a satisfactory explanation are still lacking.

Still, the recent release of *Planck* data has provided also crucial new informations on the non-Gaussian statistics of primordial perturbations [1]. Non-Gaussianity, measured by the bispectrum, provides a powerful tool to discriminate among different inflationary models and may provide a valuable window into the detailed physics of the very early universe. In the *Planck* analysis the common shapes (local, equilateral and orthogonal) and other non-standard shapes have been analyzed. But these are not the only possible: new shapes of non-Gaussianity can exist[ii].

Invariance under spatial rotations and/or parity transformations remains unbroken in the usual inflationary models based on scalar fields, so it is necessary to modify the matter content of primordial universe introducing new field(s) or assuming new configuration patterns for the background field that differs from the usual time-dependent background scalar field approach.

Motivated by all these theoretical and observational reasons, models that sustain an anisotropic expansion of the universe can have an active role and can be candidate to generate interesting imprints related to both the anomalies and primordial non-Gaussianity. It is however non trivial to realize this, since anisotropic space typically rapidly isotropizes if there is no source that sustain it. Vector fields may, in principle, support this anisotropic evolution. However massless vector fields, with a minimal $\mathcal{L}_A = -F^2/4$, are conformally invariant, which inhibits their particle production and consequently generation of perturbations. So it is necessary to break the conformal invariance in order to generate perturbations and in addition, a mechanism must be found to avoid excessively anisotropic expansion of the universe due to vector fields (it is necessary to ensure the energy density of the vector field to be subdominant in order to be consistent with the CMB observations). To our knowledge, four distinct classes of models have been constructed to achieve this; the first three of them are characterized by (i) a vector potential $V\left(A^2\right)$ [17], (ii) a fixed vector vev due to a lagrange multiplier

---

[ii]An open window for the non-Gaussianity in non-Bunch-Davies vacua from trans-Planckian effects or in features models is still open with a 2.2σ significance

[8], and (iii) a vector coupling A^2R to the scalar curvature R [18, 19]. These three proposals break the U(1) symmetry of the minimal action, and lead to an additional degree of freedom, the longitudinal vector polarization, that in all of these models turns out to be a ghost. [20, 21, 22, 23]. Also non-Abelian vector fields models have been taken into account [24, 25] but in [26] it is shown that [25] is not favoured by the CMB data.

In this thesis, and in particular in chapter 3, we study the fourth class: it is a U(1) invariant and free of ghost instabilities model, characterized by a function of a scalar inflaton φ coupled with the vector kinetic term, $\mathcal{L} = -\frac{I^2(\varphi)}{4}F_{\mu\nu}F^{\mu\nu}$. We compute the two and three point correlations functions of the curvature perturbation ζ showing that the vector field imprints a strong anisotropy, in particular a g_* associated to these modes is ~ 0.1 (respectively, ~ 0.01), if inflation lasted about 50 e-folds (respectively, about 5 e-folds) more than the final ~ 60 e-folds necessary to generate the CMB modes. We show that the infrared modes of the perturbations of the gauge field determine a classical vector field that tend to raise the level of statistical anisotropy to levels very close to the observational limits. An observable g_*, from this model, is associated to an observable bispectrum which is enhanced in the squeezed limit and which has a characteristic shape and anisotropy, and this provides a consistency relation for this kind of models.

Scalar fields, instead, are ubiquitous in cosmology since they are in accordance with the isotropy and homogeneity of the Cosmic Microwave Background. In Chapter 4, starting from a model proposed by [7], dubbed *Solid Inflation*, we show how for this model the FRW solution is not at attractor solution so it can allow for an anisotropic solution. This has been realized studying a triplet of spin zero fields with a spatially-dependent vev of the form $\langle\phi^i\rangle = x^i$ with $i = 1, 2, 3$ in a Bianchi type I metric. They show that the slight sensibility of the "solid" to the spatial expansion allows for an inflation phase. We poit out that this same property is responsible for the slow dilution of anisotropies. Specifically, we obtain that the anisotropy is erased on timescale $\Delta t = \mathcal{O}\left(\frac{1}{\varepsilon H}\right)$ where H is the Hubble parameter and ε the slow roll parameter $\varepsilon \equiv -\dot{H}/H^2$. So this provides the first example with standard gravity and scalar field of violation of the conditions of the cosmic no-hair conjecture. We compute the anisotropic contribution to the power spectrum and we show the similarities between *Solid Inflation* and the model analyzed in Chapter 3.

In Chapter 5 we have analyzed a model where a rolling pesudoscalar, gravitationally coupled to the inflaton, amplifies the vacuum fluctuations of a $U(1)$ gauge field and generates tensor chiral modes producing TB and EB correlations and parity-violating non-Gaussianity. In particular we show that the tensor non-Gaussianity breaks the parity invariance asymmetrically and creates signals in both parity-even ($\ell_1 + \ell_2 + \ell_3 =$ even) and parity-odd ($\ell_1 + \ell_2 + \ell_3 =$ odd) spaces enlarging the space of detectability of this signature. We show how the use of E-mode polarization improves of 400% the detectability and the B-modes increase of three order of magnitude the signal to noise ratio with respect to analysis with only temperature.

Departures from statistical isotropy, parity symmetry and Gaussianity involve a rich set of observable quantities, with different signatures that can be measured in the CMB or in the Large-Scale Structures. These signatures, which carry information about physical

processes on cosmological scales, have the power to reveal detailed properties of the physics responsible for generating the primordial fluctuations. This kind of observational features can give crucial informations about the fields involved (for example, how many fields and which couplings were most relevant), or alternatively, shed light on the systematic errors in the data.

<div style="text-align: right; font-size: 4em; font-weight: bold;">1</div>

BIG BANG AND INFLATION: AN OVERVIEW

In this chapter we give a general overview of the standard cosmological model and we discuss the motivations to introduce inflation and how inflation connects the microscopic physics of the quantum fluctuations to the macroscopic physics of CMB and Large Scale Structures. Finally we give all the last observational limits that suggest a more intriguing universe.

Contents

1.1   Our Universe

The cosmological observations today seem to be in favor of the (Hot) Big Bang model that explains with high accuracy the Cosmic Microwave Background (CMB), the abundances of the light nuclei and the thermal history of the universe after the Big Bang Nucleosynthesis. But this model is not sufficient to explain some questions particularly related to the early universe like, why the universe is so homogeneous? Why is it so flat? Where the structures come from? The first two questions, that are the basis of the Cosmological Principle, seem to be incompatible with a finite age for the universe. But the estimation, coming from cosmological and astrophysical observations, gives $t_0 = 13.813 \pm 0.058$ Gyr [2]. At same time the Hot Big Bang model does not include any explanation on the formation of structures that we observe today.

Inflation offers an elegant solution to the problems left unsolved by the standard cosmological model and explains how the Universe became so large, so old, and so flat providing an elegant mechanism for generating the primordial perturbations which gave rise to the structure that we see in the universe today. The general picture is that the universe underwent under a period of exponential expansion during which quantum fluctuations were inflated in scale to become the classical fluctuations that we see today. In the simplest inflationary models, the primordial fluctuations are predicted to be adiabatic, nearly scale-invariant and Gaussian. In this chapter we will briefly describe the Standard Cosmological Model, its shortcomings and the inflationary solution. Finally we will give a collection of the observational results by *Planck*, that suggest possible violation of isotropy and require the introduction of new fields in the early universe.

1.2   Friedmann-Robertson-Walker Universe

The cosmological model currently employed is based on two essential ingredients: General Relativity on one side and Standard Model of particle physics on the other. The first, with the symmetry assumptions of the metric and of the matter content of the Universe, is the fundamental tool to give the mathematical pillars to Cosmology. On this assumption of symmetry the Cosmological Principle is based and states that our Universe is homogeneous and isotropic on cosmological scales, i.e. on scales greater than 100Mpc [27]. One can easily demonstrate that, with this only *ansatz*, the spacetime element line to be considered is the Friedmann-Robertson-Walker (FRW)

$$ds^2 = dt^2 - a^2(t)\big[\frac{dr^2}{1 - kr^2} + r^2(d\theta^2 + \sin^2\theta d\varphi^2)\big] \qquad (1.1)$$

where $a(t)$ is the cosmic-scale factor, t is the cosmic time, k is the curvature parameter that determines the topology of the spatial geometry; it can assume the values +1, 0, -1 corresponding to closed, flat and open Universe respectively. The curvature parameter and the scale factor define the curvature radius $R_{curv} \equiv a(t)|k|^{-1/2}$. All the three models are without boundary: the positively curved model is finite and "curves" back on itself; the negatively curved and flat models are infinite in extent. The coordinates r, θ, φ are the comoving spherical coordinates: a particle at rest in these coordinates remains at rest, i.e., constant r, θ, φ. As a consequence a freely moving particle eventually comes to rest in these coordinates, as its momentum is red-shifted by the expansion, $p \propto a^{-1}$. The scale factor defines the distance between particles; in fact the physical separation between two points is simply $a(t)$ times the coordinate separation.

The data from high redshift supernova, Large Scale Structure (LSS) and measurements of the CMB anisotropies strongly suggest a spatially flat model of Universe [28] and then will almost always assume such a constraint.

An important quantity characterizing the FRW spacetime is the expansion rate H

$$H \equiv \frac{\dot{a}}{a} \tag{1.2}$$

The *Hubble parameter H* has unit of inverse time and is positive for an expanding Universe (negative for a collapsing Universe). It sets the fundamental scales of the FRW spacetime, i.e. the characteristic time-scale of the homogeneous Universe is the Hubble time, $t \sim H^{-1}$, and the characteristic length-scale is the Hubble length, $d \sim H^{-1}$ (in natural unit). It is useful to define the conformal FRW metric introducing the concept of *conformal time* which will be useful in the next sections. The conformal time τ is defined through the following relation

$$d\tau = \frac{dt}{a} \tag{1.3}$$

The metric (1.1) then becomes

$$ds^2 = a^2(\tau)\big[d\tau^2 - \frac{dr^2}{1 - kr^2} - r^2(d\theta^2 + \sin^2\theta d\varphi^2)\big] \tag{1.4}$$

The reason why τ is called conformal is manifest from Eq. (1.4): the corresponding FRW line element is conformal to the Minkowski line element describing a static four dimensional hypersurface. Consequently the functions of the cosmic time transform as

$$\dot{f}(t) = \frac{f'(\tau)}{a(\tau)} \tag{1.5}$$

$$\ddot{f}(t) = \frac{f''(\tau)}{a^2(\tau)} - \mathcal{H}\frac{f'(\tau)}{a^2(\tau)} \tag{1.6}$$

where

$$\mathcal{H} = \frac{a'}{a} \tag{1.7}$$

and we can set the following rules that will be very useful

$$H = \frac{\dot{a}}{a} = \frac{a'}{a^2} = \frac{\mathcal{H}}{a} \tag{1.8}$$

$$\ddot{a} = \frac{a''}{a^2} - \frac{\mathcal{H}^2}{a} \tag{1.9}$$

$$\dot{H} = \frac{\mathcal{H}'}{a^2} - \frac{\mathcal{H}^2}{a^2} \tag{1.10}$$

It is easy to see that, if the scale factor $a(t)$ scales like $a(t) \sim t^n$, then $a(\tau) \sim \tau^{\frac{n}{1-n}}$.

The Cosmological Principle imposes that the energy-momentum tensor accounting for each matter/energy component, $T_{\mu\nu}$ is precisely like the one of a perfect fluid

$$T_{\mu\nu} = (\rho + p)u_\mu u_\nu - pg_{\mu\nu} \tag{1.11}$$

where u_μ is the four-velocity of the observer (corresponding to a fluid element), $g_{\mu\nu}$ is the metric tensor, p is the pressure that is necessarily isotropic for consistence with the FRW metric, and ρ is the energy density. Within a perfect fluid approximation, defining an equation of state parameter ω which relates the pressure p to the energy density ρ by $p = \omega\rho$, the ordinary energy contributions of our Universe such as dust and radiation are distinguished by respectively $\omega = 0$ and $\omega = 1/3$. On the contrary, a cosmological constant is characterized by $\omega = -1$.

The dynamics of the expanding Universe is determined by the Einstein equations, which relate the expansion rate to the matter content, specifically to the energy density and the pressure

$$R_{\mu\nu} - \frac{1}{2}g_{\mu\nu}R = 8\pi G T_{\mu\nu} \tag{1.12}$$

where G is the Newton constant, $R_{\mu\nu}$ is the Ricci tensor and R is the Ricci scalar[i]. The solutions of Einstein equations with the FRW metric (1.1) give the Friedmann equations

$$H^2 \equiv \left(\frac{\dot{a}}{a}\right)^2 = \frac{8\pi G}{3}\rho - \frac{k}{a^2} \tag{1.13}$$

$$\frac{\ddot{a}}{a} = -\frac{4\pi G}{3}(\rho + 3p) \tag{1.14}$$

where overdots denote derivative with respect to cosmic time t. A third useful equation - not independent of the last two - is the continuity equation $\nabla_\mu T^{\mu\nu} = 0$ that leads to:

$$\dot{\rho} = -3H(\rho + p) \tag{1.15}$$

which implies that the expansion of the Universe (specified by H) can lead to local changes in the energy density. Considering the equation of state ($p = \omega\rho$)

---

[i]We have not considered the *cosmological constant* Λ *term* that can be interpreted as particle physics process yielding an effective stress-energy tensor for the vacuum of $\Lambda g_{\mu\nu}/8\pi G$ and that nowadays is considered for the actual acceleration of the Universe.

the integration of the last equation yields:

$$\rho \propto a^{-3(1+\omega)} \tag{1.16}$$

Then Eq. (1.13) in a flat Universe and with $\omega \neq -1$ is solved by:

$$a(t) \propto t^{2/[3(1+\omega)]} \tag{1.17}$$

General qualitative features of the future evolution of FRW Universe can now be seen. If $k = 0, -1$, Friedmann equation (1.13) shows that $\dot{a}$ can never become zero (apart for $t = 0$); thus, if the Universe is presently expanding, it must continue to expand forever. Indeed, for any energy content with $p \geq 0$, ρ must decrease as a increases at least as rapidly as a^{-3}, the value for dust. Thus $\rho a^2 \to 0$ as $a \to \infty$. Hence for $k = 0$ the expansion velocity $\dot{a}$ asymptotically approaches zero as $t \to \infty$, while if $k = -1$ we have $\dot{a} \to 1$ as $t \to \infty$. Otherwise, if $k = +1$, the Universe cannot expand forever but there is a critical value a_c such that $a \leq a_c$: at a finite time after $t = 0$ the Universe achieves a maximum size a_c and then it begins to recontract. The presence of a possible cosmological constant alters the fate of the Universe [29].

The Friedmann equations allow to relate the curvature of the Universe to the energy density and to the expansion rate; in fact if we define a *critical density* ρ_c and a cosmological *density parameter* Ω:

$$\rho_c = \frac{3H^2}{8\pi G} \qquad \Omega = \frac{\rho}{\rho_c} \tag{1.18}$$

Eq. (1.13) can be rewritten as

$$\Omega - 1 = \frac{k}{a^2 H^2} \tag{1.19}$$

There is a one to one correspondence between Ω and the spatial curvature of the Universe: positively curved, $\Omega > 1$; negatively curved, $\Omega < 1$; and flat $\Omega = 1$; so the "fate of the Universe" is determined by the energy density[ii].

The FRW spacetimes have two characteristics that it is important to discuss: the existence of an initial singularity, the Big Bang, and the existence of particle horizon that we encounter a lot of times when we consider the evolution of the perturbations generated by inflation. For the first we know that under the assumption of homogeneity and isotropy, General Relativity predicts that at a time $t = \int_0^1 \frac{da}{aH(a)} = \frac{2}{3(1+\omega)H_0} \sim H_0^{-1}$ ago the Universe was in a singular state where the density, the temperature and the curvature of the Universe were infinite. It is important to know that the nature of this singularity is the result of a homogeneous contraction of space down to zero size and that the Big Bang does not represent an explosion of matter at a preexisting point because the spacetime structure itself is created a $t = 0$. This singularity does not depend on the assumption of homogeneity and isotropy: in fact the Singularity

---

[ii]The critical density today is $\rho_c = 1.88 \cdot 10^{-29} h^2$ g cm^{-3} where $h = 0.72 \pm 0.07$ is the present Hubble rate in unit of 100 Km s^{-1} Mpc^{-1} [27].

Theorem of General Relativity [30] shows that singularities are generic features of cosmological solutions. We must remember that at the time of the Big Bang quantum effects were important and the General Relativity does not give exhaustive predictions.

The second and more important characteristic is the existence of *particle horizon* for FRW cosmological models. As we will see in the next section, the existence of this "boundary" is in conflict with the evidence of the isotropy of the Universe and has brought to the introduction of the inflationary paradigm.

So far it seems that the standard cosmological model is perfect in order to describe the Universe but there are some problems that it cannot solve; the most famous ones are the horizon problem, the flatness or oldness problem, the unwanted relics problem and entropy problem. We will briefly review them here. For a more concise description [27].

1.3   Shortcomings of Standard Cosmology

The standard cosmology has brought a lot of confirmations with the observational data and the most notable achievements of the Hot Big Bang FRW standard model are:

- The prediction of the cosmological expansion of the Universe;

- The explanation of the cosmic abundance of light elements (D, Li, He) deriving from the Nucleosynthesis;

- The prediction and explanation of the presence of a relic background radiation with temperature of few K, the CMB;

But several puzzles remain unsolved and it is necessary to go beyond the standard cosmological model introducing the inflationary paradigm.

1.3.1   The horizon problem

Under the term "horizon problem" a wide range of facts is included, all related to the existence of a *particle horizon* in FRW cosmological models. The particle horizon defines the boundary of the observable region at a generic time t. Physically the distance that a photon could have travelled since the Big Bang until time t, the distance to the particle horizon, is

$$R_H(t) = a(t) \int_0^t \frac{dt'}{a(t')} \tag{1.20}$$

The convergence of this integral defines the regions that are causally connected and it is not difficult to see that the integral converges in all FRW models with equation of state parameter $\omega \in (0,1)$

$$R_H = \begin{cases} 2t = & H^{-1}(t) \propto a^2 \quad (radiation) \\ 3t = & 2H^{-1}(t) \propto a^{3/2} \quad (dust) \end{cases} \qquad (1.21)$$

As $H^{-1}(t)$ is the age of the Universe, $H^{-1}(t)$ is called the Hubble radius and it is the distance that the light can travel in a Hubble time[iii].

According to standard cosmology, photon decoupled from the rest of the components (electrons and baryons) at a temperature of the order of 0.3eV. This happened when the rate of interaction of photons Γ became of the order of the Hubble size (that is, of the horizon size), and the expansion made not possible the reverse reaction of $p + e^+ \rightarrow H + \gamma$. This phase defines the so-called "surface of last scattering" at a redshift of about 1100 and an age of about $180,000(\Omega_0 h^2)^{-1/2}$yrs [31]. From the epoch of last-scattering onwards, photons free-stream and reach us basically untouched. So now, they are measurable in the CMB, whose spectrum is consistent with that of a black-body at a temperature of 2.726 ± 0.01K . Detecting primordial photons is therefore equivalent to take a picture of the Universe when the latter was about 300,000 yrs old. The length corresponding to our present Hubble radius (which is approximately the radius of our observable Universe) at the time of last-scattering was

$$\lambda_H(t_{LS}) = R_H(t_0)\left(\frac{a_{LS}}{a_0}\right) = R_H(t_0)\left(\frac{T_0}{T_{LS}}\right) \qquad (1.22)$$

During the matter-dominated period the Hubble length has decreased with a different law

$$H^2 \propto \rho_M \propto a^{-3} \propto T^3 \qquad (1.23)$$

At last scattering

$$H_{LS}^{-1} = R_H(t_0)\left(\frac{T_{LS}}{T_0}\right)^{-3/2} \ll R_H(t_0) \qquad (1.24)$$

The length corresponding to our present Hubble radius was much larger than the horizon at that time. This can be shown comparing the volumes built with these two scales

$$\frac{\lambda_H^3(T_{LS})}{H_{LS}^{-3}} = \left(\frac{T_0}{T_{LS}}\right)^{-3/2} \approx 10^6 \qquad (1.25)$$

So there were about 10^6 causally disconnected regions within the volume that now corresponds to our horizon. Because CMB experiments like COBE and WMAP tell us that our two photons have nearly the same temperature with a precision of 10^{-5} [32], we are forced to say that those two photons were very similar even if they could not talk to each other, and that the Universe at

---

[iii] In standard cosmology the distance to the horizon is finite, and up to numerical factors, equal to the age of the Universe or the Hubble radius, H^{-1}. For this reason, we will use horizon and Hubble radius interchangeably

last-scattering was homogeneous and isotropic in a physical region to a certain extent greater than the causally connected one.

Another feature of the horizon problem is related to the problem of initial conditions for the cosmological perturbations. In fact photons which were causally disconnected at the last-scattering surface have the same small anisotropies. The existence of particle horizons in the standard cosmology precludes the explanation of the smoothness as a result of microphysical events: the horizon at decoupling, the last time one could imagine temperature fluctuations being smoothed by particle interactions, corresponds to an angular scale on the sky of about $1°$, which precludes temperature variations on larger scales from being erased [31]. To account for the small-scale lumpiness of the Universe today, density perturbations with horizon-crossing amplitudes of 10^{-5} on scales of 1 Mpc to 10^4 Mpc or so are required. However, in the standard cosmology the physical size of a perturbation, which grows as the scale factor, begins larger than the horizon relatively late in the history of the Universe. This precludes a causal microphysical explanation for the origin of the required density perturbations.

1.3.2 The flatness problem

To understand where the problem comes from, it is necessary to extrapolate the validity of Einstein equations back to the Planck era, when the temperature of the Universe was $T_{Pl} \sim m_{Pl} \sim 10^{19}$ GeV. From Eq. (1.19) we note that if the Universe is perfectly spatially flat (k=0), then $\Omega = 1$ at all times. During the radiation-dominated period, the expansion rate $H^2 \propto \rho_R \propto a^{-4}$ and $\Omega - 1 \propto a^2$, while during the matter-dominated era, $\rho_M \propto a^{-3}$ and $\Omega - 1 \propto a$. In both cases $(\Omega - 1)$ decreases going backwards in time. Since we know that $(\Omega_0 - 1)$ is of order unity at present [33], we can deduce its value at t_{Pl}

$$\frac{|\Omega - 1|_{T=T_{Pl}}}{|\Omega - 1|_{T=T_0}} \sim \left(\frac{a_{Pl}^2}{a_0^2} \right) \sim \left(\frac{T_0^2}{T_{Pl}^2} \right) \sim \mathcal{O}(10^{-64}) \qquad (1.26)$$

where "0" stands for the present epoch, and $T_0 \simeq 10^{-13}$GeV is the present day temperature of the CMB radiation. In order to get the correct value of $(\Omega_0 - 1)$ at present, the value of $(\Omega - 1)$ at early times has to be fine-tuned to values amazingly close to zero, but without being exactly zero.

If this value had been initially less than 1 the Universe would have expanded and collapsed during its earliest stages; if it had been a little greater than 1 the Universe would have expanded extremely rapidly (10^{-43}s) cooling to a temperature above the absolute zero. So the flatness problem is also known as a problem of fine-tuning.

1.3.3 | The unwanted relics problem

The Hot Big Bang occurs at very high temperatures. Physics at these high energies has not yet been probed by particle accelerators, so we can only proceed through particle physics theories such as supersymmetry and string theory. The breaking of gauge symmetries during the evolution leads to the production of many unwanted relics such as monopoles, cosmic strings, and other topological defects [34]. The string theories also predict supersymmetric particles such as gravitinos, Kaluza-Klein particles, and moduli fields. The densities of these unwanted particles would decrease at the same rate as matter (a^{-3}), which means they should have a density of the same order of the matter content today $(\Omega_m \simeq 0.3$ [27]). None of these have been observed in the Universe today, either directly or through their effects on structure formation. There is also the possibility that the unwanted relics decayed into radiation some time after they were created.

1.3.4 | The entropy problem

This problem is connected with the flatness problem. In fact starting from the Friedmann equation (1.13) we can see that in radiation dominated period [31]

$$H^2 \simeq \rho_R \sim \frac{T^4}{m_{Pl}^2} \tag{1.27}$$

from which we can deduce

$$\Omega - 1 = \frac{k m_{Pl}^2}{a^2 T^4} = \frac{k m_{Pl}^2}{S^{2/3} T^2} \tag{1.28}$$

where we have introduced the entropy $S \sim a^3 T^3$. Since an adiabatic expansion implies conservation of S over the evolution of the Universe we have

$$|\Omega - 1|_{t=t_{Pl}} = \frac{m_{Pl}^2}{T_{Pl}^2} \frac{1}{S^{2/3}} = \frac{1}{S^{2/3}} \sim 10^{-60} \tag{1.29}$$

from which we deduce that Ω is so close to 1 because the total entropy of our Universe is so incredibly large. So it is possible that the problem would be solved if the cosmic expansion was non adiabatic for some finite time steps [27].

1.4 The Inflationary Paradigm

From what we have just explained, it appears that solving the shortcomings of the standard Big Bang theory requires two basic modifications of the assumptions made so far:

- The Universe has to go through a non-adiabatic period. This is necessary to solve the entropy and the flatness problem. A non-adiabatic phase may give rise to the large entropy S that we observe today.

- The Universe has to go through a primordial period during which the physical scales λ evolve faster than the horizon scale H^{-1}.

Cosmological inflation is such a mechanism. The fundamental idea of inflation is that the Universe undergoes a period of accelerated expansion, defined as a period when $\ddot{a} > 0$, at early times. From Eq. (1.14) we learn that:

$$\ddot{a} > 0 \Longleftrightarrow (\rho + 3p) < 0 \tag{1.30}$$

so for an accelerated expansion it is necessary that the pressure of the Universe is negative $p < -\frac{\rho}{3}$. Neither a radiation-dominated phase nor a matter-dominated phase (for which $p = \frac{\rho}{3}$ and $p = 0$) satisfies such a condition. In order to study the properties of the period of inflation, usually the extreme condition $p = -\rho$ is assumed, which considerably simplifies the analysis. A period with these characteristics is called a *de Sitter* stage. From Eqs. (1.13) and (1.15) derive that in a *de Sitter* phase:

$$\rho = const \quad H_I = const \tag{1.31}$$

and from the Friedmann equation (1.13)

$$a = a_i e^{H_I(t-t_i)} \tag{1.32}$$

where t_i denotes the time at which inflation starts and H_I the value of the Hubble rate during inflation.

It is possible to demonstrate that a period of accelerated expansion can solve the shortcomings of the standard Big Bang model. As we will see from the dynamics of the vacuum-dominated case, the scale factor will grow very quickly in this period while the Hubble value will remain roughly constant. This means that $(aH)^{-1}$, the comoving Hubble radius, will decrease with proper time during inflation. Effectively this means that, in coordinates fixed with the expansion, the horizon is actually shrinking. This solves the flatness problem since the $k/a^2 H^2$ term in Eq. (1.13) will rapidly shrink during inflation, pushing Ω back towards unity. The unwanted relics problem is solved as the density of such relics will be greatly diluted, providing that the relics are produced before inflation. Since the comoving Hubble length $(aH)^{-1}$ decreases with time during inflation, the length

over which regions are casually connected becomes larger than the comoving Hubble length. The observable Universe today originates from a smooth patch that was much smaller than the particle horizon size before inflation began. However, for the resolution of these problems it is necessary to know "how much" inflation is required and this is quantified by the number of *e-fold*, defined by:

$$N(t) = \ln\left(\frac{a(t_f)}{a(t_i)}\right) \tag{1.33}$$

To solve the previous problems it is enough that $N \gtrsim 60$ [29].

1.5 Inflation as driven by a slowly-rolling scalar field

Knowing the various advantages of having a period of accelerated expansion, the next task consists in finding a model that satisfies the conditions mentioned above. There are many models of inflation [29] but the most accredited and stable is based on a scalar field ϕ, the *inflaton*.
The dynamics of these fields, if it dominates on the other matter/energy components, is given by the action

$$S = \int d^4x \sqrt{-g}\mathcal{L} \tag{1.34}$$

where $\mathcal{L}$ is the Lagrangian density of the inflaton

$$\mathcal{L} = \frac{1}{2}\partial_\mu\phi\partial^\mu\phi + V(\phi) \tag{1.35}$$

g is the metric determinant and $V(\phi)$ specifies the scalar field potential. By varying the action with respect to ϕ we obtain

$$\partial_\mu \frac{\delta(\sqrt{-g}\mathcal{L})}{\delta\partial_\mu\phi} - \frac{\delta(\sqrt{-g}\mathcal{L})}{\delta\phi} = 0 \tag{1.36}$$

that in a FRW metric (1.1) gives

$$\ddot{\phi} + 3H\dot{\phi} - \frac{\nabla^2\phi}{a^2} + V'(\phi) = 0 \tag{1.37}$$

where $V'(\phi) = dV(\phi)/d\phi$ and $H = \dot{a}/a$ is the Hubble parameter. The second term in the previous equation is fundamental; it is a *friction term*: a scalar field rolling down its potential suffers a friction due to the expansion of the Universe. The second important quantity for the description of the inflaton field is the energy-momentum tensor $T_{\mu\nu}$ that is obtained from the variation of the action with respect to the metric $g^{\mu\nu}$

$$T_{\mu\nu} = \frac{2}{\sqrt{-g}}\frac{\delta\mathcal{L}}{\delta g^{\mu\nu}} \tag{1.38}$$

17

The (0,0) and (i,i) components of the energy-momentum tensor give the energy density ρ_ϕ and pressure density p_ϕ respectively

$$T_{00} = \rho_\phi = \frac{\dot{\phi}^2}{2} + V(\phi) + \frac{(\nabla\phi)^2}{2a^2} \tag{1.39}$$

$$T_{ii} = p_\phi = \frac{\dot{\phi}^2}{2} - V(\phi) - \frac{(\nabla\phi)^2}{6a^2} \tag{1.40}$$

It is easy to notice that if the gradient term dominates we have $p_\phi = -\frac{\rho_\phi}{3}$ that is not enough to drive inflation. We can split the inflaton field as $\phi(t, \mathbf{x}) = \phi_0(t) + \delta\phi(t, \mathbf{x})$ where ϕ_0 is the "classical" (infinite wavelength) field, that is the expectation value of the inflaton field on the initial isotropic and homogeneous state, while $\delta\phi(t, \mathbf{x})$ represents the quantum fluctuations around ϕ_0. Considering only the homogeneous part, which behaves like a perfect fluid, we have

$$T_{00} = \rho_\phi = \frac{\dot{\phi}^2}{2} + V(\phi) \tag{1.41}$$

$$T_{ii} = p_\phi = \frac{\dot{\phi}^2}{2} - V(\phi) \tag{1.42}$$

And, if

$$V(\phi) >> \dot{\phi}^2 \tag{1.43}$$

we obtain:

$$p_\phi \simeq -\rho_\phi \tag{1.44}$$

It is simple to notice that a scalar field whose energy is dominant in the Universe and whose potential energy dominates over the kinetic term gives rise to accelerated expansion. Inflation is thus driven by the vacuum energy of the inflaton field. Ordinary matter fields and spatial curvature k are usually neglected during inflation because their contribution to the energy density is redshifted away during the accelerated phase. For the same reason we have neglected the small inhomogeneities justifying the use of the background FRW metric.

1.5.1 Slow-roll conditions

A period of inflation requires that the scalar field must satisfy some conditions. A homogeneous scalar field has the following equation of motion

$$\ddot{\phi} + 3H\dot{\phi} + V'(\phi) = 0 \tag{1.45}$$

If we require that $\dot{\phi}^2 << V(\phi)$, the scalar field is slowly rolling down its potential. Such a *slow roll* period can be achieved if the inflaton field ϕ is in a region where the potential is sufficiently flat so $\ddot{\phi}$ is negligible. The Friedmann equation (1.13) becomes

$$H^2 \simeq \frac{8\pi G}{3} V(\phi) \tag{1.46}$$

where it is assumed that the inflaton field dominates the energy density of the Universe. With this assumption the equation of motion becomes

$$3H\dot{\phi} \approx -V'(\phi) \qquad (1.47)$$

Then slow-roll conditions require

$$\dot{\phi}^2 \ll V(\phi) \Rightarrow \frac{(V')^2}{V} \ll H^2 \qquad (1.48)$$

and

$$\ddot{\phi} \ll 3H\dot{\phi} \Rightarrow V'' \ll H^2 \qquad (1.49)$$

It is possible to define the *slow-roll parameters*

$$\varepsilon \equiv -\frac{\dot{H}}{H^2} = 4\pi G \frac{\dot{\phi}^2}{H^2} = \frac{1}{16\pi G}\left(\frac{V'}{V}\right)^2 \qquad (1.50)$$

$$\eta = \frac{1}{8\pi G}\left(\frac{V''}{V}\right) = \frac{1}{3}\frac{V''}{H^2} \qquad (1.51)$$

and the fate of inflation is described by the parameter ε: in fact inflation can occur if $\varepsilon \ll 1$ and it ends when this condition is not satisfied.
Within this approximation, the total number of e-folds between the beginning and the end of inflation is

$$N_{tot} \equiv \ln\left(\frac{a(t_f)}{a(t_i)}\right) = \int_{t_i}^{t_f} H dt \simeq -8\pi G \int_{\phi_i}^{\phi_f} \frac{V}{V'}d\phi \qquad (1.52)$$

In conclusion, inflation is cosmologically attractive but serious problems are left unsolved: on the one hand, we cannot know if the Universe in its earliest stages satisfied the conditions for inflation to light up; on the other hand, there are no experimental evidences even for the existence of a neutral spin zero boson and even less for the existence of the inflaton in particular.

1.6   Inflation and cosmological perturbations

As shown, inflationary cosmology provides the mechanism for solving the initial condition problems of the Big Bang model. In addition inflation generates the spectra of both density perturbations and gravitational waves that explain the temperature anisotropies in the CMB [32] and also the structure formation in the Universe. In the inflationary Universe, these primordial density perturbations are generated from vacuum fluctuations of the scalar field.
Our current understanding of the origin of structures in the Universe is that once the Universe became matter dominated ($z \sim 3200$), primeval density inhomogeneities ($\delta\rho/\rho \sim 10^{-5}$) were amplified by gravity and grew into the structures

we see today [29]. In order to make structure formation occur via gravitational in-stability, there must have been small preexisting fluctuations on relevant physical scales which left the Hubble radius in the radiation-dominated and matter-dominated eras. In the standard Big-Bang model these small perturbations have to be put "by hand", because it is impossible to produce fluctuations on any length scale when it is larger than the horizon size. Inflation elegantly solves this issue; in fact during inflation the Hubble radius H^{-1} remains almost constant with time while the scale factor grows quasi-exponentially. Consequently the wavelength of a quantum fluctuation in the scalar field whose potential energy drives inflation soon exceeds the Hubble radius. The quantum fluctuations arise on scales which are much smaller than the Hubble radius, which is the scale beyond which causal process cannot operate. On such small scales one can use the usual flat space-time quantum field theory to describe the scalar field vacuum fluctuations. The inflationary expansions stretch the wavelength of quantum fluctuations outside the horizon; thus, gravitational effects become more important and amplify the quantum fluctuations. When the wavelength of any particular fluctuation becomes greater than H^{-1}, microscopic physics does not affect the evolution and then the amplitude of fluctuations is "frozen-in" and fixed at some non-zero value $\delta\phi$ at the horizon crossing, because of a large friction term $3H\dot{\phi}$ in the equation of motion of the field ϕ (1.45). The amplitude of the fluctuations on super-horizon scales then remains almost unchanged for a very long time, whereas its wavelength grows exponentially. Therefore the appearance of such frozen fluctuations is equivalent to the appearance of a classical field $\delta\phi$ that does not vanish after averaging over some macroscopic intervals of time.

The fluctuations of the scalar field generate primordial perturbations in the energy density ρ_ϕ, which are then inherited by the radiation and matter to which the inflaton decays during reheating after inflation [29]. Once inflation has ended, however, the Hubble radius increases faster than the scale-factor, so the fluctuations eventually re-enter the Hubble radius during the radiation or matter-dominated eras. The fluctuations that exit around 60 e-foldings or so before reheating reenter with physical wavelengths in the range accessible to cosmological observations. These spectra are therefore distinctive signatures of inflation and give us a direct observational connection to the physics of inflation. The data of the WMAP satellite confirm the presence of adiabatic super-horizon fluctuations in the CMB and this is a distinctive signature of an early stage of acceleration. To understand the behaviour of the fluctuations consider that, since gravity acts on any component of the Universe, small fluctuations of the inflaton field are intimately related to the fluctuation of the space-time metric, giving rise to perturbations of the curvature ζ, which may loosely considered as a gravitational potential [35]. The physical wavelengths λ of these perturbations grow exponentially and leave the horizon when $\lambda > H^{-1}$. On super-horizon scales, curvature perturbations are frozen in and considered as classical. Finally, when the wavelength of these fluctuations reenters the horizon, at some radiation or matter-dominated epoch, the curvature (gravitational potential) perturbations of the space-time give rise to matter (and temperature) perturbations $\delta\rho$ via the

Poisson equation [35]. These fluctuations will then start growing, thus giving rise to the structures we observe today.

The mechanism for the generation of perturbations during inflation is not peculiar only for the inflaton field but since it dominates the energy density of the Universe it can possibly produce also metric perturbations.

We now see how the quantum fluctuations of a generic scalar field evolve during an inflationary stage [31].

1.6.1 Quantum fluctuations of a generic scalar field during inflation

We now consider the case of a generic scalar field χ with an effective potential $V(\chi)$ in a pure de Sitter stage, during which H is constant. The field χ is not necessarily the inflaton that drives the accelerated expansion.

We split the scalar field $\chi(\tau, \mathbf{x})$ as

$$\chi(\tau, \mathbf{x}) = \chi_0(\tau) + \delta\chi(\tau, \mathbf{x}) \tag{1.53}$$

where $\chi_0(\tau)$ is the homogeneous classical value of the scalar field and $\delta\chi$ are its fluctuations; τ is the conformal time. The scalar field χ is quantized by implementing the standard technique of second quantization.

The equation of motion for the background field is

$$\ddot{\chi} + 3H\dot{\chi} - \frac{1}{a^2}\bigtriangledown^2\chi + V'(\chi) = 0 \tag{1.54}$$

Perturbing Eq. (1.54) we obtain the following equation for the fluctuations

$$\ddot{\delta\chi} + 3H\dot{\delta\chi} - \frac{1}{a^2}\bigtriangledown^2\delta\chi + V''(\chi)\delta\chi = 0 \tag{1.55}$$

Let us give a heuristic explanation of why we expect that such fluctuations are generated.

If we differentiate the equation for the classical field with respect to time, we obtain

$$\dddot{\chi_0} + 3H\ddot{\chi_0} + V''\dot{\chi_0} = 0 \tag{1.56}$$

In the limit $k^2 \ll a^2$ we have neglected the gradient term and we see that $\delta\chi$ and $\dot{\chi_0}$ solve the same equation. They have indeed the same solution, because the Wronskian of the equation is $W(t) = W_0 exp[-3\int^t H d\tilde{t}]$ and goes to zero for large t. Therefore $\delta\chi$ and $\dot{\chi_0}$ have to be related to each other by a constant of proportionality depending only on $\mathbf{x}$:

$$\delta\chi = -\dot{\chi_0}\delta t(\mathbf{x}) \tag{1.57}$$

so the field $\chi(t, \mathbf{x})$ will be of the form

$$\chi(t, \mathbf{x}) = \chi_0(t - \delta t(\mathbf{x}), \mathbf{x}) \tag{1.58}$$

This equation says that the scalar field at given time t does not acquire the same value in all the space. Rather, when the field is rolling down its potential, it acquires different values at different spatial points $\mathbf{x}$, so it is not homogeneous and fluctuations are present.

Using the conformal time the Eq. (1.55) becomes

$$\delta\chi'' + 2\mathcal{H}\delta\chi' - \nabla^2\delta\chi + a^2 m_\chi^2 \delta\chi = 0 \tag{1.59}$$

where $m_\chi^2(\tau) \equiv \frac{d^2 V(\chi)}{d\chi^2}$ is an effective time-dependent mass for the field.

Expanding the scalar field χ in Fourier modes

$$\delta\chi(\tau, \mathbf{x}) = \int \frac{d^3 k}{(2\pi)^{3/2}} \delta\chi_{\mathbf{k}} e^{i\mathbf{k}\cdot\mathbf{x}} \tag{1.60}$$

and performing the following redefinition

$$\delta\chi_{\mathbf{k}} = \frac{\delta\sigma_{\mathbf{k}}}{a} \tag{1.61}$$

we obtain the equation

$$\delta\sigma_{\mathbf{k}}'' + \left(k^2 + a^2 m_\chi^2 - \frac{a''}{a}\right)\delta\sigma_{\mathbf{k}} = 0 \tag{1.62}$$

which is the Klein-Gordon equation with a time-dependent mass term, and can be derived from the effective action

$$\delta S_{\mathbf{k}} = \int d\tau \left[\frac{1}{2}(\delta\sigma_{\mathbf{k}}')^2 - \frac{1}{2}\left(k^2 + a^2 m_\chi^2 - \frac{a''}{a}\right)\delta\sigma_{\mathbf{k}}^2\right] \tag{1.63}$$

which is the canonical action for a simple harmonic oscillator.

Using the well-known techniques of quantum field theory, we can quantize the field writing it as

$$\delta\sigma_{\mathbf{k}} = u_k(\tau)a_{\mathbf{k}} + u_k^*(\tau)a_{\mathbf{k}}^\dagger \tag{1.64}$$

where we have introduced the creation and annihilation operators, which satisfy the commutation relations

$$[a_{\mathbf{k}}, a_{\mathbf{q}}] = 0 \qquad [a_{\mathbf{k}}, a_{\mathbf{q}}^\dagger] = \delta^{(3)}(\mathbf{k} - \mathbf{q}) \tag{1.65}$$

and the modes $u_k(\tau)$ are normalized as

$$u_k^* u_k' - u_k u_k^{*'} = -i \tag{1.66}$$

to satisfy the usual canonical commutation relations between $\delta\sigma$ and its conjugate momentum $\Pi = \delta\sigma'$.

The modes $u_k(\tau)$ obey the equation of motion

$$u_k'' + \left(k^2 + a^2 m_\chi^2 - \frac{a''}{a}\right)u_k = 0 \tag{1.67}$$

which has an exact solution in the case of a de Sitter stage; however, before recovering it, it is instructive to study its behaviour in the sub-horizon and super-horizon limits.

The conformal scale factor in a de Sitter stage is $a = -\frac{1}{H\tau}$ ($\tau < 0$), so $a' = \frac{1}{H\tau^2}$ and $a'' = -\frac{2}{H\tau^3} = \frac{2}{\tau^2}a$; on subhorizon scales we have $k^2 >> a^2 H^2 \simeq \frac{a''}{a}$, so Eq. (1.67) reduces to

$$u_k'' + k^2 u_k = 0 \tag{1.68}$$

whose solution is a plane wave

$$u_k(\tau) = \frac{1}{\sqrt{2k}} e^{-ik\tau} \tag{1.69}$$

Thus we find that fluctuations with wavelength within the horizon oscillate as in flat space-time. This is what we expect, because in this limit the space-time can be approximated as flat.

On superhorizon scales $k^2 \ll \frac{a''}{a}$, Eq. (1.67) becomes

$$u_k'' + \left(a^2 m_\chi^2 - \frac{a''}{a} \right) u_k = 0 \tag{1.70}$$

which is easy to be solved for a massless field ($m_\chi^2 = 0$); there are two solutions, a growing and a decaying mode

$$u_k(\tau) = B_+(k)a + B_-(k)\frac{1}{a^2} \tag{1.71}$$

We can fix the amplitude of the growing mode by matching this solution to the plane wave solution when the fluctuation with wavenumber k leaves the horizon ($k = aH$), finding

$$|B_+(k)| = \frac{1}{a\sqrt{2k}} = \frac{H}{\sqrt{2k^3}} \tag{1.72}$$

so the quantum fluctuations of the original field χ are constant on superhorizon scales

$$|\delta\chi_k| = \frac{|u_k|}{a} \simeq \frac{H}{\sqrt{2k^3}} \tag{1.73}$$

Now we derive the exact solution of Eq. (1.67), which in the case of a massless field is

$$u_k(\tau) = \frac{1}{\sqrt{2k}} e^{-ik\tau} \left(1 + \frac{i}{k\tau} \right); \quad (m_\chi^2 = 0) \tag{1.74}$$

with the initial condition $u_k(\tau) \simeq \frac{1}{\sqrt{2k}} e^{-ik\tau}$ for $k \gg aH$. In a de Sitter phase we have

$$\frac{a''}{a} - m_\chi^2 a^2 = \frac{2}{\tau^2} \left(1 - \frac{1}{2}\frac{m_\chi^2}{H^2} \right) \tag{1.75}$$

so we can rewrite Eq. (1.67) as

$$u_k''(\tau) + \left(k^2 - \frac{\nu_\chi^2 - \frac{1}{4}}{\tau 2} \right) u_k(\tau) = 0 \tag{1.76}$$

23

where

$$\nu_\chi^2 = \frac{9}{4} - \frac{m_\chi^2}{H^2} \tag{1.77}$$

When the mass is constant in time, Eq. (1.76) is a Bessel equation whose general solution for real ν_χ, that is, for light fields such that $m_\chi < \frac{3}{2}H$, reads

$$u_k(\tau) = \sqrt{-\tau}\left[c_1(k) H_{\nu_\chi}^{(1)}(-k\tau) + c_2(k) H_{\nu_\chi}^{(2)}(-k\tau) \right] \tag{1.78}$$

where $H_{\nu_\chi}^{(1)}$, $H_{\nu_\chi}^{(2)}$ are the Hankel functions of first and second kind, respectively. If we impose, as boundary condition, that in the ultraviolet regime $k \gg aH$ ($-k\tau \gg 1$) the solution matches the plane-wave solution $\frac{1}{\sqrt{2k}}e^{-ik\tau}$ that we expect in flat space-time and knowing that

$$H_{\nu_\chi}^{(1)}(x \gg 1) \simeq \sqrt{\frac{2}{\pi x}} e^{i(x - \frac{\pi}{2}\nu_\chi - \frac{\pi}{4})}; \quad H_{\nu_\chi}^{(2)}(x \gg 1) \simeq \sqrt{\frac{2}{\pi x}} e^{-i(x - \frac{\pi}{2}\nu_\chi - \frac{\pi}{4})} \tag{1.79}$$

we then set $c_2(k) = 0$ and $c_1(k) = \frac{\sqrt{\pi}}{2} e^{i(\nu_\chi + \frac{1}{2})\frac{\pi}{2}}$ which also satisfy the normalization condition (1.66).
So the exact solution becomes

$$u_k(\tau) = \frac{\sqrt{\pi}}{2} e^{i(\nu_\chi + \frac{1}{2})\frac{\pi}{2}} \sqrt{-\tau} H_{\nu_\chi}^{(1)}(-k\tau) \tag{1.80}$$

On superhorizon scales, since

$$H_{\nu_\chi}^{(1)}(x \ll 1) \simeq \sqrt{\frac{2}{\pi}} e^{-i\frac{\pi}{2}} 2^{\nu_\chi - \frac{3}{2}} \frac{\Gamma(\nu_\chi)}{\Gamma(\frac{3}{2})} x^{-\nu_\chi} \tag{1.81}$$

the solution (1.80) has the limiting behaviour

$$u_k(\tau) \simeq e^{i(\nu_\chi - \frac{1}{2})\frac{\pi}{2}} 2^{\nu_\chi - \frac{3}{2}} \frac{\Gamma(\nu_\chi)}{\Gamma(\frac{3}{2})} \frac{1}{\sqrt{2k}} (-k\tau)^{\frac{1}{2} - \nu_\chi} \tag{1.82}$$

Thus we find that on superhorizon scales the fluctuations of the scalar field $\delta\chi_k = \frac{u_k}{a}$ are not exactly constant, but acquire a tiny dependence upon time

$$|\delta\chi_{\mathbf{k}}| = 2^{\nu_\chi - \frac{3}{2}} \frac{\Gamma(\nu_\chi)}{\Gamma(\frac{3}{2})} \frac{H}{\sqrt{2k^3}} \left(\frac{k}{aH}\right)^{\frac{3}{2} - \nu_\chi} \quad (k \ll aH) \tag{1.83}$$

We introduce the parameter $\eta_\chi = \frac{m_\chi^2}{3H^2}$; if the field is very light $\frac{3}{2} - \nu_\chi \simeq \eta_\chi$, and to the lowest order in η_χ we have

$$|\delta\chi_{\mathbf{k}}| \simeq \frac{H}{\sqrt{2k^3}} \left(\frac{k}{aH}\right)^{\eta_\chi} \quad (k \ll aH) \tag{1.84}$$

This equation shows that, when a scalar field is light, its quantum fluctuations generated on subhorizon scales are gravitationally amplified and stretched to superhorizon scales because of the accelerated expansion.

A useful quantity to characterize the properties of the perturbations is the *power spectrum* that measures the amplitude of quantum fluctuations at a given scale k. If we have a random field $f(t, \mathbf{x})$ in a flat space-time we can expand it in Fourier space

$$f(t, \mathbf{x}) = \int \frac{d^3 k}{(2\pi)^{3/2}} e^{i\mathbf{k} \cdot \mathbf{x}} f_{\mathbf{k}}(t) \tag{1.85}$$

The (dimensionless) power spectrum $\mathcal{P}_f(k)$ is defined by

$$\langle f_{\mathbf{k}_1} f_{\mathbf{k}_2}^* \rangle \equiv \frac{2\pi^2}{k^3} \mathcal{P}_f(k) \delta^{(3)}(\mathbf{k}_1 - \mathbf{k}_2) \tag{1.86}$$

where the angle brackets denote ensemble average.

The two-point correlation function is given by

$$\langle f(t, \mathbf{x}_1) f(t, \mathbf{x}_2) \rangle = \int \frac{d^3 k}{4\pi k^3} \mathcal{P}_f(k) e^{i\mathbf{k} \cdot (\mathbf{x}_1 - \mathbf{x}_2)} = \int \frac{dk}{k} \frac{\sin(kx)}{kx} \mathcal{P}_f(k) \tag{1.87}$$

where $x = |\mathbf{x}_1 - \mathbf{x}_2|$. One may notice then that the power-spectrum, $\mathcal{P}_f(k)$ is the contribution to the variance per unit logarithmic interval in the wave-number k. It is standard practice to define the *spectral index* $n_f(k)$ through

$$n_f(k) - 1 \equiv \frac{d \ln \mathcal{P}_f(k)}{d \ln k} \tag{1.88}$$

since in many models of inflation the spectrum can well be approximated by a power law.

In the case of a scalar field χ the power-spectrum $\mathcal{P}_{\delta\chi}(k)$ can be evaluated by combining equations (1.61), (1.64) and (1.65)

$$\langle \delta\chi_{\mathbf{k}} \delta\chi_{\mathbf{q}}^* \rangle = \frac{1}{a^2} \langle \delta\sigma_{\mathbf{k}} \delta\sigma_{\mathbf{q}}^* \rangle = \frac{1}{a^2} \langle (u_k a_{\mathbf{k}} + u_k^* a_{\mathbf{k}\dagger})(u_q^* a_{\mathbf{q}}^\dagger + u_q a_{\mathbf{q}}) \rangle = \tag{1.89}$$

$$= \frac{1}{a^2} \langle (u_k a_{\mathbf{k}})(u_q^* a_{\mathbf{q}}^\dagger) \rangle = \frac{1}{a^2} u_k u_q^* \langle [a_{\mathbf{k}}, a_{\mathbf{q}}^\dagger] \rangle = \frac{|u_k|^2}{a^2} \delta^{(3)}(\mathbf{k} - \mathbf{q})$$

so, using the definition (1.86), we find

$$\mathcal{P}_{\delta\chi}(k) = \frac{k^3}{2\pi^2} |\delta\chi_k|^2 \tag{1.90}$$

In the case of a scalar field in a de Sitter stage, considering $m_\chi \ll \frac{3}{2} H$, from Eq.(1.84) we compute the spectrum on superhorizon scales

$$\mathcal{P}_{\delta\chi}(k) = \left(\frac{H}{2\pi} \right)^2 \left(\frac{k}{aH} \right)^{3 - 2\nu_\chi} \tag{1.91}$$

Therefore we have a nearly scale-invariant (or Harrison Zel'dovich) spectrum; the spectral index is

$$n_{\delta_\chi} - 1 = 3 - 2\nu_\chi = 2\eta_\chi \ll 1 \tag{1.92}$$

and so for a massless field we have exactly scale-invariance on superhorizon scales.

The power spectrum of fluctuations of the scalar field χ is therefore nearly flat, that is nearly independent from the wavelength $\lambda = \pi/k$; the amplitude of the fluctuations in superhorizon scales does not (almost) depend upon the time at which the fluctuations crosses the horizon and becomes frozen in. The small tilt of the power spectrum arises from the fact that the scalar field χ is massive and because during inflation the Hubble rate is not exactly constant, but nearly constant.

2

Anisotropic Universe

This chapter is devoted to a collection of all the vector models proposed so far, their problems about instability and their possible solutions in order to have agreement with observational data.

Contents

As seen in the Introduction the idea to introduce anisotropic models comes from both theoretical and observational motivations. From the observational part there is another reason to consider anisotropic sources and in particular vector fields; it comes from the inference of intergalactic magnetic fields. In fact, magnetic fields have been inferred by an apparent lack of GeV scale γ-rays coming from blazars that produce TeV scale γ-rays. The interaction with the intergalactic medium should convert the higher energy γ-rays (E$\sim$ TeV) in lower energy but the non-observation of γ-rays with energies scale $\sim$ GeV has been associated to the presence of intergalactic magnetic fields that deflect the secondary rays [36]. Even if it is not so easy to generate primordial magnetic fields taking into account the strong coupling problem and the backreaction problem the vector fields are potential candidates to explain their formation [37, 38, 39, 40].

The conformal invariance of the basic gauge invariant Maxwell Lagrangian $\mathcal{L} = -(\sqrt{-g}/4)F_{\mu\nu}F^{\mu\nu}$ makes the use of the vector field tricky in order to drive an exponential phase of expansion and to generate curvature fluctuations on superhorizon scales. In order to do that it is necessary to modify the Lagrangian finding some mechanism to break the conformal invariance. The first attempt was made by Ford [17] who considered a single self-coupled field A_μ with a Lagrangian

$$L_A = -\frac{1}{4}F_{\mu\nu}F^{\mu\nu} + V(\xi) \tag{2.1}$$

where $F_{\mu\nu} \equiv \partial_\mu A_\nu - \partial_\nu A_\mu$ is the field strenght and V is the potential of the vector field, $\xi \equiv A_\mu A^\mu$. The author analyzes different scenarios with different form of the potential and he founds that the universe expands anisotropically at the end of the inflationary period and this anisotropy survives until late times or is damped out depending on the shape and the location of the minima of the potential[17].

A similar model, but with the vector field used like a curvaton, was proposed by [35]; the form of the Lagrangian was the same

$$L_C = -\frac{1}{4}F_{\mu\nu}F^{\mu\nu} + \frac{1}{2}m^2 A_\mu A^\mu \tag{2.2}$$

and he found that for $m^2 \simeq -2H^2$ the transverse mode of the vector field is governed by the same equation of motion of a light scalar field in a de Sitter phase so a suitable power spectrum of curvature perturbations could be obtained. In this model the inflaton drives inflation and the anisotropy is bounded because the vector field acts like a curvaton.

A more concise and instructive model was proposed by Golovnev et al. [18] where inflation is driven by a non-minimally coupled (to gravity) massive vector

field. The lagrangian was

$$L_{vec} = -\frac{R}{16\pi} - \frac{1}{4}F_{\mu\nu}F^{\mu\nu} + \frac{1}{2}\Big(m^2 + \frac{R}{6}\Big)A_\mu A^\mu \qquad (2.3)$$

where R is the Ricci scalar. The non-minimal coupling ($\xi = 1/6$) of this vector field is very similar to conformal coupling for a scalar field [41]. In the case of a scalar field this coupling converts massless scalar field into a conformal invariant field while for the vector field the non-minimal coupling has an opposite effect: precisely, it violates the conformal invariance of a massless vector field and forces it to behave in the same way as a minimally coupled scalar field. This model can provide for an inflationary phase and the problem of excessive anisotropy is avoided considering either a triplet of mutually orthogonal or a large number N of randomly oriented vector fields. The degree of anisotropy left at the end of inflation is proportional to $\frac{1}{\sqrt{N}}$. this last mechanism as originally employed for magnetogenesis [42].

Another model proposed by [8] where a fixed norm vector has been studied was described by a Lagrangian like

$$L_{FN} \supset \lambda(A_\mu A^\mu - m^2) \qquad (2.4)$$

where λ is a Langrange multiplier used to fix the norm of the vector. The expansion is anisotropic and two different expansion rates have been founded.

Most of the above models successfully solve the problem of attaining a slow-roll regime for the vector-fields without too much fine tuning on the parameters of the theory and of avoiding excessive production of anisotropy at late times. But all the three break the $U(1)$ gauge symmetry and this lead to an additional degree of freedom, the longitudinal vector polarization that in all of these models turns out to be a ghost; in particular The instabilities emerge from the linearized study of the perturbation around the anisotropic inflationary solution. As in all slow-roll inflationary backgrounds, each mode of the perturbations is initially in the small wavelength regime (the wavelength is exponentially small at early times); as the background inflates, the wavelength becomes larger than the Hubble horizon H^{-1} and the mode enters into the large wavelength regime. This transition is called horizon crossing. In the self-coupled model [17] the system of perturbations contains a ghost in the small wavelength regime while in the case of the non-minimally coupled model[18] and in the fixed-norm case[8] the ghost appears at some intervals of time close to horizon crossing [20, 43, 22].

The problem of the instabilities seems to be overcome by introducing models with varying gauge coupling. In a first work by Yokoyama and Soda [44] a vector field with a non-minimal kinetic term couples with a "waterfall" field χ in a hybrid inflation model. In such a system, the vector field gives fluctuations at the end of inflation and hence induces a subcomponent of curvature perturbations. Since the vector has a preferred direction, the statistical anisotropy could appear

in the fluctuations. The Lagrangian of this model is:

$$\mathcal{L} = \frac{1}{2}R - \frac{1}{2}g^{\mu\nu}(\partial_\mu\phi\partial_\nu\phi + \partial_\mu\chi\partial_\nu\chi) + V(\phi, \chi, A_\mu) - \frac{1}{4}g^{\mu\nu}g^{\rho\sigma}f^2(\phi)F_{\mu\rho}F_{\nu\sigma} \quad (2.5)$$

where $F_{\mu\nu} = \partial_\mu A_\nu - \partial_\nu A_\mu$ is the field strength of the vector field, $V(\phi, \chi, A_\mu)$ is the potential of fields and $f(\phi)$ is the coupling function of the inflaton field to the vector one. The potential is not specified but it does not violate the gauge invariance. In this model the inflaton field is responsible for the inflation; in fact the vector field is sub-dominant and has a small expectation value compared with the inflaton. It is treated perturbatively and considered massless. With these choices the longitudinal mode of the vector field disappears and instabilities are avoided. The "waterfall" acts as the medium through which the anisotropy in A_μ is transmitted to the inflaton. However, as we will see in chapter 3 the communication already occurs without the waterfall field but directly by coupling the inflaton with the gauge field.

The most intriguing model that we deeply analyze in Section 2.3 and in Chapter 3 is the one proposed by Watanabe, Kanno and Soda [5], an inflationary scenario where the inflaton field is coupled with the kinetic term of a massless vector field; they show that the inflationary Universe is endowed with anisotropy for a wide range of coupling functions. The following Lagrangian has been used:

$$\mathcal{L} = \frac{1}{2}R - \frac{1}{2}(\partial_\mu\phi)(\partial^\mu\phi) - V(\phi) - \frac{1}{4}f^2(\phi)F_{\mu\nu}F^{\mu\nu} \quad (2.6)$$

They note that the fate of the anisotropic expansion depends on the behaviour of the coupling function. This is the first minimal model free of instabilities. Another interesting class of models is the one in which inflation is driven by a scalar field in the presence of a non-abelian $SU(2)$ vector multiplet [24, 45, 46, 47].

$$L_{NA} = \frac{M_P^2 R}{2} - \frac{f^2(\phi)}{4}g^{\mu\alpha}g^{\nu\beta}\sum_{a=1,2,3}F_{\mu\nu}^a F_{\alpha\beta}^a - \frac{M^2}{2}g^{\mu\nu}\sum_{a=1,2,3}A_\mu^a A_\nu^a + L_\phi, \quad (2.7)$$

where L_ϕ is the Lagrangian of the scalar field and $F_{\mu\nu}^a \equiv \partial_\mu A_\nu^a - \partial_\nu A_\mu^a + g_c\varepsilon^{abc}A_\mu^b A_\nu^c$ (g_c is the $SU(2)$ gauge coupling). Both f and the effective mass M can be viewed as generic functions of time. For this kind of model cosmological correlation functions have been computed in [24, 45, 46, 47] without considering the inflationary dynamics. It is shown that a richer amount of predictions is offered compared to the Abelian case. This is due to the self interaction terms that give new contributions to the bispectrum and the trispectrum that are non negligible wrt the others present in the Abelian case.

An interesting model, based only on non-abelian vector field was proposed by [25]. Gauge-flation is a non-Abelian gauge theory minimally coupled to gravity in which inflation is driven thanks to an higher order derivative operator

$$L_{GF} = \frac{M_P^2 R}{2} - \frac{1}{4}F_{\mu\nu}^a F^{a,\mu\nu} + \frac{\kappa}{96}\left(F_{\mu\nu}^a \tilde{F}^{a,\mu\nu}\right)^2, \quad (2.8)$$

where R is the Ricci scalar, $F^a_{\mu\nu} \equiv \partial_\mu A^a_\nu - \partial_\nu A^a_\mu - g_c \varepsilon^{abc} A^b_\mu A^c_\nu$ is the field-strength tensor of a $SU(2)$ gauge field with coupling constant g, and $\tilde{F}^{a,\mu\nu} \equiv \frac{\varepsilon^{\mu\nu\alpha\beta}}{2\sqrt{-g}} F^a_{\alpha\beta}$ is its dual ($\varepsilon^{\mu\nu\alpha\beta}$ is the totally anti-symmetric tensor). In this model the gauge symmetry is not broken and there are no problems of instabilities. Moreover this model admits an isotropic solution coming from the residual global gauge symmetry present in every non-Abelian group. With this trick is possible to maintain homogeneity and isotropy even in presence of vector fields. Even if Gauge-flation model seems to be a good theoretical (non-Abelian) vector model it is rueld out by the CMB data; in fact considering the only parameter of the theory $\gamma \equiv \frac{g^2 Q^2}{H^2}$ (where g is the gauge coupling constant, Q the vector vev and H the Hubble parameter) in [26] it is found that the scalar spectral index n_s is too low at small γ, while the tensor-to-scalar ratio r is too high at large γ.

In particular regime the Gauge-flation model shares some trajectories with the Chromo-natural inflation model that is a model where the non-Abelian gauge field is coupled with a pseudoscalar axion field solving the problem of the trans-Planckian axion decay constant.[48, 49]

Finally, extensions of the previous models have been considered in [50, 51] where a system of multi-vector fields with uniform coupling between the inflaton and gauge fields has been studied. The Lagrangian of the model is the following

$$L = \frac{M_P^2 R}{2} - \frac{1}{2}\partial_\mu\phi\partial^\mu\phi - V_0 e^{\lambda\phi} - \frac{1}{4}\sum_{m=1}^{N} e^{g_m\phi} F^{(m)}_{\mu\nu} F^{(m)\mu\nu} \tag{2.9}$$

where N is the number of copies of Abelian vector field considered. The result shows that the system tends to isotropize when the number of vector fields is greater than two.

2.1.1 Pseudoscalar-Vector Model and Parity Violation

Another class of models that involves vector field is chatacterized by coupling this with pseudoscalar fields like axions. Axions are ubiquitous in particle physics: they arise whenever an approximate global symmetry is spontaneously broken and are plentiful in string theory compactifications. In cosmology they have been introduced to solve the problem of the UV completion of inflationary theories and, at same time, they also give characteristic signatures for both gravitational waves and non-Gaussianity as we will see. In model of axion-vector inflation the Lagrangian is of the form

$$L_A = \frac{M_P^2 R}{2} - \frac{1}{2}\partial_\mu\varphi\partial^\mu\varphi - V(\varphi) - \frac{1}{4}F_{\mu\nu}F^{\mu\nu} - \frac{\alpha}{f}\varphi F_{\mu\nu}\tilde{F}^{\mu\nu} \tag{2.10}$$

where φ is the inflaton that, in this case, is a pseudoscalar field, $F_{\mu\nu}$ is the field strenght of the gauge field, $\tilde{F}^{\mu\nu} \equiv \frac{1}{2}\varepsilon^{\mu\nu\alpha\beta} F_{\alpha\beta}$ its dual, f the axion decay constant and α a dimensionless parameter. This kind of model, protected by

the shift symmetry ($\varphi \to \varphi + const.$), solves the problem that characterizes the *natural inflation* model: the trans-Planckian value of the axion decay constant f. Other possibilities to solve this problem are: consider two [52] or more axions [53, 54], extra-dimensions [55] but the axion-vector coupling seems to be more natural. The interaction present in 2.10 has a particular phenomenology: the motion of the inflaton amplifies the fluctuations of the gauge field δA, that in turn produces inflaton fluctuations through inverse decay: $\delta A + \delta A \to \delta\varphi$. In [56] it was shown that for sub-Planckian value of f the signal coming from the inverse decay process dominates over the usual vacuum fluctuations giving some interesting observational signatures; in fact it is found that the amplitude of the perturbations generated by the inverse decay is an exponentially growing function of $\frac{\alpha}{f}$. These modes dominate over the vacuum ones for $\frac{\alpha}{f} > 10^{-2} M_{Pl}^{-1}$ (the precise value depending on the inflaton potential). For small values of $\frac{\alpha}{f}$ this new effect is completely negligible, and the standard results are recovered. For large values, drastically new pre- dictions are obtained. In particular, the main characteristic of is that the new contribution is highly non-Gaussian: this is due to the fact that two gauge quanta that participate in the inverse decay are gaussian (loosely speaking, the inverse contribution is proportional to the square of a Gaussian field, which is obviously not gaussian). It is also found a tachyonic instability of one of the two helicity modes of the gauge field that generates a parity violating signal (one chirality produced with much greater abundance than the other one). It is also found that the spectrum of gravity waves produced by the inverse decay is much smaller than that from vacuum.
A slight modification of the previous model by introducing a new "hidden" sector consisting of a light pseudoscalar field χ gravitationally coupled to the inflaton ϕ introduces interesting features, providing new source of inflationary gravitational waves, complementary to the usual quantum vacuum fluctuations of the tensor part of the metric. This model was introduced by [6] and then studied by [57] with particular approximation for the CMB analysis. The Lagrangian is given by

$$\mathcal{L} = -\frac{1}{2}(\partial\phi)^2 - V(\phi) - \frac{1}{2}(\partial\chi)^2 - U(\chi) - \frac{1}{4}F_{\mu\nu}F^{\mu\nu} - \frac{\chi}{4f}F_{\mu\nu}\tilde{F}^{\mu\nu} \;, \quad (2.11)$$

where f is a coupling constant like an axion decay constant and $F_{\mu\nu} \equiv \partial_\mu A_\nu - \partial_\nu A_\mu$ is the field strength and $\tilde{F}_{\mu\nu}$ its dual. In this model inflation is driven by the inflaton potential $V(\phi)$, while χ contributes to the generation of curvature and tensor perturbations through gravitational interaction with the gauge field. Such a scenario is different from the descibed before in which a direct coupling between the inflaton and the gauge field is present [56]. In that case the coupling is much stronger than the gravitational one and scalar curvature fluctuations are sourced with much more efficiency than gravitational waves [6]. Observed power spectra of curvature and tensor perturbations will consist of both these gauge-field modes and considerable normal modes generated in the slow-roll regime, which are expressed as $\mathcal{P} \equiv \frac{H^2}{8\pi^2 \varepsilon M_P^2}$ and $\mathcal{P}_h = 16\varepsilon\mathcal{P}$ with H, ε and $M_P \equiv 1/\sqrt{8\pi G}$ being the Hubble parameter, the slow-roll parameter for the inflaton and the reduced Planck mass, respectively. As we will see in Chapter 5 this model show very

interesting features like large tensor equilateral non-Gaussianity and in particular parity violating signal.

2.2   Dynamical Analysis of $f(F^2)$ Models

Although a careful perturbative analysis on the instabilities of vector models has been conducted in [20, 22, 43] a more powerful analysis has been done in [21]. It is known that Hamiltonian stability and hyperbolicity analysis are more powerful tools, because the perturbative one can only demonstrates the local stability or instability around a particular background. A fundamental theory to be well posed must satisfy two necessary conditions: the boundedness by below of its Hamiltonian[i] (otherwise the theory is unstable), and the hyperbolicity of the field equations (so that the Cauchy problem is well posed [58]). In this section we briefly review the results found in [21] where a non-linear function of the Maxwell Lagrangian plus a potential term for the vector field have been analyzed

$$\mathcal{L} = -f(F^2) - V(A^2), \tag{2.12}$$

The Hamiltonian density, defined as $\mathcal{H} = \pi^\mu \dot{A}_\mu - \mathcal{L}$, is given by

$$\mathcal{H} = \frac{\pi_i^2}{4f'} + \frac{(\partial_i \pi^i)^2}{2V'} + f(F^2) + V(A^2). \tag{2.13}$$

where $\pi^\mu \equiv \partial\mathcal{L}/\partial\dot{A}_\mu$ and $\pi^0 = 0$, so the A_0 component of the vector field is non-dynamical, while $\pi^i = 4f'F_{0i}$. The analysis of the Hamiltonian boundendness must be done case by case but in [21] they shown that some conditions can be found. First of all, f' must be positive for $\mathcal{H}$ to be bounded by below. In fact if f' is negative can be found some initial conditions where $\pi_i^2 \to \infty$ and $F_{ij}^2 \to \infty$ while keeping $\bar{F}^2 = F_{ij}^2 - 2\pi_i^2/(4f')^2$ constant so the first term diverges towards $-\infty$.

Similarly V' must also be positive for $\mathcal{H}$ to be bounded by below. If it is not the case, the second term in 2.13 would diverge towards $-\infty$. This condition is not sufficient because in the case of monomial potential, like $V(A^2) = k(A^2)^n$, if $k < 0$ and n is odd and negative, then V' is positive but $\mathcal{H}$ diverges towards $-\infty$ for initial conditions such that $\partial_i \pi^i = 0$ and $A_i^2 \to \infty$.

This analysis shows that there are no necessary and sufficiend condition that guarantee the Hamiltonian stability but the models has to be analyzed explicitly case by case.

For the hyperbolicity more general statements can be found. The equation of

---

[i]More precisely, the spatial integral of the Hamiltonian density over any localized state should be bounded by below.

motion related to the Lagrangian 2.12 is

$$\nabla_\mu(f'F^{\mu\nu}) = \frac{1}{2}V'A^\nu \tag{2.14}$$

The second derivative can be recast using the principle part of the differential operator

$$[f' \times (\delta_\mu^\nu \Box - \partial_\mu\partial^\nu) + 4f''F^{\alpha\nu}F_{\beta\mu}\partial_\alpha\partial^\beta]A^\mu \tag{2.15}$$

where the term in the square bracket can be identified with the operator $\mathcal{D}$. Hyperbolicity means that the field equations have the second derivatives of the form $G^{\mu\nu}\partial_\mu\partial_\nu$, with $G^{\mu\nu}$ an effective metric of signature $-+++$ (or $+---$)(its timelike direction, corresponding to the negative (or positive) eigenvalue, should be consistent with the standard time direction of $g^{\mu\nu}$). The spectral properties of the operator

$$D_\mu^\nu(p) \equiv (M_\mu^\nu)^{\alpha\beta}p_\alpha p_\beta \equiv \left[f' \times (\delta_\mu^\nu g^{\alpha\beta} - \delta_\mu^\alpha g^{\nu\beta}) + 4f''F^{\alpha\nu}F_\mu^\beta\right]p_\alpha p_\beta \tag{2.16}$$

One needs to diagonalize $(M_\mu^\nu)^{\alpha\beta}$ with respect to μ and ν indices, $(M_\mu^\nu)^{\alpha\beta} \to G_{(\mu=\nu)}^{\alpha\beta}\delta_\mu^\nu$ and then to study the sign of the eigenvalues of the $G^{\alpha\beta}$-matrices. The details of the calculation can be found in [21]. Here we report only the relevant results: diagonalization gives three times $G^{\alpha\beta} = f' \times g^{\alpha\beta}$ which correspond to an hyperbolic operator $f'\Box$ if and onfly if

$$f' > 0 \tag{2.17}$$

The fourth operator $G^{\alpha\beta} = f' \times g^{\alpha\beta} + 4f'' \times F^{\alpha\mu}F_\mu^\beta$ gives the following eigenvalues

$$f' + f''F_{\mu\nu}^2 \pm f''\sqrt{(F_{\mu\nu}^2)^2 + (F_{\mu\nu}\tilde{F}^{\mu\nu})^2} \tag{2.18}$$

where $\tilde{F}_{\mu\nu} = \frac{1}{2}\varepsilon_{\mu\nu\rho\sigma}F^{\rho\sigma}$, $\varepsilon_{\mu\nu\rho\sigma}$ being the totally antisymmetric Levi-Civita tensor such that $\varepsilon_{0123} = +1$. To have the simultaneous positivity of the eigenvalues it is necessary that

$$f' + f''F_{\mu\nu}^2 > |f''|\sqrt{(F_{\mu\nu}^2)^2 + (F_{\mu\nu}\tilde{F}^{\mu\nu})^2} \tag{2.19}$$

When $F_{\mu\nu}\tilde{F}^{\mu\nu} = 0$, i.e., when electric and magnetic fields are orthogonal, this inequality imposes both $f' > 0$ and $f' + f''F_{\mu\nu}^2 > 0$. So this means that these eigenvalues can be made negative by an appropriate choice of the relativistic invariants $F_{\mu\nu}^2$ and $F_{\mu\nu}\tilde{F}^{\mu\nu}$.

So, it is not so easy to find functions of the Maxwell Lagrangian that simultaneously have an Hamiltonian bounded by below and hyperbolic field equations. It seems that the only safe case is the standard Maxwell Langrangian that unfortunately is conformal invariant. [ii]

[ii] A function like $f(F^2) = kF^2 + 2\Lambda$ (where k and Λ are constants) where Λ is a cosmological constant could satisfy inequality 2.17 but no interesting anisotropic signatures can survive due to the cosmic no-hair theorem.

2.3 Possible Solutions: $f(\phi)F^2$ Model

As seen in Section 2.1 many vector inflationary models suffer from instability except for the models in which the inflaton is coupled with the gauge field and in the *gauge flation* model but this is disfavoured by CMB observations. In this section we want to describe one of the most interesting anisotropic model. This is a supergravity-inspired model, proposed by [5], where the Lagrangian recalls the bosonic one in supergravity

$$\mathcal{L} = \frac{1}{2}R - \frac{1}{2}(\partial\phi)^2 - V(\phi) - \frac{1}{4}I(\phi)^2 F_{\mu\nu}F^{\mu\nu}, \qquad (2.20)$$

$I(\phi)$ is the coupling function of the inflaton field to the $U(1)$ gauge field and, as we will see, its form depends on the kind of potential choosen for the inflaton. Its functional is determined as

$$I(\phi) = e^{2\int \frac{V}{V_\phi}d\phi} \qquad (2.21)$$

The effect of the backreaction of the vector field is not to destroy inflation and in [5] it is shown that the model admits an anisotropic inflationary attractor solution and this contrasts the dilution of the anisotropies due to the cosmic no-hair theorem. The coupling of the vector field to the inflaton produces an effective potential for the inflaton. In [5] the model has been studied in a Bianchi type I metric

$$ds^2 = -dt^2 + e^{2\alpha(t)}\left[e^{-4\sigma(t)}dx^2 + e^{2\sigma(t)}(dy^2 + dz^2)\right] \qquad (2.22)$$

where e^α represents an isotropic scale factor while σ the deviation from isotropy. The evolution equation for σ is the following

$$\ddot{\sigma} + 3\dot{\alpha}\dot{\sigma} - \frac{k^2}{3}I(\phi)^{-2}e^{-4\alpha-4\sigma} \qquad (2.23)$$

where k is a constant of integration. It is shown that in order to drive inflation the potential of the inflaton must be dominant and the anisotropy should be subdominant. Although the anisotropy is small it persist during inflation and an anistropic attractor is founded as show in Figure 2.1

In particular they also found a general result, true for a broad class of potentials, that put an upper limit on the amplitude of the anisotropy $\Sigma \equiv \dot{\sigma}$

$$\frac{\Sigma}{H} \lesssim \varepsilon \qquad (2.24)$$

and this is confirmed, in the case of a chaotic potential, by the Figure 2.2. This result is easily explained taking into account that the cosmic no hair theorem holds in the presence of the cosmological constant and that the deviation from the exact de Sitter expansion is characterized by the slow roll parameter. So the
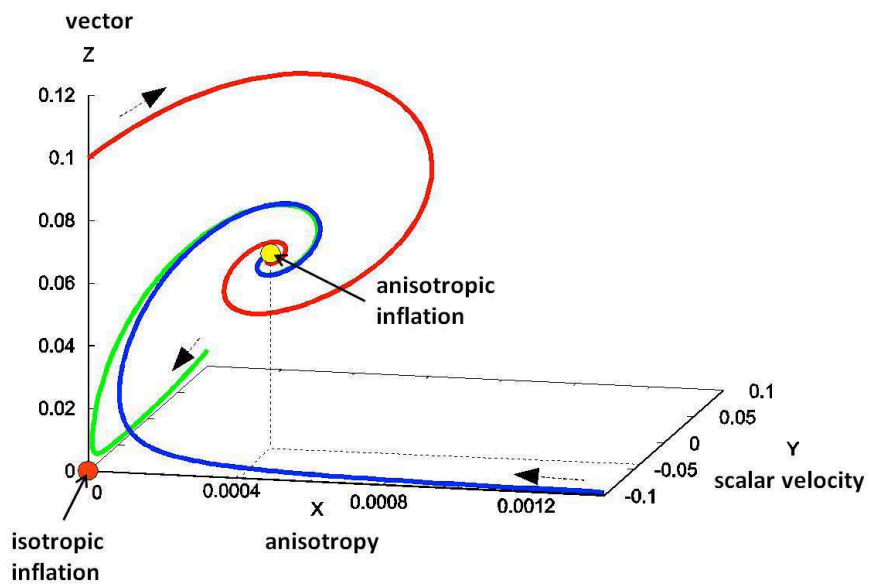
Figure 2.1: Phase space evolution that shows the convergence of the trajectories to the anisotropic fixed point [5].
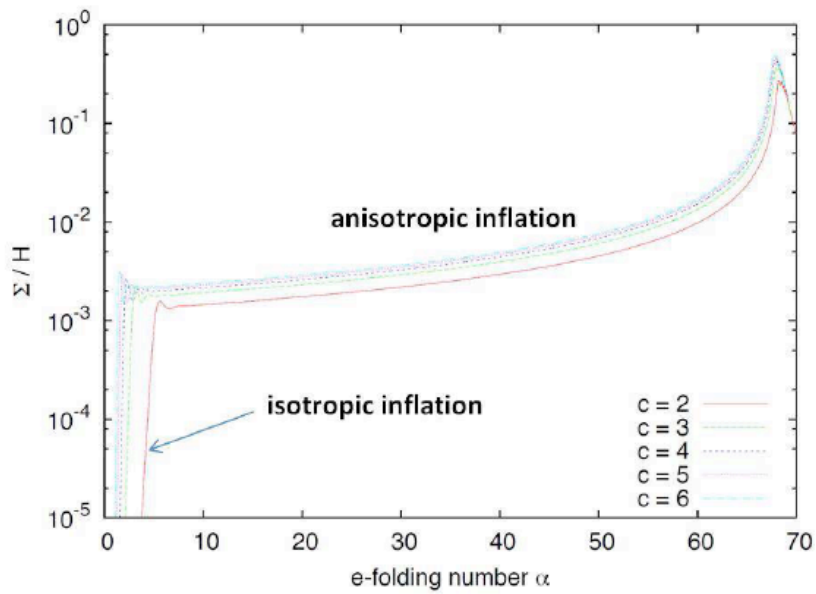
Figure 2.2: Anisotropy evolution with respect to the e-folding number [5].

deviation from the isotropic expansion must be proportional always to the same parameter.

From the point of view of connection with observations in [59] the model has been perturbed in an anisotropic space-time finding two sources of statistical anisotropy of fluctuations: the first coming from the anisotropic expansion itself and the second coming from the scalar-vector coupling. They have computed the power spectrum of the curvature perturbation and of the tensor mode finding an anisotropic contribution in both case. It is important to stress that the computation in an anisotropic space-time is very involved and as we will show in Chapter 3 not so necessary. An important feature for this kind of model is that the tensor perturbations can be induced from the curvature perturbations through the anisotropy of the background and, as a consequence, there is a mixing between curvature and tensor fluctuations that can give TB and EB mixing in the CMB data. Of course this is a very distinctive signature for this model that can be observed in the *Planck* analysis.

2.4 The Bianchi Universe

The direct consequence of having an anisotropic source that gives non-negligible contribution to the evolution of the universe is the choice of a background metric with the three spatial directions with different expansion rates. In this section we briefly describe this class of metrics that can account for homogeneous but anisotropic spacetimes: the Bianchi metrics. The Bianchi family are geometries with spatially homogeneous (constant t) surfaces which are invariant under the action of a three dimensional Lie group and can be foliated into the spatial homogeneous hypersurfaces Σ_t

$$M = \mathbb{R} \times \Sigma_t \qquad (2.25)$$

where $\mathbb{R}$ is the time variable. The Lie algebra is composed by the basis vector e_i (Killing vectors) that satisfy

$$[e_i, e_j] = C_{ij}^k e_k \qquad (2.26)$$

where C_{ij}^k are the structure constants. A Bianchi metric can be written as

$$ds^2 = -dt^2 + h_{ij}(t)e^i \otimes e^j, \qquad (2.27)$$

where $i, j = 1, 2, 3$ label the coordinates in homogeneous space-like hypersurfaces, h_{ij} represent the homogeneous spatial metric and e^i are one-forms dual to the basis e_i. The structure constants enter in the definition of the scalar curvature $^{(3)}R$

$$^{(3)}R = -C_{ij}^i C_{k}^{k\,j} + \frac{1}{2}C_{jk}^i C_i^{k\,j} - \frac{1}{4}C_{ijk}C^{ijk}, \qquad (2.28)$$

indicating that the structure constants of the algebra, define automatically the spatially homogeneous cosmological model.

So different algebras define different Bianchi models; in particular there are nine Bianchi models: Bianchi type I, that is a generalization of the flat FRW metric has an algebra where $C_{ij}^k = 0$, corresponding to a flat hypersurface. Meanwhile, Bianchi type IX corresponds to the $so(3)$ algebra with $^{(3)}R > 0$. It is important to underline that all the Bianchi metrics, except type IX, have a non-positive spatial scalar curvature [11]. This is important because is strictly related to the cosmic no-hair conjecture for which in any initial background, in presence of a positive cosmological constant, all the initial existing anisotropies are rapidly washed out. This conjecture was proven to be true for all of the Bianchi models except for the Bianchi-IX by Wald in [11]. For the Bianchi-IX this result is also true under the assumption that the cosmological constant overcomes the spatial curvature terms.

Tipically, in the study of anistropic models, Bianchi type I metric are assumed with the following form:

$$ds^2 = -dt^2 + a^2(t)dx^2 + b^2(t)(dy^2 + dz^2) \qquad (2.29)$$

where $a(t)$ and $b(t)$ are the two scale factors related to the two different direction (or rate) of expansion. This metric has been used in Chapter 4 for the analysis of the *Solid Inflation* model. A detailed study of perturbations in anisotropic space-time, like 2.29, has been conducted in [60, 10, 61].

3

THE ANISOTROPIC POWER SPECTRUM AND BISPECTRUM IN THE $I\left(\varphi\right)F^{2}$ MECHANISM

In this chapter I have mainly reported the results of our paper [62] in which we have analyzed a model where a suitable coupling between the inflaton and a gauge field can produce interesting features, like statistical anisotropy in the correlation functions and non-trivial angular dependence in the shape of the bispectrum providing distinctive signatures for this kind of models.

Contents

As introduced in Chapter 2 the first model free of instabilities is the one in which the inflaton is coupled to a $U(1)$ gauge field. In this Chapter we compute the power spectrum and the bispectrum of the cosmological curvature perturbations ζ for this model under the assumptions that

1. The dominant contribution to ζ is provided by a slowly rolling inflaton field

2. The inflaton is coupled to the kinetic term of a vector field so to produce a nearly scale invariant and frozen spectrum of vector perturbations at large scales.

These assumptions are realized in models of magnetogenesis and of statistical anisotropy of the cosmological perturbations. Despite the phenomenology of these models has been heavily studied in the literature, we obtain novel and general results, since, for the first time to our knowledge, we simultaneously take into account both the facts that (i) a strong contribution to the anisotropy (both in the power spectrum and in the bispectrum of ζ) results from the same coupling characterized in 2., and (ii) the inflationary expansion that took place before the Cosmic Microwave Background (CMB) modes left the horizon unavoidably results in a classical background vector field that is homogeneous from the point of view of the CMB modes, but breaks isotropy. Interest for models that can produce vector fields during inflation has been generated by the inference of intergalactic magnetic fields and by claims of broken statistical invariance of the CMB modes. Intergalactic magnetic fields have been inferred by an apparent lack of GeV scale $\gamma-$rays coming from blazars that produce TeV scale $\gamma-$rays; in standard models, part of the higher energy $\gamma-$rays should be converted in lower energy secondaries (which then generate the lower energy $\gamma-$rays) by their interaction with the inter galactic medium. The non-observation of the GeV scale $\gamma-$rays has been explained as intergalactic magnetic fields that deflect the secondaries [36].

Broken statistical isotropy of the CMB perturbations has instead been found in the studies [63, 64, 65] of the WMAP data. While the overall WMAP results [33] strongly support the inflationary paradigm, the above studies have shown that the statistics of the WMAP anisotropies does not possess full rotational invariance. Specifically, under the parametrization [8]

$$P_\zeta \left(\vec{k} \right) = P\left(k \right) \left[1 + g_* \cos^2 \theta_{\hat{k}, \hat{V}} \right] \tag{3.1}$$

(which can be thought of as an expansion series of the power spectrum in the limit of small anisotropy, truncated at the quadruple term) the WMAP data give $g_* = 0.29 \pm 0.031$ [65]. The "privileged" direction $\hat{V}$ lies very close to the ecliptic poles. This strongly suggests a systematical origin of the effect, and it

has been shown in [64, 66] that the instrument beam asymmetry can account for it. Fortunately, the Planck satellite will soon provide an independent test of this with an expected sensitivity to a quadrupolar anisotropy in the power spectrum as small as 0.5% at 1σ [67, 68]. On different scales (and marginalizing over the preferred direction $\hat{V}$) Large-Scale Structure data analysis constrain $-0.41 < g_* < 0.38$ at 95% C.L. [69] (the amplitude of the anisotropy may in general be scale dependent [8]).

Broken rotational invariance could be the result of anisotropic inflation [70]. It is however nontrivial to realize this, since anisotropic spaces typically rapidly isotropize in presence of a cosmological constant [11]. [i] Vector fields may in principle support the anisotropy. [ii] In this case, the problem of preserving the anisotropy translates into contrasting the quick decrease of the vector energy that takes place for a minimal $\mathcal{L}_A = -F^2/4$. To our knowledge, four distinct classes of models have been constructed to achieve this; the first three of them are characterized by (i) a vector potential $V\left(A^2\right)$ [17], (ii) a fixed vector vev due to a lagrange multiplier [8], and (iii) a vector coupling $A^2 R$ to the scalar curvature R [18, 19]. This last mechanism was originally employed for magnetogenesis in [42]. These three proposals break the U(1) symmetry of the minimal action, and lead to an additional degree of freedom, the longitudinal vector polarization, that in all of these models turns out to be a ghost [20, 22, 43]. [iii]

The fourth class is instead U(1) invariant and free of ghost instabilities. It is characterized by a function of a scalar inflaton φ multiplying the vector kinetic term,

$$\mathcal{L} = -\frac{I^2\left(\varphi\right)}{4} F_{\mu\nu} F^{\mu\nu} \qquad (3.2)$$

A suitably chosen evolution for $\langle I \rangle$ during inflation results in a (nearly) constant vector energy density, and therefore in a prolonged anisotropic expansion [5]. [iv] Also this mechanism was originally suggested for magnetogenesis [83] (this application is however problematic [38], as we discuss below). For anisotropic

---

[i]See [71] for the extension of the study of [11] to slow roll inflation

[ii]Vector fields can play a nontrivial role for the inflationary dynamics also in the isotropic case [72, 25, 73, 48].

[iii]Ref. [23] claims that some versions of the $A^2 R$ model may be healthy, arguing that the standard quantization may not apply for such models in the sub-horizon regime. We do not believe that this argument is correct; in writing the dispersion relation of a mode one customarily "accepts" the background evolution also in the sub-horizon regime; for instance, one writes that the physical momentum scales as $p = k/a$, where a is the scale factor coming from the metric. If we include $a \propto \mathrm{e}^{Ht}$ in the dispersion relation also in the sub-horizon regime, there is no reason why we should not include a term proportional to the curvature in this regime. We also point out that, even if the argument of [23] was correct, it would simply lead to the conclusion that we do not know how to quantize these models, and that all the phenomenological predictions that have been derived for them (which are based on the standard quantization in the sub-horizon regime) are invalid; there are essentially the conclusions of [20, 22, 43].

[iv]See [74, 75, 76, 50, 77] for models of anisotropic inflation that employ the idea of [5]. Also, an interesting model of vector curvaton [35] employing a varying mass m and kinetic function I has been proposed in [78] and studied in [79, 80, 81, 82]. This model also admits an attractor solution where I scales as in the model studied here. In particular, ref. [82] demonstrated that treating I and m as functions of a quantum inflaton field results in a different phenomenology than just treating them as classical external functions.

expansion, a homogeneous vector field pointing along a given direction corresponds to an "electric" component, and (3.2) enjoys an "electric" ↔ "magnetic" duality under $I^2 \leftrightarrow \frac{1}{I^2}$ [84]. A constant "electric" component is also produced through (3.2) in the mechanism of [44], in which the vector field is coupled to the waterfall field χ of hybrid inflation through a $\chi^2 A^2$ interaction. Due to this, the gauge field provides a contribution to the mass of χ, concurring to determine the moment at which inflation ends, and - thanks to this - contributing to the curvature perturbation. The waterfall field acts as the medium through which the anisotropy in A_μ is communicated to the inflation; however, as we shall see, the communication already occurs through the very same interaction (3.2) that supports the vector field. This unavoidable effect has not been accounted for neither in [44], nor in the related works [85, 86, 87, 88, 89].

The linearized theory of cosmological perturbations in the anisotropic inflationary model of [5] was worked out in [60, 90, 61, 91]. The classical equations of motion of the model admit an attractor solution, [5, 92] characterized by a non-vanishing "electric" component $\vec{E}^{(0)}$. A 10% level anisotropy ($|g_*| = \mathrm{O}\,(0.1)$) is found for an energy $|\vec{E}^{(0)}|^2/2$ which is about eight orders of magnitude smaller than the inflaton potential [90, 61, 91]. Therefore, the vector energy needs to be highly subdominant not too produce a too strong anisotropy. The work [93] computed instead the cosmological perturbations in the case in which (3.2) provides scale invariant "magnetic" components of the vector field, as in the magnetogenesis application [83, 94]. Cosmological applications in this context have also been studied in [95, 96, 39, 97, 51, 98, 99, 100]. Studies of the cosmological perturbations in [83, 94] start from the point of view that the statistics of the generated "magnetic" field is isotropic, and therefore obtain statistical isotropic results. In shorts, in the magnetogenesis context [83, 94] one does not have the analogous of the attractor solution $\vec{E}^{(0)}$ of the classical equations of motion of the anisotropic inflationary model [5] (the corresponding $\vec{B}^{(0)}$ vanishes in [83, 94]) and therefore it is simply assumed that $g_* = 0$ in this case.

However, in [5, 44] (respectively, in [83, 94]), the CMB perturbations are affected by a classical "electric" field $\vec{E}_{\mathrm{classical}}$ (respectively, classical "magnetic" field $\vec{B}_{\mathrm{classical}}$) which is in general different from the value given by the classical equations of motion. Indeed, such mechanisms are designed to result in a nearly scale invariant spectrum for the "electric" (respectively, "magnetic") perturbations. Let us denote by N_{tot} the number of e-folds of inflation. The modes that left the horizon in the first $N_{\mathrm{tot}} - N$ e-folds of inflation add up as a classical background from the point of view of the modes that leave the horizon in the final N e-folds. This is well appreciated for scalar fields during inflation [101]. The modes that leave the horizon add up in a "random walk" manner to form a classical background that is experienced as homogeneous by modes of smaller size. A homogeneous classical vector is a field that points in a given direction (that, in a given realization of the model, is determined by the random addition of the super-horizon modes) that breaks isotropy. In the magnetogenesis application, the effects of this energy $\langle \vec{B}^2 \rangle/2$ on the background evolution have

been well appreciated (see, among others, [38, 102, 103]). We point out that this energy is associated with a classical vector field, and in this work we show that this vector imprints a strong anisotropy to the power spectrum and bispectrum of ζ in all the applications of (3.2).

Specifically, we show that the natural value of g_* associated to these modes is ~ 0.1 (respectively, ~ 0.01), if inflation lasted about 50 e-folds (respectively, about 5 e-folds) more than the final ~ 60 e-folds necessary to generate the CMB modes. Generic models of slow roll inflation are characterized by a much longer duration of inflation, and, therefore, embedding the mechanism (3.2) in one of these models generically results in too anisotropic perturbations. For a tuned duration of inflation the mechanism becomes extremely predictive since, there is essentially no free parameter in (3.2). The only relevant quantity is the magnitude of the classical vector field present when the CMB modes left the horizon, and that can be "traded" for g_*. Therefore, any given value of g_* should be associated with firm predictions for other observables.

There are two such predictions that immediately come to mind: the first is a TB and an EB mixing in the CMB data [9], resulting from the coupling between scalar and tensor modes that, due to the anisotropy, takes place already in the linearized theory [70, 104, 10, 105]. The second is a directionality dependence in the bispectrum (and, in principle, in the higher point correlation functions), with a clear correlation with the one in the power spectrum. The bispectrum resulting from (3.2) is computed for the first time in the present work. [v] We show that the isotropic power spectrum and bispectrum of [93] are in fact the theoretical expectation (i.e., the theoretical average over several realizations) for the anisotropic signals that we obtain here, and which are the real quantities that are produced by any single realization of (3.2). Quite interestingly, an observable g_* produced from (3.2) is associated to an observable bispectrum which is enhanced like the local one in the squeezed limit, and which has a characteristic shape and anisotropy (immediately correlated with the one in the power spectrum).

The chapter is organized as follows. In Section 3.2 we study the spectrum of the vector field perturbations obtained from (3.2), with a particular attention for the functions I that result in scale invariant vector modes. In this section we also further discuss the role of the large-wavelength modes in determining the classical background anisotropy that affects modes of CMB wavelengths. In Section 3.3 we study how these modes δA are coupled to the modes of ζ through (3.2). The power spectrum and bispectrum of ζ are computed respectively in Sections 3.4 and 3.5. There, we show explicitly how the sum of the long-wavelength modes adds up with the solution of the classical equations of motion to determine the physical value of $\vec{E}_{\text{classical}}$ (or $\vec{B}_{\text{classical}}$) observed by the CMB modes. The resulting phenomenology is reviewed in Section 3.6. In Section 3.7 we discuss our results, that generally apply to all the realizations of (3.2) that give a nearly scale invariant vector field, in the context of anisotropic inflation [5], of the waterfall

---

[v] For previous works on anisotropic non-gaussianity, see [44, 106, 85, 107, 108, 109, 86, 110, 111, 88, 112, 89].

43

mechanism [44], and of magnetogenesis [83, 94]. A concluding discussion is given in Section 4.6.

3.2 A scale invariant vector field

Let us consider a locally U(1) invariant vector field with lagrangian (3.2). Ref. [83] identified this field with the electromagnetic one, assuming that I sets to a constant after inflation (in this case, we can simply normalize $I_{\text{end}} = 1$). The function I enters in the definition of the electric and magnetic components

$$E_i = -\frac{\langle I \rangle}{a^2} A_i' \ , \ \ B_i = \frac{\langle I \rangle}{a^2} \varepsilon_{ijk} \partial_j A_k \tag{3.3}$$

(we denote by $\langle \dots \rangle$ the vacuum expectation value of a field, or of a function), where prime denotes derivative with respect to conformal time τ, and a is the scale factor of the universe, $ds^2 = a^2(\tau)(-d\tau^2 + d\vec{x}^2)$. With the notation (3.3), the physical energy density in the vector field assumes the conventional expression $\rho = \frac{|\vec{E}|^2 + |\vec{B}|^2}{2}$ at all times. In this work, apart from where we explicitly refer to the magnetogenesis application [83] , we do not necessarily identify the vector field with our photon, but we keep the "electromagnetic" notation (3.3) for convenience. The classical equations of motion obtained from (3.2) are solved by a homogeneous "electric" field $\vec{E}^{(0)} \propto \frac{1}{a^2 \langle I \rangle}$. While the standard case, $I = \text{const}$, corresponds to $\rho_E \propto a^{-4}$, a constant "electric" energy is obtained if $\langle I \rangle \propto a^{-2}$.

A desired time evolution for $\langle I \rangle$ can be obtained for several functions $I(\varphi)$, provided they are suitably arranged with the inflaton potential [94]. Indeed,

$$a \propto \exp\left[-\int \frac{d\varphi}{\sqrt{2\varepsilon(\varphi)}M_p} \right] \tag{3.4}$$

where we have introduced the slow roll parameter

$$\varepsilon \equiv \frac{M_p^2}{2} \left(\frac{V'}{V} \right)^2 \tag{3.5}$$

(prime on a function here denotes derivative with respect to its argument) and where a monotonic slow roll inflaton evolution with $\dot{\varphi} < 0$ is assumed. Therefore, a desired behavior $\langle I \rangle = f(a)$ can be obtained by choosing the functional form of I to coincide with that function f of the right hand side of (3.4):

$$I = I_0 \exp\left[-\int \frac{n \, d\varphi}{\sqrt{2\varepsilon(\varphi)}M_p} \right] \ \ \Rightarrow \ \ \langle I \rangle \propto a^n \tag{3.6}$$

where I_0 can be chosen so that $I = 1$ after inflation. As a concrete example, the choice

$$V = \frac{1}{2} m^2 \varphi^2 \ , \ \ I = e^{\frac{c \varphi^2}{2M_p^2}} \tag{3.7}$$

results in $\langle I \rangle \propto a^{-2c}$. We thus see that a constant $\vec{E}^{(0)}$ is achieved for $c = 1$. Many other choices of V and I are clearly possible, provided that their functional forms are related to each other to produce through (3.4) the desired time dependence for $\langle I \rangle$ [94].

3.2.1   Production of vector fluctuations from the $I^2 F^2$ term

---

It is well known that, for $I = 1$, the vector field is conformally coupled to a FRW background, and so its fluctuations are not excited by the expansion of the universe. On the contrary, as we now review, the choice $\langle I \rangle \propto a^{-2}$ that allows for a constant $\vec{E}^{(0)}$ solution, also excites the vector fluctuations to produce a classical and scale invariant spectrum of "electric" fluctuations at large scales.

We quantize the vector field in the Coulomb gauge $A_0 = 0$

$$
\begin{aligned}
\vec{A} &= \vec{A}^{(0)} + \sum_{\lambda = \pm} \int \frac{d^3 k}{(2\pi)^{3/2}} \, \mathrm{e}^{i\vec{k}\vec{x}} \, \vec{\varepsilon}_\lambda \left(\vec{k}\right) \frac{\hat{V}_\lambda}{\langle I \rangle} \\
\hat{V} &\equiv a_\lambda \left(\vec{k}\right) V_\lambda (k) + a_\lambda^\dagger \left(-\vec{k}\right) V_\lambda^* (k)
\end{aligned}
\tag{3.8}
$$

where $\vec{\varepsilon}_\lambda$ are circular polarization vectors satisfying the relations $\vec{k} \cdot \vec{\varepsilon}_\pm \left(\vec{k}\right) = 0$, $\vec{k} \times \vec{\varepsilon}_\pm \left(\vec{k}\right) = \mp i k \vec{\varepsilon}_\pm \left(\vec{k}\right)$, $\vec{\varepsilon}_\pm \left(-\vec{k}\right) = \vec{\varepsilon}_\pm \left(\vec{k}\right)^*$, and normalized according to $\vec{\varepsilon}_\lambda \left(\vec{k}\right)^* \cdot \vec{\varepsilon}_{\lambda'} \left(\vec{k}\right) = \delta_{\lambda\lambda'}$. The annihilation / creation operators satisfy $\left[a_\lambda \left(\vec{k}\right), a_{\lambda'}^\dagger \left(\vec{k}'\right) \right] = \delta_{\lambda\lambda'} \, \delta^{(3)} \left(\vec{k} - \vec{k}'\right)$.

The mode functions satisfy the evolution equation

$$
V_\lambda'' + \left(k^2 - \frac{\langle I \rangle''}{\langle I \rangle} \right) V_\lambda = 0
\tag{3.9}
$$

where prime denotes derivative with respect to conformal time τ. For $\langle I \rangle \propto a^{-2} \propto \tau^2$ (we disregard slow roll corrections, so that $a = -\frac{1}{H\tau}$), the properly normalized vector modes are

$$
V_\lambda \simeq \frac{1 + ik\tau}{\sqrt{2} k^{3/2} \, \tau} \, \mathrm{e}^{-ik\tau}
\tag{3.10}
$$

We Fourier transform the "electric" and "magnetic" fields (3.3)

$$
\begin{aligned}
\vec{E} &= \vec{E}^{(0)} + \int \frac{d^3 k}{(2\pi)^{3/2}} \, \mathrm{e}^{i\vec{k}\vec{x}} \, \delta\vec{E} \left(\vec{k}\right) \\
\vec{B} &= \int \frac{d^3 k}{(2\pi)^{3/2}} \, \mathrm{e}^{i\vec{k}\vec{x}} \, \delta\vec{B} \left(\vec{k}\right)
\end{aligned}
\tag{3.11}
$$

Inserting the solutions (3.10) in (3.3) we see that the "electric" and "magnetic"

fields become classical (commuting) fields at super-horizon scales

$$\delta \vec{E}\left(\vec{k}\right) = \sum_\lambda \mathcal{E}_k \, \vec{\varepsilon}_\lambda\left(\vec{k}\right) \left[a_\lambda\left(\vec{k}\right) + a_\lambda^\dagger\left(-\vec{k}\right)\right]$$

$$\delta \vec{B}\left(\vec{k}\right) = \sum_\lambda \mathcal{B}_k \, \lambda \vec{\varepsilon}_\lambda\left(\vec{k}\right) \left[a_\lambda\left(\vec{k}\right) + a_\lambda^\dagger\left(-\vec{k}\right)\right]$$

$$\mathcal{E}_k \simeq \frac{3H^2}{\sqrt{2}k^{3/2}} \; , \; \mathcal{B}_k \simeq \frac{H^2\tau}{\sqrt{2}k^{1/2}} \; , \; -k\tau \ll 1 \qquad (3.12)$$

Namely, the "electric" field fluctuations are nearly constant outside the horizon, while the "magnetic" field fluctuations rapidly decrease. As we mentioned, the electric field fluctuations are scale invariant (slow roll corrections will slightly tilt their spectrum; however, we disregard slow roll corrections in this work whenever compared with a non-vanishing expression at $0-$th order in slow roll).

Finally, we note that this mechanism enjoys a duality symmetry $\langle I \rangle \leftrightarrow \frac{1}{\langle I \rangle}$. Under this exchange, the "electric" and "magnetic" modes interchange their role, $\left|\delta\vec{E}\right|^2 \leftrightarrow \left|\delta\vec{B}\right|^2$. The original mechanism [83] aims to produce fluctuations with scale invariant magnetic energy, and therefore has $\langle I \rangle \propto a^2$ during inflation. This corresponds to choosing $c = -1$ in the example (3.7). For definiteness, our explicit computations are done for $\langle I \rangle \propto a^{-2}$. However, our results can be readily extended to the context of [83] by exploiting this duality.

3.2.2   Classical anisotropy when the CMB modes leave the horizon

We denote by $\vec{E}^{(0)}$ the "electric" field obtained from solving the classical equations of motion of a given model. For instance, as we discuss in Subsection 3.7.1, the classical equations of motion of the anisotropic inflationary model [5], characterized by $c \simeq 1$ in (3.7), admit an attractor solution with a nearly constant $\vec{E}^{(0)}$.

We denote by $\vec{E}_{\text{classical}}$ the classical and homogeneous electric field measured by a local observer at some time τ during inflation. We can assume that at the initial time of inflation τ_{in} no classical fluctuations are present, so that $\vec{E}_{\text{classical}} = \vec{E}^{(0)}$ at τ_{in}. However, this identification is no longer exactly true at any later time. Indeed, at the time $\tau > \tau_{\text{in}}$ during inflation

$$\vec{E}_{\text{classical}} = \vec{E}^{(0)} + \vec{E}^{\text{IR}} \qquad (3.13)$$

where the second quantity (IR = "infra-red") denotes the sum of all the modes $\delta\vec{E}_k$ that left the horizon between the times τ_{in} and τ. These modes have become classical and are homogeneous from the point of view of a local observer present at τ. The same considerations apply to the "magnetic" component of the vector field. For any single realization of the mechanism (3.2) with $\langle I \rangle \propto a^{-2}$, the quantities $\vec{E}^{\text{IR}}$ and $\vec{B}^{\text{IR}}$ are drawn by, respectively, a gaussian (to very good

approximation) statistics, with vanishing mean and with variance

$$
\begin{aligned}
\sigma^2_{\vec{E}^{\mathrm{IR}}, N} &= \langle \delta \vec{E}(\vec{x})^2 \rangle = \frac{1}{\pi^2} \int_{\mathrm{IR}} dk\, k^2 |\mathcal{E}_k|^2 \simeq \frac{9H^4}{2\pi^2} \int_{\mathrm{IR}} \frac{dk}{k} \\
&= \frac{9H^4}{2\pi^2} N \\
\sigma^2_{\vec{B}^{\mathrm{IR}}} &= \cdots = \frac{3H^4}{8\pi^2}
\end{aligned}
\tag{3.14}
$$

where the IR modes are those characterized by momentum k in the interval $\frac{1}{-\tau_{\mathrm{in}}} < k < \frac{1}{-\tau}$, and where N is the number of e-folds of inflation from τ_{in} and τ.

These quantities are the natural expectation for the energy that gets progressively stored in the "electromagnetic" field during inflation

$$
\rho_{\delta E, N} = \frac{\langle \delta \vec{E}(\vec{x})^2 \rangle}{2} \simeq \frac{9H^4}{4\pi^2} N \quad , \quad \rho_B \ll \rho_{\delta E}
\tag{3.15}
$$

This has been well appreciated in the magnetogenesis applications of this mechanism (we remark that the role of the "electric" and "magnetic" energy is interchanged for $\langle I \rangle \leftrightarrow \frac{1}{\langle I \rangle}$). For example, ref. [38] computed the energy density accumulated in these super-horizon modes for all possible values of n in the $\langle I \rangle \propto a^n$ dependence. For $|n| > 2$, this energy density grows as $a^{4(|n/2|-1)}$ (while $n = \pm 2$ results in $\rho \propto \ln a = N$, as we have seen), until the backreaction of this energy is no longer negligible. Ref. [102] studied the regime of strong backreaction that takes place for $n > 2$. Ref. [103] studied magnetogenesis for a more general time dependence of I, imposing as one of the conditions that the energy density in the classical super-horizon modes remains less than that of the inflaton.

We obtain a first limit on the total duration of inflation N_{tot} by imposing that $\vec{E}^{\mathrm{IR}}$ has a negligible effect on the background evolution. The strongest backreaction constraint does not actually come from $\rho_{\delta E} \ll V$, but rather from the evolution equation of the inflaton (loosely speaking, it is "easier" for the vector field to affect the motion of the inflaton, that is slowly rolling on a flat potential, than the expansion rate). The corresponding condition is $\rho_{\delta E} \ll 2\,\varepsilon\, H^2\, M_p^2$, and it is satisfied for $N_{\mathrm{tot}} \ll \mathrm{O}\left(10^7\right)$ [93].

The variances of the three components of $\vec{E}^{\mathrm{IR}}$ are equal to each other, [vi] and equal to 1/3 of the value given in (3.14). This, however, does not mean that in a given realization the super-horizon modes add up to equal amounts in all three directions. Indeed, the difference between different directions is drawn from the

---

[vi] Actually, one can obtain a small difference proportional to the small difference ΔH in the expansion rates of the different directions. As we well see, $\Delta H / H$ needs to be $\lesssim 10^{-8}$, and therefore this difference is completely negligible for the present discussion.

statistics

$$\left\langle \delta E_x^2 - \delta E_y^2 \right\rangle = 0$$

$$\sqrt{\left\langle \left(\delta E_x^2 - \delta E_y^2 \right)^2 \right\rangle} = 2 \left\langle \delta E_x^2 \right\rangle = \frac{4}{3} \rho_{\delta E, N} \tag{3.16}$$

Therefore, $\rho_{\delta E}$ is also the typical amount of the classical anisotropy provided by the IR modes. This is not surprising since, in any given realization, $\vec{E}^{\mathrm{IR}}$ is a classical vector that points in some given direction.

Only for $|\vec{E}^{(0)}| \gg |\vec{E}^{\mathrm{IR}}|$, or, equivalently, for $\rho_{E^{(0)}} \gg \rho_{\delta_E}$, the classical electric field measured by the observer is (deterministically) given by the solution of the classical equations of motion. If this is not the case, one should conclude that the solution of the classical equations of motion is unstable under quantum corrections, and one should expect large corrections to the predictions made if only $|\vec{E}^{(0)}|$ is considered.[vii] In our computations below, both the contributions to $\vec{E}_{\mathrm{classical}}$ will be accounted for (as we will see, this amounts in considering loop contributions to the power spectrum and the anisotropic spectrum of the cosmological perturbations).

3.3 Anisotropic source of the Cosmological Perturbations

As we have discussed in length in the previous Section, for the mechanism we are studing the cosmological perturbations that we observed experienced a classical homogeneous vector field (3.13) when they left the horizon. This breaks the background isotropy, and, strictly speaking, the local patch where these modes live has a Bianchi-I geometry with residual 2d isotropy

$$ds^2 = -dt^2 + a^2(t)\, dx^2 + b^2(t) \left[dy^2 + dz^2 \right] \tag{3.17}$$

where for the definiteness the $x-$axis has been oriented along $\vec{E}_{\mathrm{classical}}$.
To characterize the anisotropy, we define

$$\frac{\Delta H}{H} \equiv \frac{3\,(H_y - H_x)}{H_x + H_y + H_z} \tag{3.18}$$

This nearly corresponds to the mechanism of anisotropic inflation of [5], where the model (3.7) has been employed, and where it is shown that the classical equations of the model admit an anisotropic solution with $\frac{\Delta H}{H} \simeq (c-1)\,\varepsilon$. In [5], and in the successive works [60, 90, 61, 91] that study the linearized perturbations of this model, it is assumed that $\vec{E}_{\mathrm{classical}} = \vec{E}^{(0)}$, while, as we have discussed, these two quantities are in general different. Therefore, this model leads to

---

[vii]Before eq. (3.13), we set $\vec{E}_{\mathrm{classical}} = \vec{E}^{(0)}$ at the start of inflation. We note that if this is not the case the departure of the classical electric field from the solution of the classical equation of motion will in general be even greater.

anisotropic inflation even for $c = 1$. Given this strong correspondence, our study has several relations with [5], and for example we will show that our results for the power spectrum coincides with that of [90, 61, 91], once the value of $\vec{E}^{(0)}$ used there is replaced by the full $\vec{E}_{\text{classical}}$ (for the bispectrum instead, our result is completely new, since the perturbations of [5] have been so far studied only at the linearized level).

In the studies [60, 90, 61, 91], the perturbations are separated according to how they transform under an SO(2) rotation in the symmetry plane orthogonal to the vector vev, as originally done in [70, 10]. This simplifies the problem, as modes that transform differently are not coupled to each other at the linearized level. Still, the non-FRW background results in a very involved computation, once the perturbations of all the fields (metric included) are taken into account. In particular, the anisotropy does not increase the number of physical modes, but results in couplings between these modes that would be absent in the FRW case [70, 10]. The main result of [90, 61, 91], which is somewhat surprising a-priori, is that an anisotropic parameter $g_* = \mathcal{O}(0.1)$ is obtained for a $\frac{\Delta H}{H} = \mathcal{O}(10^{-8})$ background anisotropy. Motivated by this result, one can instead use a different approach, and perform the standard quantization of the cosmological perturbations on a FRW background, ignoring at zeroth order the couplings between the different modes. Such couplings can be taken into account as perturbative mass insertions in the in-in formalism. This is effectively the procedure adopted in [90, 91] when they solve analytically the linearized theory. Moreover ref. [91] showed that the dominant operator that determines g_* in this perturbative evaluation is the $\delta\varphi - \delta A_\mu$ coupling obtained from expanding the vector kinetic term, and with no contribution from the metric perturbations. This analytic approximated result is in excellent agreement [91] with the one obtained from an exact numerical evolution of g_* (in which the full quadratic action of all the 2d scalar modes is retained). Moreover, the analytical and numerical results of [91] agree with those of [90] and [61], respectively.

We use the same computational scheme for the bispectrum computation. Specifically, we disregard metric perturbations, and we use in the in-in formalism the $0th$ order eigenmodes obtained from the approximate FRW quantization. The bispectrum is produced by interactions, and we know that for slow roll FRW inflation the interactions of the metric perturbations produce an unobservable bispectrum. We will see instead that the interaction between the vector and the scalar field, which is encoded in the vector kinetic term, results in a larger, and potentially observable, signal. Ref. [93] proved this explicitly for the case of $\vec{E}_{\text{classical}} = 0$, by solving the second order equation for the curvature perturbation in spatially flat gauge $\zeta = -\frac{\mathcal{H}}{\varphi'}\delta\varphi$ (we recall that prime denotes derivative with respect to conformal time τ, while $\mathcal{H} = \frac{a'}{a}$). It was shown in [93] that the contribution from the direct vector-scalar interaction is slow-roll enhanced with respect to that coming from the interactions of the metric. There is no reason to expect that the relative strength of the effects should change for a $\mathrm{O}(10^{-8})$

background anisotropy. [viii]

Therefore we retain the FRW quantization of the vector field performed in the previous Section. The remaining perturbations (of the scalar field and of the metric) are also quantized as in the standard FRW case. We then expand the vector kinetic term into δA and $\delta\varphi$. We use the resulting interactions to determine the dominant anisotropic contribution to the power spectrum of ζ and the dominant contribution to the bispectrum.

Therefore, all the dominant effects arise from expanding the only interaction term between the inflaton and the vector field,

$$\Delta\mathcal{L} = \frac{-a^4}{4}\left(\langle\frac{\delta I^2}{\delta\varphi}\rangle\delta\varphi + \frac{1}{2}\langle\frac{\delta^2 I^2}{\delta\varphi^2}\rangle\delta\varphi^2 + \dots\right)(\langle F_{\mu\nu}\rangle + \delta F^{\mu\nu})^2$$

(3.19)

In spatially flat gauge, $\delta\varphi = -\frac{\varphi'}{\mathcal{H}}\zeta = \sqrt{2\varepsilon}\,M_p\zeta$. We note that, in principle, ζ has additional contributions proportional to the perturbations of the vector field. Ref. [93] showed that these contributions are completely subdominant in the case of $\vec{E}_{\text{classical}} = 0$. We believe that it is very natural to assume that this continues to be the case also in the current context. Indeed, as we shall see, $\frac{\rho_E}{\rho_\varphi}$ needs to be $\lesssim \mathrm{O}\left(10^{-8}\right)$ during inflation or otherwise the power spectrum is too anisotropic. This ratio further decreases between the end of inflation and the inflaton decay, when the inflation field performs coherent oscillations, so that $\rho_\varphi \propto a^{-3}$, while the vector kinetic term becomes standard, and $\rho_E \propto a^{-4}$. If this is the case,

$$\frac{a_{\text{end infl}}}{a_{\text{reh}}} \simeq 10^{-10}\left(\frac{T_{\text{reh}}}{10^9\,\text{GeV}}\right)^{4/3}\left(\frac{10^{15}\,\text{GeV}}{H_{\text{end infl}}}\right)^{2/3}$$

(3.20)

where T_{reh} and a_{reh} are, respectively, the temperature of the inflation decay products and the scale factor at the inflaton decay. We see that it is therefore natural to disregard ρ_E and $\delta\rho_E$ at reheating. In this way, the only relevant contribution of δA to the final curvature perturbation is the modification of $\delta\varphi$ induced by the vector-inflaton coupling (which is precisely the effect that we are computing). We note that this assumption is also made in [90, 61, 91] when they give the power spectrum of ζ in the model [5].

Using the expression (3.6), we have, for the first two terms in the expansion of

---

[viii]We note that metric perturbations are also disregarded in the computations [44, 85, 86, 87, 88, 89] of the anisotropic bispectrum through the waterfall mechanism.

I^2,

$$\left\langle \frac{\partial I^2}{\partial \varphi} \right\rangle \delta\varphi \;=\; -2n \left\langle \frac{I^2}{\sqrt{2\varepsilon}M_p} \right\rangle \delta\varphi = -2n \left\langle I^2 \right\rangle \zeta$$

$$\frac{1}{2} \left\langle \frac{\partial^2 I^2}{\partial \varphi^2} \right\rangle \delta\varphi^2 \;=\; \left\langle \left[\frac{n^2}{\varepsilon M_p^2} - \frac{n}{M_p^2} \left(1 - \frac{\eta}{2\varepsilon} \right) \right] I^2 \right\rangle \delta\varphi^2$$

$$\simeq 2n^2 \left\langle I^2 \right\rangle \zeta^2 \qquad\qquad (3.21)$$

where $\eta = M_p^2 \frac{V''}{V}$ is a slow roll parameter, and where in the final approximation we retained only the dominant term in slow roll approximation.

We inserted these expressions in (3.19), taking $n = -2$ (which corresponds to a constant "electric" field). We expanded also the vector part as in (3.8), and we computed the contributions to the power spectrum and the bispectrum combining the resulting vertices. We verified that the leading diagrams do not contain interactions coming from the second order term $\frac{\delta^2 I^2}{\delta\varphi^2}$ (if this was not the case, we should worry about the convergence of the $I\left[\langle\varphi\rangle + \delta\varphi\right]$ expansion). Therefore we have the two dominant $\propto \delta\varphi A^{(0)} \delta A$ and $\propto \delta\varphi \delta A^2$ interactions [ix]

$$\mathcal{L}_{\text{int}} \;\supset\; a^4 \left[4E_x^{(0)} \delta E_x \zeta + 2\, \delta\vec{E} \cdot \delta\vec{E}\, \zeta \right]$$

$$\equiv\; \mathcal{L}_{\text{int},1} + \mathcal{L}_{\text{int},2} \qquad\qquad (3.22)$$

We note that the vector field enters in the quadratic term $\mathcal{L}_{\text{int},1}$ only in the combination $\propto 2\langle E_x\rangle \delta E_x \subset \vec{E}^2 - \vec{B}^2 \propto F_{\mu\nu}F^{\mu\nu}$. We also note that the cubic term $\mathcal{L}_{\text{int},2}$ should also have the term $-2a^4\delta\vec{B}\cdot\delta\vec{B}\,\zeta$; this term however gives a subdominant contribution to ζ with respect to contribution from the "electric" components, since the "electric" modes are much greater than the "magnetic" ones at super-horizon scales - see eq. (3.12) - which is where they provide the greatest contribution to ζ (as discussed in [93] and below).

We stress that, although in this Section we have often mentioned the anisotropic inflationary model [5], this interaction lagrangian applies to all models that verify the two assumptions spelled out at the beginning of the introduction. We actually see that the precise functional forms of I and V do not enter in (3.22), apart from the fact that the relation (3.6) has been imposed, with $n = -2$. Identical results would be obtained for $n = 2$, exploiting the "electric" – "magnetic" duality of the mechanism. We recall that $n = \pm 2$ precisely correspond to enforcing the assumption 2. made at the beginning of the Introduction. For the choice (3.7), one has $n = -2c$. However, we stress that (3.22) is valid independently of this choice.

The interaction lagrangian (3.22) enters in the $n-$point correlation functions

---

[ix]When we perform the expansion, linear terms in the perturbations are removed by the background equations of motion; we commit a mistake by disregarding the effect of the gauge field vev in the background evolution, but, as we remarked, we work in a regime where this effect is negligible.
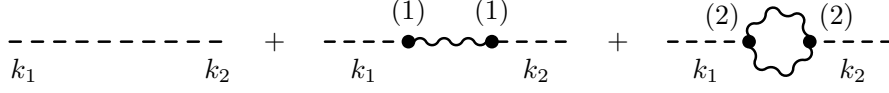
Figure 3.1: Leading diagrams for $\langle \zeta^2 \rangle$, with the vertices labelled as in (3.26).

through the in-in formalism relation

$$
\left\langle \hat{\zeta}_{\vec{k}_1} \hat{\zeta}_{\vec{k}_2} \ldots \hat{\zeta}_{\vec{k}_n} (\tau) \right\rangle = \sum_{N=0}^{\infty} (-i)^N \int^{\tau} d\tau_1 \ldots \int^{\tau_{N-1}} d\tau_N
$$
$$
\left\langle \left[\left[\ldots \left[\hat{\zeta}_{\vec{k}_1}^{(0)} \hat{\zeta}_{\vec{k}_2}^{(0)} \ldots \hat{\zeta}_{\vec{k}_n}^{(0)} (\tau), \ H_{\text{int}}(\tau_1) \right], \ldots \right], \ H_{\text{int}}(\tau_N) \right] \right\rangle
$$

(3.23)

where in our computational schemes the quantity $\hat{\zeta}_{\vec{k}}^{(0)}$ is the Fourier transform of the (unperturbed) FRW quantized field

$$
\zeta^{(0)} = \int \frac{d^3 k}{(2\pi)^{3/2}} e^{i\vec{k}\cdot\vec{x}} \hat{\zeta}_{\vec{k}}^{(0)} \quad , \quad \hat{\zeta}_{\vec{k}}^{(0)} \equiv \zeta_{\vec{k}}^{(0)} a_{\vec{k}} + \zeta_{\vec{k}}^{(0)*} a_{-\vec{k}}^{\dagger}
$$

(3.24)

At leading order in slow roll, we have

$$
\zeta_k^{(0)}(\tau) \simeq \frac{H(1 + i k \tau)}{2\sqrt{\varepsilon} M_p k^{3/2}} e^{-ik\tau}
$$

(3.25)

The unperturbed fields are also employed in the interaction hamiltonian $H_{\text{int}}(\tau) = -\int d^3x \, \mathcal{L}_{\text{int}}(\tau, \vec{x})$. The two terms in (3.22) give, respectively, rise to the two terms

$$
H_{\text{int},1}(\tau) = -\frac{4 E_x^{(0)}}{H^4 \tau^4} \int d^3k \, \delta E_x \left(\tau, \vec{k} \right) \hat{\zeta}_{-\vec{k}}^{(0)}(\tau)
$$
$$
H_{\text{int},2}(\tau) = -\frac{2}{H^4 \tau^4} \int \frac{d^3k d^3p}{(2\pi)^{3/2}} \delta\vec{E}\left(\tau, \vec{k} \right) \cdot \delta\vec{E}(\tau, \vec{p}) \, \hat{\zeta}_{-\vec{k}-\vec{p}}^{(0)}(\tau)
$$

(3.26)

Once inserted into (4.45), the two interaction terms give rise to the leading contributions to the power spectrum and bispectrum described by the diagrams shown, respectively, in Figures (4.2) and (3.2). These quantities are computed in the following Section.

3.4   Anisotropic power spectrum

The total power spectrum $P_\zeta \left(\vec{k} \right)$ is related to the full two-point correlation function (4.45) by

$$\left\langle \hat{\zeta}_{\vec{k}_1} \hat{\zeta}_{\vec{k}_2} \right\rangle = 2\pi^2 \frac{\delta^{(3)} \left(\vec{k}_1 + \vec{k}_2 \right)}{k_1^3} P_\zeta \left(\vec{k}_1 \right) \tag{3.27}$$

We denote the contributions of the first and of the last two diagrams in Figure 4.2 as, respectively,

$$\left\langle \hat{\zeta}_{\vec{k}_1} \hat{\zeta}_{\vec{k}_2} \right\rangle = \left\langle \hat{\zeta}_{\vec{k}_1}^{(0)} \hat{\zeta}_{\vec{k}_2}^{(0)} \right\rangle + \delta \left\langle \hat{\zeta}_{\vec{k}_1} \hat{\zeta}_{\vec{k}_2} \right\rangle \tag{3.28}$$

and, correspondingly,

$$P_\zeta = \mathcal{P}^{(0)} + \delta P \tag{3.29}$$

These quantities are computed in the following Subsections.

3.4.1   Tree level contributions

The first diagram in Figure 4.2 gives the (unperturbed) FRW power spectrum

$$\mathcal{P}^{(0)} = \frac{H^2}{8\pi^2 \varepsilon M_p^2} = \frac{H^4}{4\pi^2 \dot{\varphi}^2} \tag{3.30}$$

at super-horizon scales, where the slow roll expression (3.25) has been used.

The second diagram in Figure 4.2 gives the anisotropic contribution

$$\begin{aligned} \delta \langle \hat{\zeta}_{\vec{k}_1} \hat{\zeta}_{\vec{k}_2} \left(\tau \right) \rangle|_1 \;\; = \;\; & -\int_{\tau_{\min}}^{\tau} d\tau_1 \int_{\tau_{\min}}^{\tau_1} d\tau_2 \\ & \left\langle \left[\left[\hat{\zeta}_{\vec{k}_1}^{(0)} \hat{\zeta}_{\vec{k}_2}^{(0)} \left(\tau \right), \mathcal{H}_{\mathrm{int},1} \left(\tau_1 \right) \right], \mathcal{H}_{\mathrm{int},1} \left(\tau_2 \right) \right] \right\rangle \end{aligned} \tag{3.31}$$

We are interested in the power spectrum at super horizon scales, $k|\tau| \ll 1$. The time integral (3.31) is dominated by the times for which the modes in $H_{\mathrm{int}} \left(\tau_i \right)$ are also outside the horizon (mathematically, the contribution in the sub-horizon phase is suppressed by the oscillatory phases in the mode functions). This condition will be relevant for setting $\tau_{\min}$ (see below). As remarked before eq. (3.12), in this regime the vector field is classical, and does not contribute to the

commutators. The only nontrivial elements in the commutators are therefore

$$\left[\hat{\zeta}^{(0)}_{\vec{k}}(\tau), \hat{\zeta}^{(0)}_{\vec{k}'}(\tau')\right] = \left(\zeta^{(0)}_k(\tau)\zeta^{(0)*}_k(\tau') - \text{c.c.}\right)\delta^{(3)}\left(\vec{k} + \vec{k}'\right)$$

$$\simeq \frac{-iH^2\left[\tau^3 - \tau'^3\right]}{6\varepsilon M_p^2}\delta^{(3)}\left(\vec{k} + \vec{k}'\right) \tag{3.32}$$

where the last result is true in the super-horizon regime. We insert (3.26) into (3.31) and perform the commutators between the $\hat{\zeta}^{(0)}$ fields. The two resulting $\delta-$functions are employed to perform the two integrals over momenta, leading to

$$\delta\langle\hat{\zeta}_{\vec{k}_1}\hat{\zeta}_{\vec{k}_2}(\tau)\rangle|_1 \simeq \frac{4\,E_x^{(0)2}}{9\varepsilon^2 M_p^4 H^4}\prod_{i=1}^{2}\int_{\tau_{\min}}^{\tau}\frac{d\tau_i}{\tau_i^4}\left[\tau^3 - \tau_i^3\right]$$

$$\left\langle\delta E_x\left(\tau_1, \vec{k}_1\right)\delta E_x\left(\tau_2, \vec{k}_2\right)\right\rangle \tag{3.33}$$

Requiring that the vector field in this expression is in the super-horizon regime limits each time integral to $\tau_i > -\frac{1}{k_i}$. This sets the value of $\tau_{\min}$ in the two integrals. Using the expressions (3.12), and the identity

$$\sum_\lambda \varepsilon_{\lambda,i}\left(\vec{k}\right)\varepsilon_{\lambda,j}^*\left(\vec{k}\right) = \delta_{ij} - \hat{k}_i\,\hat{k}_j \tag{3.34}$$

we obtain

$$\delta\langle\hat{\zeta}_{\vec{k}_1}\hat{\zeta}_{\vec{k}_2}(\tau)\rangle|_1 \simeq \frac{2E_x^{(0)2}}{\varepsilon^2\,M_p^4}\frac{\delta^{(3)}\left(\vec{k}_1 + \vec{k}_2\right)}{k_1^3}\sin^2\theta_{\hat{k}_1,\hat{E}^{(0)}}\times$$

$$\times\left\{\int_{-\frac{1}{k_1}}^{\tau}\frac{d\tau'}{\tau'^4}\left[\tau^3 - \tau'^3\right]\right\}^2 \tag{3.35}$$

Changing variable $y' \equiv \frac{\tau'}{\tau}$, and recalling that $-k_1\tau \ll 1$, the time integral in the second line becomes

$$\int_1^{-\frac{1}{k_1\tau}}dy'\,\frac{y'^3 - 1}{y'^4} \simeq \ln\frac{1}{-k_1\,\tau} \tag{3.36}$$

At the end of inflation this quantity becomes N_{k_1}, namely the number of e-folds before the end of inflation at which the modes with wavenumber k_1 left the horizon. Using this result,

$$\delta P_1\left(\tau_{\text{end}}, \vec{k}\right) \simeq \frac{24}{\varepsilon}\frac{E_x^{(0)2}}{V(\varphi)}N_k^2\mathcal{P}^{(0)}\sin^2\theta_{\hat{k},\hat{E}^{(0)}} \tag{3.37}$$

where τ_{end} denotes the end of inflation (we assume that I rapidly approaches 1 at the end of inflation, so that the vector field is rapidly diluted away by the expansion, and the power spectrum of ζ freezes out). For the anisotropic inflationary model of [5], eq. (3.37) coincides with the analytic result of [90, 91], which, as we remarked, is in excellent agreement with the full numerical computation of [61, 91]. This confirms the validity of all the approximations

that we have performed.

The expression for the loop diagram in Figure 4.2 is analogous to eq. (3.31), with $\mathcal{H}_{\text{int},2}$ replacing $\mathcal{H}_{\text{int},1}$. We perform the commutators, again keeping in mind that the time integrals are dominated by fields in the super-horizon regime. We obtain

$$
\delta \langle \hat{\zeta}_{\vec{k}_1} \hat{\zeta}_{\vec{k}_2} (\tau) \rangle |_2 \simeq \frac{1}{9\varepsilon^2 H^4 M_p^4} \int \frac{d^3 p \, d^3 q}{(2\pi)^3} \prod_{i=1}^{2} \int_{\tau_{\min}}^{\tau} \frac{d\tau_i}{\tau_i^4} \left[\tau^3 - \tau_i^3 \right]
$$
$$
\left\langle \delta E_i (\tau_1, \vec{p}) \, \delta E_i \left(\tau_1, \vec{k}_1 - \vec{p} \right) \delta E_j (\tau_2, \vec{q}) \, \delta E_j \left(\tau_2, \vec{k}_2 - \vec{q} \right) \right\rangle
$$
(3.38)

Evaluating the full correlator (disregarding the disconnected contraction) gives

$$
\left(\delta \langle \hat{\zeta}_{\vec{k}_1} \hat{\zeta}_{\vec{k}_2} (\tau) \rangle |_2 \right)_{\text{theory}} \simeq \frac{9 H^4 \delta^{(3)} \left(\vec{k}_1 + \vec{k}_2 \right)}{2\varepsilon^2 M_p^4}
$$
$$
\int \frac{d^3 p}{(2\pi)^3} \frac{1 + \cos^2 \theta_{\widehat{p,k_1-p}}}{p^3 |\vec{k}_1 - \vec{p}|^3} \prod_{i=1}^{2} \int_{\tau_{\min}}^{\tau} \frac{d\tau_i}{\tau_i^4} \left[\tau^3 - \tau_i^3 \right]
$$
(3.39)

where also in this case we recall that the main contribution comes from the times when all the fields are in the superhorizon regime (for the same reasons mentioned after eq. (3.31)). This corresponds to $\tau_{\min} = \text{Max} \left[-\frac{1}{p}, -\frac{1}{|\vec{k}_1 - \vec{p}|} \right]$. Performing the time integrals, and keeping only the logarithmically enhanced term, leads to

$$
\left(\delta \langle \hat{\zeta}_{\vec{k}_1} \hat{\zeta}_{\vec{k}_2} (\tau) \rangle |_2 \right)_{\text{theory}} \simeq \frac{9 H^4 \delta^{(3)} \left(\vec{k}_1 + \vec{k}_2 \right)}{2\varepsilon^2 M_p^4}
$$
$$
\int \frac{d^3 p}{(2\pi)^3} \frac{1 + \cos^2 \theta_{\widehat{p,k_1-p}}}{p^3 |\vec{k}_1 - \vec{p}|^3} \ln^2 \left(\text{Min} \left[\frac{1}{-\tau \, p}, \frac{1}{-\tau \, |\vec{k}_1 - \vec{p}|} \right] \right)
$$
(3.40)

The final momentum integral naively diverges logarithmically at the two poles $\vec{p} \to \vec{0}, \vec{k}_1$. We need however to impose that the the fields $\delta \vec{E}$ in (3.38) were inside the horizon at the start of inflation (or they would not be excited by the mechanism described in the previous Section). Therefore $p, |\vec{k}_1 - \vec{p}| > -\frac{1}{\tau_{\text{in}}}$, where τ_{in} denotes the conformal time at the start of inflation. With this cut-off

$$
\delta P_2 \left(\tau_{\text{end}}, \vec{k} \right) |_{\text{theory}} \simeq 192 \, \mathcal{P}^{(0)2} N_k^2 \left(N_{\text{tot}} - N_k \right)
$$
(3.41)

This result accounts only for the contribution of the two poles and therefore is accurate only as long as the logarithmic enhancement encoded in the last term is $\gg 1$. For $N_{\text{tot}} \simeq N_k$ this last factor should be replaced by a $\mathrm{O}\left(1\right)$ factor. The result (3.41) was first derived in [93] using the Green function method.

We note that the modes contributing to the logarithmic enhancement are precisely the modes that left the horizon during the first $N_{\text{tot}} - N_{\text{CMB}}$ e-folds of inflation, and that contribute to the classical field $\vec{E}^{\text{IR}}$. As we discussed after eq. (3.13), this quantity adds up with the solution $\vec{E}^{(0)}$ of the classical equations of motion to give $\vec{E}_{\text{classical}}$, which is the homogeneous and classical "electric" field observed by the CMB modes. The quantity (3.41) is the theoretical expectation value associated with the loop diagram; it is the result that one would obtain if one could average over several realizations of the mechanism (see also [113]). However (assuming that this mechanism describes our universe) the CMB modes exit the horizon after a single realization of the first $N_{\text{tot}} - N_{\text{CMB}}$ e-folds of inflation. They therefore are not affected by the theoretical average $\langle |\vec{E}^{\text{IR}}|^{\,2} \rangle$ (which is statistically isotropic), but by the value that $\vec{E}^{\text{IR}}$ happened to assume in that single realization.

Therefore, if we want to compute the contribution of δP_2 to the power spectrum that is observed in a single realization, we need to replace the quantum operator of the IR modes entering in (3.38) with the classical Fourier transform of $\vec{E}^{\text{IR}}$. If we do so, the expression (3.38) becomes formally identical to (3.33), with the quantity $E_x^{(0)2} \equiv |\vec{E}^{(0)}|^2$ replaced by $|\vec{E}^{\text{IR}}|^2$ and with $\delta E_x\left(\tau_i, \vec{k}_i\right)$ (namely, the component of the fluctuations along the direction of $\vec{E}^{(0)}$) replaced by the component of $\delta\vec{E}\left(\tau_i, \vec{k}_i\right)$ in the direction of $|\vec{E}^{\text{IR}}|^2$. As a consequence, the value of $\delta P_2\left(\tau_{\text{end}}, \vec{k}\right)$ for a single realization coincides with (3.37), with $\vec{E}^{(0)}$ replaced by $\vec{E}^{\text{IR}}$,

$$\delta P_2\left(\tau_{\text{end}}, \vec{k}\right)|_{1\,\text{realization}} \simeq \frac{24}{\varepsilon} \frac{|\vec{E}^{\text{IR}}|^2}{V\left(\varphi\right)} N_k^2 \mathcal{P}^{(0)} \sin^2 \theta_{\hat{k}, \hat{E}^{\text{IR}}} \qquad (3.42)$$

Computing the theoretical expectation for this contribution amounts in replacing $\sin^2 \theta_{\hat{k}, \hat{E}^{\text{IR}}} E^{\text{IR}2}$ with $\frac{2}{3}\sigma^2_{\vec{E}^{\text{IR}}, N}$. The resulting expression coincides with (3.41).

We note that taking the classical IR value for one propagator is equivalent to taking the classical IR value for one of the two vector fields in the interaction hamiltonian $H_{\text{int},2}$ given in eq. (3.26). This interaction term then becomes identical to $H_{\text{int},1}$ apart from the fact that $\vec{E}^{(0)}$ is replaced by $\vec{E}^{\text{IR}}$. The two expressions than become a unique vertex in terms of the vector $\vec{E}_{\text{classical}} = \vec{E}^{(0)} + \vec{E}^{\text{IR}}$. This is the expected physical result, since the CMB modes "measure" the sum $\vec{E}_{\text{classical}}$ and cannot distinguish the two components. Even at the diagrammatic level, taking the IR limit in the third diagram of Figure 4.2 amounts in shrinking to zero one of the propagators, and one thus recovers the second diagram with a different external vector in the vertex (clearly, all this discussion applies also to the bispectrum computation). Therefore, from the last two diagrams of Figure 4.2 we obtain

$$\delta P\left(\tau_{\text{end}}, \vec{k}\right) \simeq \frac{24}{\varepsilon} \frac{E_{\text{classical}}^2}{V\left(\varphi\right)} N_k^2 \mathcal{P}^{(0)} \sin^2 \theta_{\hat{k}, \hat{E}_{\text{classical}}} \qquad (3.43)$$
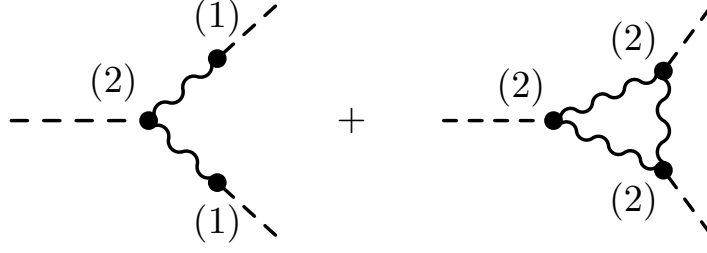
Figure 3.2: Leading diagrams for $\langle \zeta^3 \rangle$, with the vertices labelled as in (3.26).

3.5 Anisotropic Bispectrum

The bispectrum of ζ is defined as

$$\mathcal{B}_\zeta \left(\tau, \vec{k}_1, \vec{k}_2, \vec{k}_3 \right) \delta^{(3)} \left(\sum_i \vec{k}_i \right) = \left\langle \hat{\zeta}_{\vec{k}_1} \hat{\zeta}_{\vec{k}_2} \hat{\zeta}_{\vec{k}_3} (\tau) \right\rangle \tag{3.44}$$

The diagrams shown in Figure 3.2 give the dominant contributions to the bispectrum. The computation is presented in the following Subsections.

3.5.1 Tree level contributions

We evaluate the contribution of the first diagram $\mathcal{B}_1$ as we did for δP_1 in the previous Subsection. We start from

$$\begin{aligned}
\left\langle \hat{\zeta}_{\vec{k}_1} \hat{\zeta}_{\vec{k}_2} \hat{\zeta}_{\vec{k}_3} (\tau) \right\rangle_1 &= i \int d\tau_1 d\tau_2 d\tau_3 \left\langle \left[\left[\left[\hat{\zeta}^{(0)}_{\vec{k}_1} \hat{\zeta}^{(0)}_{\vec{k}_2} \hat{\zeta}^{(0)}_{\vec{k}_3} (\tau), \right. \right. \right. \right. \\
&\quad \left. \left. \left. \left. \mathcal{H}_{\text{int},2} (\tau_1) \right], \mathcal{H}_{\text{int},1} (\tau_2) \right], \mathcal{H}_{\text{int},1} (\tau_3) \right] \right\rangle + \dots
\end{aligned} \tag{3.45}$$

where the dots denote two additional terms obtained by permuting the position of $\mathcal{H}_{\text{int},2}$. Performing the commutators between the $\hat{\zeta}^{(0)}$ fields results into

$$\begin{aligned}
\left\langle \hat{\zeta}_{\vec{k}_1} \hat{\zeta}_{\vec{k}_2} \hat{\zeta}_{\vec{k}_3} (\tau) \right\rangle_1 &\simeq \frac{4 \, E_x^{(0)2}}{27 \varepsilon^3 H^6 M_p^6} \prod_{i=1}^{3} \int_{\tau_{\min}}^{\tau} d\tau_i \frac{\tau^3 - \tau_i^3}{\tau_i^4} \\
&\quad \int \frac{d^3 p}{(2\pi)^{3/2}} \left\langle \delta E_x \left(\tau_1, \vec{k}_1 \right) \delta E_x \left(\tau_2, \vec{k}_2 \right) \right. \\
&\quad \left. \delta \vec{E} \left(\tau_3, \vec{p} \right) \cdot \delta \vec{E} \left(\tau_3, \vec{k}_3 - \vec{p} \right) + \dots \right\rangle
\end{aligned} \tag{3.46}$$

where dots denote two additional terms obtained by permuting $\vec{k}_3$ with the other two momenta. As for the diagrams evaluated in the previous Subsection, the time integrals are dominated by the times for which the mode functions are classical and do not oscillate. For the term that is explicitly written in (3.46) this gives the three lower limits $\tau_1 > -\frac{1}{k_1}$, $\tau_2 > -\frac{1}{k_2}$, and $\tau_3 > \text{Max} \left[-\frac{1}{k_1}, -\frac{1}{k_2} \right]$

(the limit on τ_3 is most easily seen after taking the expectation value). Taking the expectation value and performing the time integral, we obtain

$$
\mathcal{B}_1\left(\tau_{\text{end}}, \vec{k}_i\right) \simeq \frac{288\sqrt{2}\,\pi^{5/2}}{\varepsilon}\,\frac{E_x^{(0)2}}{V(\varphi)}\,\mathcal{P}^{(0)2}
$$
$$
\times\left\{\frac{N_{k_1}\,N_{k_2}\,\text{Min}\left[N_{k_1},\,N_{k_2}\right]}{k_1^3\,k_2^3}\,\mathcal{C}_{\hat{k}_1,\hat{k}_2,\hat{E}^{(0)}} + 2\text{ permutations}\right\}
$$
(3.47)

where we have defined

$$
\mathcal{C}_{\hat{k}_1,\hat{k}_2,\hat{V}} \equiv 1 - \cos^2\theta_{\hat{k}_1,\hat{V}} - \cos^2\theta_{\hat{k}_2,\hat{V}}
$$
$$
+ \cos\theta_{\hat{k}_1,\hat{V}}\cos\theta_{\hat{k}_2,\hat{V}}\cos\theta_{\hat{k}_1,\hat{k}_2}
$$
(3.48)

3.5.2 | Including the loop contribution

For the second diagram in Figure 3.2 we obtain

$$
\left\langle\hat{\zeta}_{\vec{k}_1}\,\hat{\zeta}_{\vec{k}_2}\,\hat{\zeta}_{\vec{k}_3}\left(\tau_{\text{end}}\right)\right\rangle_2 \simeq \frac{1}{27\varepsilon^3 H^6 M_p^6}
$$
$$
\left\langle\prod_{i=1}^{3}\int\frac{d^3p_i}{(2\pi)^{3/2}}\int d\tau_i\frac{\tau^3 - \tau_i^3}{\tau_i^4}\delta\vec{E}\left(\tau_i, \vec{p}_i\right)\cdot\delta\vec{E}\left(\tau_i, \vec{k}_i - \vec{p}_i\right)\right\rangle
$$
(3.49)

where again we restrict the time integrals to when the modes are outside the horizon. The full correlator gives

$$
\left\langle\hat{\zeta}_{\vec{k}_1}\,\hat{\zeta}_{\vec{k}_2}\,\hat{\zeta}_{\vec{k}_3}\left(\tau_{\text{end}}\right)\right\rangle_2\Big|_{\text{theory}} \simeq \frac{27H^6\delta^{(3)}\left(\sum_i\vec{k}_i\right)}{\varepsilon^3 M_p^6}\int\frac{d^3p}{(2\pi)^{9/2}}
$$
$$
\prod_{i=1}^{3}\int d\tau_i\frac{\tau^3 - \tau_i^3}{\tau_i^4}\frac{Q_{ki}\left[\hat{p}\right]\,Q_{ij}\left[\widehat{p - k_1}\right]\,Q_{jk}\left[\widehat{p + k_3}\right]}{p^3\,|\vec{p} - \vec{k}_1|^3\,|\vec{p} + \vec{k}_3|^3}
$$
(3.50)

where we have defined $Q_{ij}\left[\hat{p}\right] \equiv \delta_{ij} - \hat{p}_i\,\hat{p}_j$ and where the time integrals are restricted to $\tau_1 > \text{Max}\left[-\frac{1}{p}, -\frac{1}{|\vec{p} - \vec{k}_1|}\right]$, $\tau_2 > \text{Max}\left[-\frac{1}{|\vec{p} - \vec{k}_1|}, -\frac{1}{|\vec{p} + \vec{k}_3|}\right]$, and $\tau_3 > \text{Max}\left[-\frac{1}{p}, -\frac{1}{|\vec{p} + \vec{k}_3|}\right]$.

The final momentum integral has three poles where it naively diverges logarithmically. The integral is regulated by the same argument used after (3.40), which in the present case enforces $p, |p - \vec{k}_1|, |\vec{p} + \vec{k}_3| > -\frac{1}{\tau_{\text{in}}}$. Performing the integrals

gives

$$\mathcal{B}_2\left(\tau_{\text{end}}, \vec{k}_i\right)\big|_{\text{theory}} \simeq 1152\sqrt{2}\pi^{5/2}\mathcal{P}^{(0)3}\Big\{N_{k_1}N_{k_2}$$

$$\times \text{Min}\left[N_{k_1}\left(N_{\text{tot}} - N_{k_1}\right), N_{k_2}\left(N_{\text{tot}} - N_{k_2}\right)\right]\frac{1 + \cos^2\theta_{\hat{k}_1\hat{k}_2}}{k_1^3 k_2^3}$$

$$+ 2\text{ permutations}\Big\} \tag{3.51}$$

As for (3.41), this result is accurate for $N_{\text{tot}} \gg N_{k_i}$; if this is not the case, the factor $N_{\text{tot}} - N_{k_i}$ should be replaced by a O (1) factor. The result (3.51) was first derived in [93] using the Green function method.

As for δP_2, the result is dominated by the regime in which one propagator has an IR mode. Also in this case, the value for a single realization is obtained by replacing the quantum operator of the IR field entering in (3.49) by a classical Fourier transform. We recover an expression formally identical to (3.46), with $\vec{E}^{(0)}$ replaced by $\vec{E}^{\text{IR}}$. Therefore, precisely as for the power spectrum, the total contribution of the two diagrams to the bispectrum is given by

$$\mathcal{B}\left(\tau_{\text{end}}, \vec{k}_i\right) \simeq \frac{288\sqrt{2}\,\pi^{5/2}}{\varepsilon}\frac{|\vec{E}_{\text{classical}}|^2}{V\left(\varphi\right)}\mathcal{P}^{(0)2}$$

$$\times \left\{\frac{N_{k_1}N_{k_2}\text{Min}\left[N_{k_1}, N_{k_2}\right]}{k_1^3 k_2^3}\mathcal{C}_{\hat{k}_1, \hat{k}_2, \hat{E}^{\text{classical}}} + 2\text{ permut.}\right\} \tag{3.52}$$

where we recall that $\mathcal{C}$ is given in (3.48).

3.6 Phenomenology

The total power spectrum is given by

$$P_\zeta = \mathcal{P}^{(0)}\left[1 + \frac{24}{\varepsilon}\frac{E_{\text{classical}}^2}{V\left(\varphi\right)}N_k^2\left(1 - \cos^2\theta_{\hat{k}, \hat{E}_{\text{classical}}}\right)\right] \tag{3.53}$$

corresponding to a negative g_* parameter in (4.64)

$$g_* = -\frac{24}{\varepsilon}\frac{E_{\text{classical}}^2}{V\left(\varphi\right)}N_k^2 \Big/ \left[1 + \frac{24}{\varepsilon}\frac{E_{\text{classical}}^2}{V\left(\varphi\right)}N_k^2\right]$$

$$\simeq -\frac{24}{\varepsilon}\frac{E_{\text{classical}}^2}{V\left(\varphi\right)}N_k^2 \tag{3.54}$$

where the approximation is due to the fact that $|g_*|$ is phenomenologically constrained to be < 1.

Inverting this relation for the CMB modes, and denoting by $\rho_{E_{\text{cl}}} \equiv \frac{E_{\text{classical}}^2}{2}$ the energy of the classical "electric" field present when the CMB modes left the

horizon

$$\frac{\rho_{E_{\mathrm{cl}}}}{V(\varphi)} \simeq 5.8 \cdot 10^{-9} \, \frac{\varepsilon}{0.01} \, \frac{|g_*|_{\mathrm{CMB}}}{0.1} \left(\frac{60}{N_{\mathrm{CMB}}}\right)^2 \tag{3.55}$$

and therefore we see that even a very subdominant vector field can produce an appreciably anisotropic power spectrum. Conversely, this indicates that the classical "electric" field must be extremely subdominant not to conflict with the phenomenological limits on the isotropy of the power spectrum.

We recall that, in any given realization, $\vec{E}_{\mathrm{classical}} = \vec{E}^{(0)} + \vec{E}^{\mathrm{IR}}$, where $\vec{E}^{(0)}$ is the solution of the classical equations of motion of the model, and $\vec{E}^{\mathrm{IR}}$ is drawn by a gaussian statistics of zero mean, and variance (3.14)

$$\left\langle \vec{E}^{\mathrm{IR}\ 2} \right\rangle_N = \frac{9H^4}{2\pi^2} \, N \tag{3.56}$$

The variance grows with the number of e-folds of inflation.
It is instructive to evaluate the ratio

$$R_N \equiv \frac{\rho_{E_{\mathrm{cl}}}}{\rho_{\delta E, N}} = \frac{\left|\vec{E}^{(0)} + \vec{E}^{\mathrm{IR}}\right|^2}{\left\langle \vec{E}^{\mathrm{IR}\ 2} \right\rangle_N} \tag{3.57}$$

at the moment that the CMB fluctuations left the horizon. Combining (3.55) and (3.56), and using the observed value [33] for the dominant term $\mathcal{P}^{(0)} \simeq P_\zeta \simeq 2.5 \cdot 10^{-9}$, we obtain

$$R_{N_{\mathrm{tot}}-N_{\mathrm{CMB}}} \simeq \frac{|g_*|_{\mathrm{CMB}}}{0.1} \left(\frac{60}{N_{\mathrm{CMB}}}\right)^2 \frac{37}{N_{\mathrm{tot}} - N_{\mathrm{CMB}}} \tag{3.58}$$

The numerator of (3.57) is the observed value, while the denominator the theoretical variance. Therefore, a value $R_{N_{\mathrm{tot}}-N_{\mathrm{CMB}}} \geq 1$ should be naturally expected for this ratio. Indeed, $R_{N_{\mathrm{tot}}-N_{\mathrm{CMB}}} \ll 1$ indicates either that the sum of the IR modes is unnaturally small in that realization (i.e. $|\vec{E}^{(0)}|^2$, $|\vec{E}^{\mathrm{IR}}|^2 \ll \left\langle \vec{E}^{\mathrm{IR}\ 2} \right\rangle_{N_{\mathrm{tot}}-N_{\mathrm{CMB}}}$), or that it unnaturally cancels against $\vec{E}^{(0)}$. Assuming a natural $R_{N_{\mathrm{tot}}-N_{\mathrm{CMB}}} \gtrsim 1$ realization, [x]

$$|g_*|_{\mathrm{CMB}} \gtrsim \mathrm{Min}\left[0.1 \left(\frac{N_{\mathrm{CMB}}}{60}\right)^2 \frac{N_{\mathrm{tot}} - N_{\mathrm{CMB}}}{37}, \, 1\right] \tag{3.59}$$

In generic slow roll inflationary potentials , the total duration of inflation exceeds (by much) the minimal N_{CMB} amount. One naturally finds an order one anisotropy in these models.
Another important conclusion can be drawn from (3.58). As it is exponentially unlikely to have $|\vec{E}^{\mathrm{IR}}|^2$ much greater than its variance, a value $R_{N_{\mathrm{tot}}-N_{\mathrm{CMB}}} \gg 1$ implies that $|\vec{E}^{(0)}|$ is much greater than the sum of the IR modes. Only in this case the solution of the classical equations of motion provides an accurate value

---

[x]Strictly speaking, eq. (3.55), and those derived from it, are only valid for $|g_*| < 1$. A value of $N_{\mathrm{tot}} - N_{\mathrm{CMB}}$ that results in a $|g_*| > 1$ in (3.58) should be associated to a $|g_*| = \mathrm{O}(1)$ in the natural $R_{N_{\mathrm{tot}}-N_{\mathrm{CMB}}} \gtrsim 1$ regime.

for the classical vector field that affects the observables curvature perturbations (as it is typically assumed in many works). A value $R_{N_{\text{tot}}-N_{\text{CMB}}} \simeq 1$ indicates instead that the contribution of the IR modes is no longer negligible, and that the solution of the classical equations of motion is unstable under quantum fluctuations (more appropriately, under the sum of the quantum fluctuations that have become classical). We see from (3.58) that $R_{N_{\text{tot}}-N_{\text{CMB}}} \gg 1$ can be obtained only for $N_{\text{tot}} - N_{\text{CMB}} \ll 37$.

Therefore, this mechanism can result in a $|g_*|_{\text{CMB}} \simeq 0.1$ anisotropy for either a tuned short duration of zinflation or an unnaturally small $\vec{E}_{\text{classical}}$. Assuming that this is the case, we can obtain a firm prediction from the anisotropy, the shape, and the magnitude of the non-gaussianity in the model. The bispectrum from this mechanism is given in eq. (3.52). To quantify whether this bispectrum is of observable magnitude, we notice that it is enhanced in the squeezed limit precisely as the local template. We therefore insert (3.52) into the relation

$$\mathcal{B}_\zeta \left(\tau_{\text{end}}, \vec{k}_i \right) \equiv \frac{3}{10} \left(2\pi \right)^{5/2} f_{\text{NL}} P_\zeta \left(k \right)^2 \frac{\sum_i k^3}{\prod_i k_i^3} \tag{3.60}$$

which, for the local bispectrum template, results in a constant $f_{\text{NL}}^{\text{local}}$ with the correct normalization (the non conventional factor of "2π-dependence" is due to our choice (3.24) for the Fourier transform). In the squeezed limit, we obtain

$$f_{\text{NL}} \simeq \frac{480}{\varepsilon} \frac{\mathcal{P}^{(0)2}}{P_\zeta^2} \frac{\rho_{E_{\text{cl}}}}{V \left(\varphi \right)} N_{k_1} N_{k_2}^2 \mathcal{C}_{\hat{k}_1, \hat{k}_2, \hat{V}} \quad , \quad k_1 \ll k_2 \simeq k_3 \tag{3.61}$$

where $\mathcal{C}$ is given in (3.48). Recalling that $\mathcal{P}^{(0)}$ dominates the power spectrum, using (3.55), and simply denoting $N_{k_1} \simeq N_{k_2} \equiv N_{\text{CMB}}$ (assuming that the momenta are not too hierarchical; this is certainly the case in the CMB analysis), we arrive to the final estimate

$$f_{\text{NL}} \simeq 26 \frac{|g_*|_{\text{CMB}}}{0.1} \frac{N_{\text{CMB}}}{60} \frac{\mathcal{C}_{\hat{k}_1, \hat{k}_2, \hat{V}}}{4/9} \quad , \quad k_1 \ll k_2 \simeq k_3 \tag{3.62}$$

where the value 4/9 has been inserted in the last factor so that this factor averages to one if we average over all directions of $\vec{k}_1$ and $\vec{k}_2 \simeq \vec{k}_3$. This result holds independently of the type of inflationary potential considered. In the estimate (3.62) we have averaged over all directions, with the assumption that this is what is done when extracting the value of f_{NL} from the full-sky data. The estimate (3.62) indicates that a $|g_*|$ in the $0.01 - 0.1$ range from this mechanism can likely be associated to a detectable bispectrum. A detection of a non-vanishing f_{NL} of the local shape will motivate a more detailed analysis, where the full shape and the anisotropy of (3.52) are retained.

3.7 Applications

In the following subsections we discuss how our findings apply to three well studied models in which vector fields are employed to either break statistical isotropy or to generate primordial magnetic fields.

3.7.1 Anisotropic inflation

Ref. [5] studied anisotropic inflation from the model (3.7). It was shown that the classical equation of the system admit an attractor solution characterized by the geometry (4.29) and by

$$E_x^{(0)} \simeq \sqrt{3\,\varepsilon\,(c-1)}\, H\, M_p \tag{3.63}$$

This values corresponds to [5]

$$\frac{\Delta H}{H} \simeq \frac{2\,\rho_{E^{(0)}}}{V\,(\varphi)} \simeq \frac{(c-1)\,\varepsilon}{c^2} \tag{3.64}$$

The power spectrum in this model was computed in [90, 61, 91] that however disregarded the contribution of $\vec{E}^{\text{IR}}$. Our computation reproduces their result (which confirms the validity of our computational scheme and the accuracy of our approximations) in this limit. Moreover, we have computed for the first time the bispectrum of this model, using the same computational scheme used to compute the power spectrum. The contribution of $\vec{E}^{(0)}$ to the anisotropy of the power spectrum forces $c - 1 \lesssim 10^{-6}$ [90, 61, 91]. The implicit assumption in this result is that choosing a $c - 1 \to 0$ in the lagrangian would result in a $g_* \to 0$ parameter. However, taking also $\vec{E}^{\text{IR}}$ into consideration, leads to the general conclusions on the natural amount of g_* and on the instability of (3.63) that we have presented in the previous section.

3.7.2 Waterfall mechanism

Ref. [44] embedded the mechanism (3.2) in hybrid inflation, through the lagrangian

$$\begin{aligned}
\mathcal{L} &= -\frac{I^2\,(\varphi)\,F^2}{4} - \frac{1}{2}\,(\partial\varphi)^2 - \frac{1}{2}\,(\partial\chi)^2 - V \\
V &= \frac{\lambda}{4}\left(\chi^2 - v^2\right)^2 + \frac{1}{2}g^2\varphi^2\chi^2 + \frac{1}{2}m^2\varphi^2 + \frac{1}{2}h^2 A^\mu A_\mu \chi^2
\end{aligned} \tag{3.65}$$

The additional coupling of the vector A_μ to the waterfall field χ provides a contribution to ζ through the mechanism of modulated perturbations [114, 115, 116]. Specifically, the value of the vector field contributes to determine the end of inflation, that happens when

$$m_\chi^2 = -\lambda v^2 + g^2 \varphi^2 + h^2 A_\mu A^\mu = 0 \tag{3.66}$$

so that perturbations δA_μ get converted into ζ at the end of inflation. This results in the additional contributions [44]

$$\Delta g_* \sim -\frac{h^4 |A|^2}{g^4 \varphi_e^2} \quad , \quad \Delta f_{\rm NL} \sim \eta_e \left(\frac{h^2}{g^2} \Delta g_* - \Delta g_*^2 \right) \tag{3.67}$$

where φ_e and η_e are, respectively, the value of the inflaton and of the slow roll parameter η at the end of inflation, and where we have normalized the coupling in (3.2) to $\langle I \rangle \equiv 1$ at the end of inflation.[xi]

These additional contributions to the anisotropy obviously vanish in the limit in which the vector field is not coupled to the waterfall field ($h \to 0$). On the contrary, (4.65) and (3.62) are general results unavoidably present when the function I in (3.65) is arranged to provide a constant vector field (which is also necessary to have non-negligible values in (3.67)). These unavoidable contributions have not been included in the many works that studied [44]. Given that (4.65) nearly saturates the phenomenological limit, the contribution (3.67) to g_* is at most comparable to (4.65). On the contrary, the additional coupling h present in (3.65) can allow for a greater non-gaussianity than (3.62). Indeed, in the minimal model (3.2), the parameter $f_{\rm NL}$ is uniquely related to g_* through (3.62), and this strict relation increases the predictivity of the mechanism. For the model (3.65), non-gaussianity can be enhanced for $h \gg g$. The shape of the contribution to the bispectrum resulting from the waterfall coupling [44] is in general different from the shape of (3.52); the two shapes coincide for $h \gg g$.

3.7.3 │ Magnetogenesis

Using the "electric" $\leftrightarrow$ "magnetic" duality that we have mentioned [84], the results for the perturbations that we have obtained are also valid in the case of $\langle I \rangle \propto a^2$, which results in a scale invariant "magnetic" field [83]. In fact, the two results (3.41) and (3.51) have been first obtained in [93] for $\langle I \rangle \propto a^2$. Although the mechanism (3.2) was first introduced with this motivation, the magnetogenesis application suffers a strong coupling problem [38]. Indeed, with (3.2) the fine structure constant scales as $\alpha \propto \langle I \rangle^{-2}$. The choice $\langle I \rangle \propto a^2$ corresponds to a fast decreasing $\alpha \propto a^{-4}$ during inflation. Assuming that α reaches the present value

---

[xi]Ref. [89] studied the additional contributions to ζ from the waterfall coupling in the case in which the vev of the vector field varies with time. For a discussion of the effects from a time varying inflaton coupling in modulated reheating see [117].

at the end of inflation implies $\alpha \gg 1$ during inflation, and a quantum field theory of electromagnetism that is (at the very least) out of computational control [38]. Alternatively, for $\alpha \lesssim 1$ at the start of inflation, one obtains $\alpha \sim e^{-4N_{\text{tot}}}$ at the end of inflation, and requiring that α grows back to its present value before big-bang nucleosynthesis does not appear feasible [93]. [xii]

Clearly, the strong coupling problem is a problem of the magnetogenesis application and not of the mechanism (3.2), as one can always assume that a generic U(1) field is sufficiently weakly coupled to other fields. For a growing $\langle I \rangle$ the coupling decreases during inflation, and one can assume that the vector field has couplings $\lesssim 1$ at the beginning of inflation. For a decreasing $\langle I \rangle$ the coupling grows during inflation, and one can require a coupling $\lesssim 1$ when inflation ends. In principle one may hope that a field with such properties is produced during inflation by this mechanism, and it is then (partially) converted to the magnetic one through some coupling. Some attempts so far in this direction have been unsuccessful [93], but a general study remains to be done. If this, or some other idea [95, 96, 39, 97, 51, 98, 99, 100], can circumvent the strong coupling problem, our findings provide a signature that may be correlated with the magnetic field.

3.8 Conclusions

There are two questions associated to the attempt of reconciling a non vanishing anisotropy g_* with a model of inflation. The first one is "what are the other signatures that would accompany the measured value of g_* ?"; the second one is "what is the natural value of g_* in the model? ". A first difficulty that is encountered in answering these questions is that anisotropic hairs are typically erased by inflation [11, 71], so that one has to design specific models that preserve the anisotropy. Vector fields appear as the simplest possibility, as their vev breaks isotropy. Several mechanisms have been designed to prevent the rapidly erosion of the vector vev by the inflationary expansion. As shown in [20, 22, 43], however, many of them (for instance, the use of a potential as in [17], of a lagrange multiplier as in [8], or of a coupling to the curvature as in [18] and as in analogous models of vector curvaton) have ghosts. The use of (3.2) for preserving the vector vev [5, 44] has resulted in a rather exceptional mechanism where the above two questions can be formulated.

With the mechanism (3.2), the answer to the first question appears to be very positive. The anisotropy in the power spectrum is correlated with a characteristic and very likely detectable bispectrum. The bispectrum, whose full shape is given in (3.52), is enhanced as the local one in the squeezed limit, where it has an

---

[xii]A scale invariant magnetic field is also obtained at the start of inflation for $\langle I \rangle \propto a^{-3}$. However, too much energy gets stored in the electric field in this case [38], and the system enters in a strong backreaction regime in which a too small magnetic field is produced [102].

effective local parameter (see (3.62) for more details)

$$f_{\mathrm{NL}} \simeq 26 \, \frac{|g_*|_{\mathrm{CMB}}}{0.1} \qquad (3.68)$$

A larger bispectrum can be obtained if the vector field has additional interactions with the inflationary sector, as in the waterfall mechanism of [44]. However these additional interactions are not needed, and the result (6.1) is the direct contribution that comes from the interaction (3.2). Therefore, this is the result in the most minimal and predictive implementation of (3.2). We see that an anisotropy in the power spectrum at the $1\% - 10\%$ level, could be associated with a detectable bispectrum.

For the second question, one needs to take into account that, for a mechanism that results in a scale invariant field (as in the implementations [5, 44]), a classical background value of this field is unavoidably generated by the sum of the modes that have left the horizon during inflation [101]. The crucial point for our discussion is that a background vector field breaks isotropy. It is unnatural to require that the anisotropy experienced by the CMB modes when they leave the horizon is smaller than the theoretical expectation value $\left\langle \delta \vec{E}^2 \right\rangle \sim H^4 \left(N_{\mathrm{tot}} - N_{\mathrm{CMB}} \right)$, where H is the Hubble rate during inflation, and $N_{\mathrm{tot}} - N_{\mathrm{CMB}}$ is the number of e-folds of inflation that took place before the CMB modes are generated, and during which the classical background of long-wavelength modes experienced by the CMB modes has accumulated. Taking this into account, we find that the natural value for the anisotropy is (see (4.65) for more details)

$$|g_*|_{\mathrm{CMB}} \gtrsim \mathrm{Min} \left[0.1 \, \frac{N_{\mathrm{tot}} - N_{\mathrm{CMB}}}{37}, \, 1 \right] \qquad (3.69)$$

which can easily overcome the phenomenological bounds (particularly with the improvement expected from Planck [67, 68]). We note that this saturation takes place for a very subdominant vector field, with very negligible backreaction on the background inflaton evolution. This ensures that the result (3.69) is robust. However, as already obtained in [90, 61, 91], even a very subdominant vector field can result in a substantial anisotropy parameter.

Remarkably, these considerations apply also to the magnetogenesis applications of (3.2). The role of the background magnetic field has been so far disregarded in the study of the cosmological perturbations obtained in that context. However, the result (3.69) applies also to this case. We stress that the magnetogenesis application suffers from a serious strong coupling problem [38]. If this problem can be solved, a magnetic field through this mechanism would be naturally correlated with an observable anisotropy of the perturbations.

Analogously, an anisotropic signal should also be expected in models where a triad of vectors is arranged to produce isotropic expansion or isotropic perturbations [118], since the long-wavelength background values of the different vectors fields will in general be different.

Although our study has been limited to the mechanism (3.2), one may expect

that an anisotropic background field and a large anisotropy of the perturbations may be a general outcome of all models that sustain higher than 0 spin fields during inflation. For instance, it would be interesting to study the natural level of anisotropy to be expected in the mechanism of [78] (for which statistical isotropy has been obtained for very specific choices of the kinetic and the mass function [82]) or in the case of inflation or magnetic fields from p-forms [119, 120, 121, 122, 123, 124, 125, 126].

4

ANISOTROPY IN SOLID INFLATION

In this chapter, based on [127], we have computed the curvature perturbations on an anisotropic solution of the "solid inflation" model defined as a system of three derivatively coupled scalar fields obeying certain symmetries that differ drastically from that of standard inflationary models: time translations are unbroken. We show that FRW is not an attractor of this model and anisotropic features can be generated with standard gravity and scalar fields.

Contents

4.1 Introduction

The CMB data strongly support the inflationary framework and allow to rule out several specific inflationary models [128]. Still, a large number of models remains compatible with the data. It proves useful to classify and study them in terms of an effective field theory description of inflation [129, 130], where the behavior of the perturbations and the possible signatures can be understood in terms of symmetries and symmetry breaking. For instance, several models of inflation are characterized by a shift symmetry $\phi \to \phi + C$ (where ϕ is the inflaton, and C a constant), which protects the required flatness of the inflaton potential against radiative corrections (for a recent review see [131]). In the limit of exact shift symmetry the potential coincides with a cosmological constant, and the spacetime geometry is the de Sitter one. A small and controlled breaking of the symmetry ensures a slow roll inflaton evolution, which breaks time translational invariance. This set-up has one scalar perturbation, which can be identified as the Goldstone boson of this broken symmetry.

While the requirement that inflation ends demands that time translation invariance is broken, and, more in general, cosmology studies time-evolving backgrounds, the vast majority of the models assumes invariance under spatial translations, in agreement with the observed homogeneity and isotropy of the universe at large scales. In fact, one of the many features of inflation is that it can dynamically lead to the observed homogeneity and isotropy [34], which are otherwise hard to achieve starting from more general initial conditions [132].

The simplest way to enforce isotropy and homogeneity is to assume that only spin zero fields are dynamically relevant during inflation, and that their vacuum expectation value (vev) is independent of the spatial coordinates. These assumptions characterize the vast majority of the models of inflation. However, in principle, one could imagine that different sources are present, which individually break the invariance under spatial transformations, but that their combined effect - due to some underlying symmetry - preserves the background isotropy and homogeneity. Due to this different symmetry breaking pattern, such a possibility could result in specific phenomenological signatures that are not obtained in the more conventional inflationary models.

Isotropy with spin one sources can be achieved through (i) a triplet of orthogonal vectors with equal vev [**?**], (ii) a large number $N \gg 1$ of randomly oriented vectors [18] - resulting in a $\mathrm{O}\left(1/\sqrt{N}\right) \ll 1$ anisotropy - or massive vectors oscillating about the minimum of the potential [**?**] - resulting in an effective isotropic equation of state once averaged over the oscillations.

Homogeneity and isotropy with spin zero fields with a spatially-dependent vev can be achieved with a triplet of scalars with [133, 7]

$$\langle \phi^i \rangle = x^i \, , \tag{4.1}$$

where $i = 1, 2, 3$. In particular, ref. [7] dubbed this model *Solid Inflation*. It is assumed in [7] that the medium driving inflation can be coarse-grained at the level of fundamental cells, and that only the position of these cells is relevant for inflationary cosmology. The three scalars $\phi^i(t, \vec{x})$ can be viewed as the three coordinates that provide the position at the time t of the cell element that at the time $t = 0$ was at position $\vec{x}$. Therefore, the vevs (4.1) characterize a medium at rest in comoving coordinates. The properties of the solid are defined through a lagrangian, which is a functional of ϕ^i. As we describe below, (i) only derivatives of the scalars enter in the lagrangian, so that the vev (4.1) can be compatible with homogeneity of the background solution, and (ii) only SO(3) invariant combination of the derivatives enter in the lagrangian, so that the vev (4.1) can be compatible with isotropy. As discussed in [7], this description provides a complementary formulation of [134], which also suggested a coarse-grained description of the inflationary medium dubbed *Elastic Inflation.*

By construction, the background evolution of solid inflation is isotropic, and the power spectrum of the scalar perturbations is statistically isotropic [134, 7]. However, the bispectrum presents a characteristic shape not encountered in previous models of scalar field inflation [7]. Specifically, it is enhanced in the squeezed limit as the local template, but it manifests a nontrivial dependence on the angle between the small and large momentum in the correlator. It turns useful to adopt the parametrization [135]

$$B_\zeta(k_1, k_2, k_3) = \sum_L c_L P_L\left(\hat{k}_1 \cdot \hat{k}_2\right) P_\zeta(k_1) P_\zeta(k_2) + 2\,\text{perm.}, \qquad (4.2)$$

where P_ζ and B_ζ are, respectively, the power spectrum and bispectrum of the curvature perturbation in the uniform density gauge and P_L are the Legendre polynomials. The local template is characterized by $c_i = \frac{6}{5} f_{\text{NL}} \delta_{i0}$. More in general, typical models of scalar field inflation are characterized by $c_i = 0$, for $i \neq 0$ in the squeezed limit. The reason for this is the following [136, 137]: in the squeezed limit $k_3 \ll k_{1,2}$, the long wavelength mode modulates the two short wavelength modes when they leave the horizon. From the point of view of the short wavelength modes, the long wavelength mode can be accurately described by a mean and a gradient. The gradient defines a local basis for a quadrupolar dependence of the small-scale power, thus in principle contributing to the c_2 coefficient above. However, the gradient vanishes in the long wavelength limit $k_3 \to 0$.

On the contrary, the nonvanishing scalar vevs (4.1) provide a directionality modulation of the bispectrum that does not vanish in the squeezed limit, and the bispectrum of solid inflation is dominated by the c_2 term in the squeezed limit [7]. Quite interestingly, a nontrivial angular dependence in that limit had previously been obtained in [93] and further studied in [62, 138, 135, 139, 12, 140] [i] in

---

[i] Ref. [141] rederived the results of [62], claiming that their rederivation uses only the classical mode functions, and it is therefore "simpler and more complete" than the computation of [62]. The rederivation is not more complete, since, by admission, it disregards the contribution from the modes in the quantum regime. We argue that it is also not simpler, since also the results of [93, 62] are due to the classical super-horizon contribution, as repeatedly stressed in [62].

the model $f(\phi)F^2$, where ϕ is the inflaton and F^2 the square of a vector field strength $F_{\mu\nu}$, in the case in which $f(\phi)$ is chosen so to produce a scale invariant spectrum for the vector field. In this case, the nontrivial angular dependence of the bispectrum is due to the fact that a homogeneous vector breaks isotropy locally, and so the anisotropic modulation survives also in the $k_3 \to 0$ limit. [ii] This has further nontrivial consequences, as we discuss in the Conclusions. For the $f(\phi)F^2$ model, $c_2 = c_0/2$, while all other c_i coefficients vanish.

Motivated by the above models, the Planck collaboration [1] has constrained the first coefficients of the series (4.2), as $c_0 = 3.24 \pm 6.96$, $c_1 = 11.0 \pm 113$, and $c_2 = 3.8 \pm 27.8$ (all at 68% CL), with error bars in agreement with the forecasts of [135].

The $f(\phi)F^2$ mechanism is constructed to generate and sustain a nontrivial vector field in cosmology (see [142] for a recent review and for a more extended list of relevant works). A vector field with standard $\mathcal{L} = -\frac{1}{4}F^2$ lagrangian is conformally coupled to a FRW background, and so its fluctuations are not excited by the expansion of the universe. Moreover, if a vector vev is present as an initial condition, it is rapidly diluted away by the expansion of the universe. Therefore, any signature associated to the vector - including the angular dependence in (4.2) - would be negligible in this case. Several models have been proposed for which a classical vector vev is not diluted by the expansion. Several of them break the gauge invariance associated with the vector field. Such models are characterized by (i) a suitable vector potential $V(A^2)$ [17], (ii) a specific coupling to the scalar curvature $\mathcal{L} \supset \frac{1}{12}RA^2$ [42, 18, 106], or (iii) a lagrange multiplier λ that enforces a fixed norm for the vector, $\mathcal{L} \supset \lambda(A^2 - v^2)^2$ [8]. Due to the broken gauge invariance, the vector field has also a longitudinal mode. This mode turns out to be a ghost [?] in all the above models. On the contrary, the $f(\phi)F^2$ mechanism preserves gauge invariance, and it is therefore stable [60]. A suitable choice of $f(\phi)$ can result in frozen and scale invariant super-horizon perturbations, and in a constant vev, for the magnetic or electric component of the vector field. The first possibility has been suggested as a model for inflationary magnetogenesis [83, 94, 84] (although this application is highly nontrivial to realize [38, 93, 103, 143]), while the second one has been used to obtain a prolonged stage of anisotropic inflationary expansion [5]. [iii]

The $f(\phi)F^2$ mechanism and solid inflation constitute the two only examples known so far of a primordial bispectrum with a nontrivial angular dependence in the squeezed limit. It is natural to ask whether the two models have other common aspects, and in fact the present investigation originated by an argument that convinced us that the analogy between the models already starts at the background level: a remarkable property of the medium of solid inflation is that it is very weakly affected by the huge inflationary expansion. This property, which is completely at odds with that of the solids that we ordinarily deal

---

[ii] Notice that in the $f(\phi)F^2$ model with a non-vanishing vev of the vector field, a bispectrum that breaks statistical isotropy is generated, and its angle-average does assume the form (4.2). A statistically isotropic bispectrum is obtained from a triplet of orthogonal vectors of equal magnitude.

[iii] See [?] for models of anisotropic inflation that employ the idea of [5].

with, is encoded by an extremely weak dependence of the energy of the solid on its volume. Cosmological perturbations in solid inflation are supported by deformation of this solid - the "phonons". [iv] Stability of these perturbations, and the existence of a weak coupling regime, require that the medium is not only very weakly sensitive to the overall volume expansion, but to all spatial deformations [7]. This naturally led us to conjecture that the solid should be extremely inefficient to respond to anisotropic background deformations, and that, consequently, it should also admit prolonged anisotropic solutions. The computations of the present work show that this is indeed the case.

Specifically, we obtain that the anisotropy is erased on a timescale $\Delta t = \mathrm{O}\left(\frac{1}{\varepsilon H}\right)$, where H is the Hubble rate, and ε the slow roll parameter $\varepsilon \equiv -\dot{H}/H^2$ (dot denoting a time derivative). This corresponds to the isotropization rate $\Delta t^{-1} = \mathrm{O}\left(\varepsilon H\right)$. This rate is suppressed with respect to the isotropization rate $\Delta t^{-1} = \mathrm{O}\left(H\right)$ that is typically encountered in inflationary models [11, 71]. Ref. [11] showed that a $\mathrm{O}\left(H\right)$ isotropization rate is the norm for practically all homogeneous and anisotropic backgrounds (with the possible exception of a Bianchi type-IX geometry) in the presence of a cosmological constant and a fluid that satisfies the dominant and strong energy conditions. This result is often denoted in the literature as the "cosmological no-hair conjecture" (or "theorem"), as it implies that no information on the anisotropy survives, analogously to what would happen for a black-hole solution. The above cited vector field models are attempts to evade the results of [11], and, as we discussed, only those based on the $f\left(\phi\right)F^2$ represent viable solutions. Besides using vector fields, other works that have attempted to evade the result of [11] involve either higher order curvature terms [**?**] or higher forms [**?**, 147, 148]. Ref. [148] supports the higher form through the same mechanism as [5], and it is therefore stable. To our knowledge, a full study of the perturbations for the proposals [**?**, 147] remains to be done. The one we present here is the first counter example of [11] with standard gravity and only scalar fields. This counter example has no pathologies: as we show below, the slow isotropization in solid inflation precisely originates by the demand that the phonons have a well behaved propagation in this unconventional medium.

The work is organized as follows. In Section 4.2 we present the model of solid / elastic inflation, and its FRW solution, as formulated in [7]. In Section 4.3 we review the curvature perturbation on the FRW solution, again mostly summarizing the original study of [7]. In Section 4.4 we study the simplest anisotropic solution in this model and we discuss why the result of [11] is evaded. In Section 4.5 we study the scalar curvature perturbation on this anisotropic solution and we obtain the corresponding phenomenological limit on the anisotropy. In the concluding Section 4.6 we further discuss the analogy between solid inflation and the $f\left(\phi\right)F^2$ model, and we review some interesting open questions.

[iv]See [144] for an early lagrangian formulation of the cosmological medium as a fluid, and for the description of its perturbations in terms of phonons. A different lagrangian formulation of a fluid driving inflation has also been recently studied in [145, 146].

4.2   The model and the FRW background solution

The action of solid inflation is [7]

$$S = \int d^4x \sqrt{-g} \left\{ \frac{M_p^2}{2} R + F\left[X, Y, Z\right] \right\} , \qquad (4.3)$$

where R is the scalar curvature, M_p the (reduced) Planck mass, and F a function that characterizes the solid, as we now discuss. The solid is divided in several infinitesimal cells. The three scalars $\phi^i\left(t, \vec{x}\right)$ can be viewed as the three coordinates that provide the position at the time t of the cell element that at the time $t = 0$ was at position $\vec{x}$. Therefore, the vevs (4.1) characterize a medium at rest in comoving coordinates. To reconcile a homogeneous and isotropic solution with background fields that are $\mathbf{x}-$dependent, ref. [7] imposes that the function F is invariant under translations $\phi^i \to \phi^i + C^i$, and SO(3) rotations, $\phi^i \to O^i_j \phi^j$, with C^i, O^i_j constant. Specifically, it is assumed that F is a function of SO(3) invariants of

$$B^{ij} \equiv g^{\mu\nu} \partial_\mu \phi^i \partial_\nu \phi^j . \qquad (4.4)$$

Only three independent such invariants, exist, that in [7] are chosen as [v]

$$X \equiv \operatorname{Tr} B = B^{ii} \quad , \quad Y \equiv \frac{\operatorname{Tr}\left(B^2\right)}{\left(\operatorname{Tr} B\right)^2} \quad , \quad Z \equiv \frac{\operatorname{Tr}\left(B^3\right)}{\left(\operatorname{Tr} B\right)^3} . \qquad (4.5)$$

As we shall see, the SO(3) invariance in the "internal $\{\phi^i\}$ space", together with the "diagonal" vevs (4.1), allows for an isotropic background solution for the model. However, it is important to stress that this is not the only admissible solution. In fact, in Section 4.4 we will see that the vev (4.1) is compatible with anisotropic solutions, for which the anisotropy is encoded in different scale factors for the different spatial directions (a Bianchi-I background). In the reminder of this Section we concentrate on the isotropic background solution

$$ds^2 = -dt^2 + a^2\left(t\right) dx^i dx^i , \qquad (4.6)$$

and we also state the conditions for the validity of the theory obtained in [7] (which apply to generic backgrounds).

The energy momentum tensor obtained from (4.3) is

$$T_{\mu\nu} = g_{\mu\nu} F - 2 \partial_\mu \phi^i \partial_\nu \phi^j \, \frac{\partial F}{\partial B^{ij}} , \qquad (4.7)$$

---

[v]The determinant of B^{ji} can be written as the combination $\det B = \frac{X^3}{6}\left(1 - 3Y + 2Z\right)$. Since the energy of a perfect fluid is only sensitive to volume deformations, we can regard the special case in which F only depends on this combination as the field theoretical description of a fluid. Such a case was also discussed in [7] and studied in [149].

72

where,

$$\frac{\partial F}{\partial B^{ij}} = \left(F_X - \frac{2Y}{X} F_Y - 3\frac{Z}{X} F_Z \right) \delta^{ij}$$
$$+ \frac{2F_Y}{X^2} B^{ij} + \frac{3F_Z}{X^3} B^{ik} B^{kj} \ . \tag{4.8}$$

On the background (4.6), the three above invariants have the vevs $\langle X \rangle = \frac{3}{a^2}, \langle Y \rangle = \frac{1}{3}, \langle Z \rangle = \frac{1}{9}$, and we obtain $\langle T^\mu_\nu \rangle = \mathrm{diag}\,(-\rho, p, p, p)$, with

$$\rho = -F \ , \quad p = F - \frac{2}{a^2} F_X \tag{4.9}$$

where the subscript denotes partial derivative. The background Einstein equations are the standard ones in terms of the above energy density and pressure

$$3H^2 = \frac{\rho}{M_p^2} \ , \quad -2\dot{H} - 3H^2 = \frac{p}{M_p^2} \tag{4.10}$$

In addition, one has the equations obtained by extremizing the action with respect to the scalar fields:

$$\partial_\mu \left[\sqrt{-g} \frac{\partial F}{\partial \partial_\mu \phi^i} \right] = \partial_\mu \left[\sqrt{-g} \frac{\partial F}{\partial B^{ab}} \frac{\partial B^{ab}}{\partial \partial_\mu \phi^i} \right] = 0 \ . \tag{4.11}$$

For the above background configuration (4.1),

$$\frac{\partial B^{ab}}{\partial \partial_\mu \phi^i} \bigg|_{\phi^i = x^i} = \delta^a_i g^{\mu b} + \delta^b_i g^{\mu a} \ . \tag{4.12}$$

As the indices a and b only range from 1 to 3, as long as the metric is diagonal the expression (4.11) automatically vanishes when $\mu = 0$. Moreover, as long as the metric is $\vec{x}$-independent, the expression in square parenthesis is also $\vec{x}$-independent. Therefore, the equations (4.11) are automatically (that is, for any functional form of $F[X, Y, Z]$) satisfied by (4.1), both on a FRW and on a Bianchi-I background.

Following [7], we define the slow roll parameters,

$$\varepsilon \equiv \frac{-\dot{H}}{H^2} = \frac{X\,F_X}{F} \ , \quad \eta \equiv \frac{\dot\varepsilon}{\varepsilon H} = 2 \left(\varepsilon - \frac{XF_{XX} + F_X}{F_X} \right) \ , \tag{4.13}$$

and we impose that $\varepsilon, |\eta| \ll 1$, as required for successful inflation. From eq. (4.9), we see that $F < 0$. We then impose that $\dot{H} < 0$ during inflation, which forces $F_X < 0$.

Let us now discuss the validity of the effective field theory that describes the solid [7]. To do this, it is sufficient to study the perturbations of a solid with $|XF_X| \ll |F|$ on a Minkowski background (as always, this study reproduces the study of cosmological perturbations in the sub-horizon regime [7]). We decompose an arbitrary deformation of the solid (namely, a "phonon"), $\phi^i = x^i + \pi^i(x)$ into

longitudinal plus transverse one, $\vec{\pi} = \vec{\pi}_L + \vec{\pi}_T$, with, respectively, the properties $\vec{\nabla} \times \vec{\pi}_L = 0$ and $\vec{\nabla} \cdot \vec{\pi}_T$. The sound speed of such perturbations is [vi] [7]

$$c_T^2 = 1 + \frac{2}{3} \frac{F_Y + F_Z}{F_X X} \quad , \quad c_L^2 \simeq \frac{4}{3} c_T^2 - 1 \; . \tag{4.14}$$

It is then immediate to verify that the requirements of subluminal propagation of the perturbations ($c_{L,T}^2 < 1$) and of the absence of tachyonic modes ($c_{L,T}^2 > 0$) are obtained for [7]

$$0 < F_Y + F_Z < \frac{3}{8} \varepsilon \, |F| \; . \tag{4.15}$$

As the "phonons" enter derivatively in F, their nonlinear interactions necessarily become strong at energies E greater than some scale Λ. We need to require that $\Lambda \gg H$, so that there exist a finite window of sub-horizon scales in which the theory (4.3) is weakly coupled. A detailed study performed in [7] shows that this is the case for $\varepsilon c_L^3 \gg \left(\frac{H}{M_p}\right)^{2/3}$. This condition can be satisfied at sufficiently small H. This condition, together with (4.15) ensures that the field theoretical description (4.3) of the solid is under perturbative control.

To conclude this Section, we note that F_X is the only derivative of the function F that enters in the expression for the pressure, since, by construction, Y and Z are insensitive to the overall spatial volume [7]. Therefore, F_X is the only quantity that characterizes the sensitivity of the solid to the volume expansion. We need to impose that $\varepsilon \ll 1$, or, equivalently, that this sensitivity is extremely small. This is not a surprising condition: the source of inflation needs to have an equation of state sufficiently close to that of a cosmological constant, which is, by definition, insensitive to the volume expansion. This property is in complete contrast with that of solids that we ordinary deal with, but nonetheless it is logically conceivable, and it has a perfectly valid field theoretical description [7]. From the study of the perturbations of such an unusual medium, we learn that also the combination $F_Y + F_Z$ needs to be small. As we shall see in Section 4.4, this combination, obtained from the sound speed of the phonons, controls the response of the solid to anisotropic deformations. We therefore learn that the solid not only needs to be extremely insensitive to the volume expansion, but also to an anisotropy of the geometry. This property is the basis for the prolonged anisotropic inflationary solution that we obtain in Section 4.4.

4.3   Scalar curvature perturbations on the FRW solution

In this section we summarize the linearized study [7] of the perturbations on the FRW background of solid inflation discussed in the previous Section. We

---

[vi]The approximation made in the second equation in (4.14) is $|X F_{XX} + F_X| \ll |F_X|$, as it is required to have $|\eta| \ll 1$ in eq. (4.13). The full expression for the longitudinal sound speed that we use in the following computations is $c_L^2 = \frac{4}{3} c_T^2 - 1 + \frac{2}{3}\varepsilon - \frac{1}{3}\eta$.

decompose the fields in background plus perturbations

$$
\begin{aligned}
\phi^i &= x^i + \pi^i\left(t, \vec{x}\right) \quad , \quad \pi^i\left(t, \vec{x}\right) = \frac{\partial_i}{\sqrt{-\partial^2}}\pi_L + \pi_T^i \ , \\
g_{00} &= -1 - 2\Phi\left(t, \vec{x}\right) \ , \\
g_{0i} &= B^i\left(t, \vec{x}\right) \quad , \quad B^i\left(t, \vec{x}\right) = \frac{\partial_i}{\sqrt{-\partial^2}}B_L + B_T^i \ , \\
g_{ij} &= a^2\left(t\right)\left(\delta_{ij} + h_{ij}\left(t, \vec{x}\right)\right) \ ,
\end{aligned}
\tag{4.16}
$$

where π_T^i and B_T^i are transverse, and h_{ij} is transverse and traceless. The perturbations of the metric are classified according to how they transform under spatial rotations. The perturbations Φ and B_L transform as two scalar modes, the perturbations B_T^i form a vector multiplet (of two degrees of freedom, given the transversality condition), and the perturbations h_{ij} form a tensor multiplet (again of two degrees of freedom). Modes with different transformation properties are decoupled from one another at the linearized level. We note that we have set to zero two scalar modes and one vector mode in δg_{ij}, leading to the so called spatially flat gauge. This can always be done using infinitesimal coordinate transformations, and actually this fixes completely this gauge freedom (equivalently, one may choose to use gauge invariant combinations of the perturbations [150, 151]).

In addition, also the perturbations of the scalar field are separated into a "longitudinal" and a "transverse" part. The π_T^i multiplet is not a vector multiplet under spatial rotations, given that all fields ϕ^i are scalar fields, and the index i is in this case just a label for the three fields. However, due to the fact that at the background level $\langle\phi^i\rangle = x^i$, one can verify that, at the linearized level, π_L only couples to the scalar modes of the metric, while π_T^i only couples to the vector multiplet of the metric. Therefore, with an abuse of notation, in the following we refer to π_L as a scalar perturbation, and to π_T^i as a vector multiplet. Therefore, after fixing the freedom of infinitesimal coordinate transformation, the system of perturbations has a scalar sector of 3 degrees of freedom (π_L, Φ, B_L), a vector sector of 4 degrees of freedom (π_T^i, B_T^i) and a tensor sector of 2 degrees of freedom. However, not all these degrees of freedom represent physically propagating independent degrees of freedom. The modes Φ, B_L, B_T^i, that form the $\delta g_{0\mu}$ elements enter in the quadratic action of the perturbations without time derivatives, and are not independent degrees of freedom [152]. In Fourier space, the equations of motion for these non-dynamical fields are algebraic in them, and can be solved to give the non-dynamical fields as a function of the dynamical fields, without introducing any additional degree of freedom. Therefore the system of physically propagating perturbations of the model consists of one scalar degree of freedom, π_L, two "vector" degrees of freedom, π_T^i, and two tensor degrees of freedom, h_{ij} (the latter are the two polarizations of the gravitational waves). For our purposes we are interested only in the scalar sector at the linearized level and we refer the interested reader to [7] for a detailed analysis of the vector and tensor modes at the linearized level, and for the calculation of the three point function of the scalar mode at the non-linear level in a FRW

background.

The scalar / vector decomposition appearing in (4.16) is better understood in Fourier space. We Fourier transform each perturbation $\delta(t, \vec{x})$ as

$$\delta(t, \vec{x}) = \int \frac{d^3k}{(2\pi)^{3/2}} e^{i\vec{x} \cdot \vec{k}} \delta\left(t, \vec{k}\right) , \qquad (4.17)$$

(we use the same symbol for the mode in real and in Fourier space, as the context always makes manifest which of the two our following equations refer to). Then, if $\hat{k}_i$ denotes the unit vector in the direction of the momentum of the mode, we have $\pi_L = -i\hat{k}_i \cdot \pi^i$, and $\pi_T^i = \pi^i + i\hat{k}_i \pi_L$ (and identically for B^i).

To study the scalar sector at the linearized level, we expand the action (4.3) at quadratic order in the Fourier modes of π_L, Φ, B_L. The algebraic equations for Φ and B_L obtained by extremizing this action are, respectively, solved by

$$\Phi = k\varepsilon a^2 H \frac{\dot{\pi}_L + \varepsilon H \pi_L}{k^2 + 3\varepsilon a^2 H^2} ,$$

$$B_L = \varepsilon a^2 H \frac{-3a^2 H \dot{\pi}_L + k^2 \pi_L}{k^2 + 3\varepsilon a^2 H^2} . \qquad (4.18)$$

Inserting these solutions back into the quadratic action we obtain the free action for the scalar physical degree of freedom

$$S = \int dt d^3 k a^3 M_p^2 \left(\frac{\varepsilon a^2 H^2 k^2}{k^2 + 3\varepsilon a^2 H^2} |\dot{\pi}_L + \varepsilon H \pi_L|^2 \right.$$

$$\left. -\varepsilon H^2 c_L^2 k^2 |\pi_L|^2 \right) , \qquad (4.19)$$

in agreement with [7]. From this expression we recognize that the speed of the scalar perturbations is indeed c_L in the flat space-time / sub-horizon regime. We are interested in the gauge invariant variable ζ, that represents the curvature perturbation on uniform-density hypersurfaces. In our gauge

$$\zeta\Big|_{\delta g_{ij,\text{scalar}}=0} \equiv -H\frac{\delta\rho}{\dot{\rho}} = -\frac{k}{3}\pi_L , \qquad (4.20)$$

As shown in [7], the variable ζ is continuous if the end of inflation and reheating occur due to a sharp phase transition that modifies F. Therefore, we are interested in the value that ζ assumes on super-horizon scales during inflation. The initial condition for ζ is obtained by computing the canonically normalized variable, in terms of which the action (4.19) acquires the form

$$S = \frac{1}{2} \int d\tau d^3 k \left[|V'|^2 - \omega^2 |V|^2 \right] \Rightarrow V_{\text{in}} = \frac{e^{-i \int^\tau \omega d\tau' + i\phi_0}}{\sqrt{2\omega}} . \qquad (4.21)$$

(the relation between ζ and V is immediately obtained by comparing the kinetic

term of (4.19) and of (4.21)). In this expression, prime denotes derivative with respect to conformal time τ, and ϕ_0 is an arbitrary unphysical phase. The initial condition is the so called adiabatic vacuum solution, set in the deep sub-horizon regime, where the frequency is adiabatically evolving, $\omega' \ll \omega^2$.

As shown in [7], it is actually convenient to consider the curvature perturbations $\mathcal{R}$, that in spatially flat gauge, is related to ζ by

$$\mathcal{R} = \frac{1}{\varepsilon H} \frac{\dot{\zeta} + \varepsilon H \zeta}{1 + k^2/(3a^2\varepsilon H^2)} \quad , \tag{4.22}$$

since the equation of motion for $\mathcal{R}$,

$$\mathcal{R}'' + (2 + \eta - 2s_L) aH\mathcal{R}' + k^2 c_L^2 \mathcal{R} + \left[3\varepsilon - 6s_L + 3c_L^2\varepsilon \right.$$

$$\left. - \varepsilon(2\varepsilon + \eta) + 2s_L(2\varepsilon - \eta) + s_\eta \eta \right] a^2 H^2 \mathcal{R} = 0 \quad , \tag{4.23}$$

is significantly simpler than the one for ζ. In this expression, $s_L \equiv \frac{\dot{c}_L}{c_L H}$ [7], and $s_\eta \equiv \frac{\dot{\eta}}{\eta H}$ are slow roll-suppressed quantities. Eq. (4.23) is exact, but the second line (not explicitly given in [7]) is second order in slow roll and negligible for all the following considerations. Up to first order in slow roll, the solution is

$$\mathcal{R} = C \left(\frac{\tau}{\tau_c} \right)^{-\alpha} H_\nu^{(1)}(-c_L k\tau(1 + s_{L,c})) \quad ,$$

$$\alpha \equiv -\frac{1}{2}(3 + 2\varepsilon_c + \eta_c - 2s_{L,c}) \quad ,$$

$$\nu \equiv \frac{1}{2}\left(3 + 5s_{L,c} - 2c_{L,c}^2\varepsilon_c + \eta_c\right) \quad , \tag{4.24}$$

where τ_c is some time during inflation, and the suffix c indicates that the corresponding quantity is evaluated at τ_c. We have already eliminated the solution $\propto H_\nu^{(2)}$ which approximates to a negative frequency mode in the asymptotic past. We take the time derivative of eq. (4.22) and we combine it with the equation of motion for ζ following from (4.19), [vii] so to eliminate $\dddot{\zeta}$. We obtain an equation relating $\dot{\mathcal{R}}$, ζ, and $\dot{\zeta}$. The system formed by this equation and by eq. (4.22) con be formally solved to express ζ and its derivative in terms of $\mathcal{R}$ and its derivative. We then insert the explicit solution (4.24) and its time derivative into these formal expressions, and obtain

$$\zeta = C \left(\frac{\tau}{\tau_c} \right)^{3/2} \left[1 + \left(\varepsilon_c + \frac{\eta_c}{2} - s_{L,c} \right) \ln \frac{\tau}{\tau_c} \right]$$

$$\times \left[-\frac{\varepsilon_c}{3} H_\nu^{(1)}(Q) + \frac{k\tau}{3c_L}(1 - \varepsilon_c) H_{1+\nu}^{(1)}(Q) \right] \quad , \tag{4.25}$$

where, for brevity, $Q \equiv -k\tau c_L(1 + s_{L,c})$. This expression is valid up to first

---

[vii] We also need to use the explicit solutions for the background quantities given in Appendix A of [7].

order in slow roll. [viii] The coefficient C can be now set from evaluating the solution (4.25) at the asymptotic past $\tau_{\text{in}} \to -\infty$, and from the consideration made right after eq. (4.21):

$$C = -i\sqrt{\frac{\pi}{2}} \frac{(-\tau_c)^{3/2} c_{L,c} H_c}{2M_p \sqrt{\varepsilon_c}} \tag{4.26}$$

(up to subdominant slow roll corrections), where the arbitrary phase has been chosen so that ζ is real and positive in the asymptotic past during inflation. In fact, using (4.25) and (4.26), we can finally write the expression for ζ in the late time / super-horizon regime ($-kc_L\tau \ll 1$):

$$\zeta_{\text{late}} \simeq \frac{H_c}{2k^{3/2} c_L^{5/2} M_p \sqrt{\varepsilon_c}} \left\{ 1 + \varepsilon_c \left[\left(1 + c_{L,c}^2\right) \log\frac{\tau}{\tau_c} + \mathrm{O}\,(1) \right] \right\} , \tag{4.27}$$

in agreement with [7]. It is worth pointing out that the variable ζ presents a (slow roll suppressed) growth outside the horizon [7]. One of the conditions for the conservation of ζ on super-horizon scales is that the anisotropic part of the stress-energy tensor vanishes in that regime [150]. This is the case for minimally coupled scalar fields with $\vec{x}-$independent vev [153]. In the present model, however,

$$\delta T_{ij,\text{scalar}} = a^2 M_p^2 \dot{H} \zeta \Big[2\,(3 - 2\varepsilon + \eta)\,\delta_{ij}$$

$$- \left(3 + 3c_L^2 - 2\varepsilon + \eta\right) \left(3\hat{k}_i\hat{k}_j - \delta_{ij}\right) \Big] , \tag{4.28}$$

where we recall that $\hat{k}_i$ is the unit-vector in the direction of the momentum of the mode. In the standard case, the anisotropic part can be at best proportional to spatial gradients, and therefore vanishes in the large scale limit. This is not the case in the present model, due to the $\vec{x}-$dependent scalar field vevs. We note that $\delta T_{ij,\text{scalar}}$ is slow roll suppressed, which explain why the evolution of ζ on super-horizon scales is also slow-roll suppressed.

[viii]The explicit expression (4.25) has not been given in [7], and we reported its derivation since some of the subdominant terms in ζ and ζ' are needed for the power spectrum computation that we perform in Section 4.5. We have written this expression in the most compact way; doing so, however, it contains also terms which are second or higher order in slow roll, and which should be disregarded. Such terms do not enter in any of our computations.

4.4   Prolonged anisotropic background solution

Let us now consider a Bianchi-I background

$$ds^2 = -dt^2 + a^2\left(t\right)dx^2 + b^2\left(t\right)\left[dy^2 + dz^2\right] \ ,$$
$$a \equiv \mathrm{e}^{\alpha - 2\sigma} \ , \quad b \equiv \mathrm{e}^{\alpha + \sigma} \ , \tag{4.29}$$

where, for simplicity, we have assumed a residual 2d isotropy in the $y - z$ plane (we expect that dropping this assumption would complicate the algebra, without affecting the main physical conclusions of this and of the next Section). We follow the notation of [5] of parametrizing by e^{α} the "average" scale factor (the volume scales as $\sqrt{-g} = \mathrm{e}^{3\alpha}$) and by e^{σ} the anisotropy. In principle, one could also consider anisotropic vevs for the scalar fields, $\langle \phi^i \rangle = c^i x^i$, with c^i being three different constants. However, starting from such configuration, one can always rescale coordinates so that the relation (4.1) is maintained, and the line element is still of the form (4.29).

As we discussed after eq. (4.11), the scalar fields equations of motion are solved by the ansatz (4.1) and (4.29). Let us therefore turn our attention to the Einstein equations $\mathrm{Eq}^{\mu}_{\nu} \equiv G^{\mu}_{\nu} - \frac{T^{\mu}_{\nu}}{M_p^2}$, and, using (4.7) and (4.8), we obtain

$$\dot{\alpha}^2 - \dot{\sigma}^2 + \frac{F}{3M_p^2} = 0 \ ,$$

$$\ddot{\alpha} + 3\dot{\sigma}^2 - \frac{\mathrm{e}^{4\sigma} + 2\mathrm{e}^{-2\sigma}}{3M_p^2}\mathrm{e}^{-2\alpha}F_X = 0 \ ,$$

$$\ddot{\sigma} + 3\dot{\alpha}\dot{\sigma} - \frac{2}{3}\frac{\mathrm{e}^{4\sigma} - \mathrm{e}^{-2\sigma}}{M_p^2}\mathrm{e}^{-2\alpha}F_X$$
$$- \frac{4\mathrm{e}^{6\sigma}\left(\mathrm{e}^{6\sigma} - 1\right)F_Y}{\left(\mathrm{e}^{6\sigma} + 2\right)^3 M_p^2} - \frac{6\mathrm{e}^{6\sigma}\left(\mathrm{e}^{12\sigma} - 1\right)F_Z}{\left(\mathrm{e}^{6\sigma} + 2\right)^4 M_p^2} = 0 \ ,$$

$$\tag{4.30}$$

which correspond, respectively, to the $\frac{\mathrm{Eq}^0_0}{3}$, $\frac{\mathrm{Eq}^1_1 + 2\mathrm{Eq}^2_2 - 3\mathrm{Eq}^0_0}{6}$, and $\frac{\mathrm{Eq}^1_1 - \mathrm{Eq}^2_2}{3}$ combinations of the Einstein equations. Due to the background symmetries, $\mathrm{Eq}^3_3 = \mathrm{Eq}^2_2$, while Eq^{μ}_{ν} identically vanish for $\mu \neq \nu$. Moreover, the three equations (4.30) are actually not independent, since they are related by a nontrivial Bianchi identity $\left(\frac{d}{dt} + 3\dot{\alpha}\right)\mathrm{Eq}^0_0 - \left(\dot{\alpha} - 2\dot{\sigma}\right)\mathrm{Eq}^1_1 - 2\left(\dot{\alpha} + \dot{\sigma}\right)\mathrm{Eq}^2_2 = 0$. Therefore, a closed set of sufficient equations for the two scale factors is obtained by taking for instance the first two, or the first and the third one among (4.30).

The observed statistical isotropy of the CMB constrains the background anisotropy to be small (we quantify this statement in the next Section). Therefore, we restrict the study of the Einstein equations to the $\sigma \ll 1$ regime. Up to $\mathrm{O}\left(\sigma^2\right)$ corrections, the first two equations in (4.30) reduce to the FRW equations

(4.10), where $H = \dot{\alpha}$. The third equation gives instead

$$\ddot{\sigma} + 3\dot{\alpha}\dot{\sigma} - \frac{4\mathrm{e}^{-2\alpha}F_X + \frac{8}{9}\left(F_Y + F_Z\right)}{M_p^2}\sigma + \mathrm{O}\left(\sigma^2\right) = 0 \ . \tag{4.31}$$

Using (4.14), this equation rewrites

$$\ddot{\sigma} + 3H\dot{\sigma} + 4\varepsilon H^2 c_T^2 \sigma + \mathrm{O}\left(\sigma^2\right) = 0 \ ,$$

$$H \equiv \dot{\alpha} \ , \ \ \varepsilon \equiv -\frac{\dot{H}}{H^2} \ . \tag{4.32}$$

where we have recalled the definitions of the "average" Hubble rate H, and of the slow roll parameter ε. As $\mathrm{O}\left(\sigma^2\right)$ are disregarded in (4.32), such quantities can be evaluated from the FRW equations (4.10), disregarding the anisotropy.

In the case of standard scalar field inflation, the normalization of the scale factors is unphysical (for a flat geometry), and the anisotropy is encoded in the "anisotropic Hubble rate" $h \equiv \dot{\sigma}$. This quantity obeys the equation $\dot{h} + 3Hh = 0$ (see for instance [10]), which corresponds to the first two terms in (4.32). This equation is solved either by the FRW geometry, $h = 0$, or by an exponentially decreasing anisotropy, $h \propto \mathrm{e}^{-3Ht}$ (we disregard the slow roll decrease of H). This is at the basis of the cosmic no-hair conjecture, according to which inflation is expected to rapidly erase any background anisotropy.
In the present model, with the scale factors appearing in B^{ij} (see eq. (4.4)), also σ, and not only its derivative, is physical. To solve eq. (4.32), we perform the ansatz

$$\sigma\left(t\right) \propto \mathrm{e}^{\int^t dt' \lambda(t')H(t')} \ \ \Rightarrow \ \ \frac{\dot{\lambda}}{H} + \lambda^2 + \left(3 - \varepsilon\right)\lambda + 4\varepsilon c_T^2 = 0 \ . \tag{4.33}$$

where we recall that ε, H, c_T in this equation are evaluated on the FRW geometry. We solve this equation to leading order in the slow roll parameters. We obtain

$$\lambda_1 = -3 + c_1\left(t\right)\varepsilon + \mathrm{O}\left(\varepsilon^2\right) \ , \ \ \lambda_2 = c_2\left(t\right)\varepsilon + \mathrm{O}\left(\varepsilon^2\right) \ , \tag{4.34}$$

where, in turns,

$$\frac{\dot{c}_1}{H} + 6 - 3c_1 + 3c_L^2 = 0 \ , \ \ \frac{\dot{c}_2}{H} + 3c_2 + 4c_T^2 = 0 \ . \tag{4.35}$$

Given eqs. (4.13) and (4.14), and given that Y and Z are constant on a FRW background, it is very reasonable to assume that $\dot{c}_{L,T} = \mathrm{O}\left(\varepsilon H\right)$ or less. In this case, [ix]

$$c_1 = 2 + c_L^2 \ , \ \ c_2 = -\frac{4}{3}c_T^2 \ . \tag{4.36}$$

Therefore, to leading order, the anisotropy evolves as

$$\sigma\left(t\right) \simeq \sigma_1 \mathrm{e}^{-\int\left[3 - \left(2 + c_L^2\right)\varepsilon\right]Hdt} + \sigma_2 \mathrm{e}^{-\int \frac{4}{3}c_T^2 \varepsilon Hdt} \ , \ \ \sigma, \varepsilon \ll 1 \ , \tag{4.37}$$

[ix] We stress that the prolonged anisotropy is not consequence of $\dot{c}_T = \mathrm{O}\left(\varepsilon H\right)$. Even if $\dot{c}_T = \mathrm{O}\left(H\right)$, the exponent $\lambda_2 = \mathrm{O}\left(\varepsilon\right)$, which guarantees a slow isotropization.
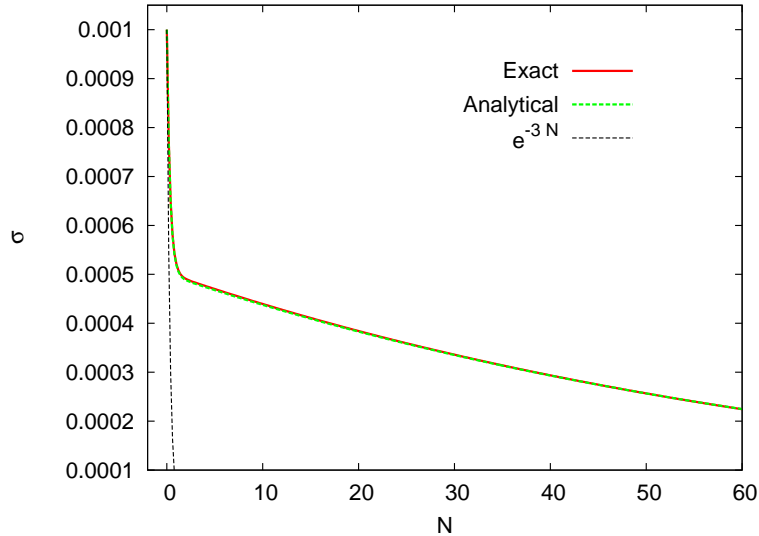
Figure 4.1: Evolution of the anisotropy σ (defined in eq. (4.29)) as a function of the number of e-folds (of the average scale factor α) for the model (4.38), and for an initial approximately equal admixture of the two modes in (4.37). The analytical solution (4.37) shows a perfect agreement with the exact one. The line $\propto \mathrm{e}^{-3N}$ shows the decrease of the fast decreasing mode. We note that this is also the rate at which the anisotropy $\dot{\sigma}$ decreases in standard inflationary models

where σ_1 and σ_2 are integration constant. The first term is (up to the subleading slow-roll correction) the fast decreasing solution found in standard slow roll inflation. The second term is a new, slowly decreasing solution, that is peculiar of this model. We note that, as we anticipated, the coefficient λ_2 is proportional to the sound speed of the transverse modes; this testifies that the evolution of the phonons and of the anisotropy are determined by how the medium reacts to deformations. As we already showed, the solid that drives inflation needs to be extremely inefficient in responding to changes in the volume, and to the anisotropy.

In Figure 4.1 we compare the approximate solution (4.37) for the anisotropy against the exact solution obtained by numerically evolving the system (4.30). We choose the simplest possibility

$$F = F_0 X^{\varepsilon} \ . \tag{4.38}$$

It is immediate to verify that, at $\mathrm{O}\left(\sigma^0\right)$, the parameter ε introduced in this function coincides with the slow roll parameter $\varepsilon = -\frac{\dot{H}}{H^2}$. With this choice, we obtain the sound speeds $c_T^2 = 1$, and $c_L^2 = \frac{1}{3}$.

In the evolution shown in the Figure, we choose $\varepsilon = 0.01$ and $\sigma_{\mathrm{in}} = 0.001$. We want to verify the validity of the approximate analytical solution (4.37). Therefore, we assume that it is valid, and we choose an initial condition that

is an approximately equal admixture of both modes in (4.37). We do so by taking the initial value $\dot{\sigma}_{\text{in}} = \frac{\sigma_{\text{in}}}{2} H \left[-3 + \left(2 + c_L^2 \right) \varepsilon - \frac{4}{3} c_T^2 \varepsilon \right]$. We then use the first equation in (4.30) to set the initial condition $\dot{\alpha}_{\text{in}}$, and evolve numerically the last two equations in (4.30) (for the choice (4.38), the initial value α_{in} can be reabsorbed in F_0, which can then be rescaled away from the system of equations). If eq. (4.37) is a good approximation of the exact solution, we must obtain that the anisotropy drops to about half its initial value within the first few e-folds [x] - corresponding to the fast decreasing component in (4.37) - followed by a much smaller decrease - corresponding to the second term in (4.37). This is precisely what the evolution in the figure shows. More precisely, we show both the exact numerical solution, and the analytic solution (4.37), and we see that the analytic solution is in excellent agreement with the exact one. In the figure, we also show the curve $\sigma = \sigma_{\text{in}} e^{-3N}$. This curve has the same decrease of the fast decreasing mode. As we discussed, this reproduces the decrease of the anisotropy in standard models of scalar field inflation.

Finally, we note that, strictly speaking, inflation never terminates for the choice (4.38). As in ref. [7], we are assuming that (4.38) describes the function only for a finite range of X, and then inflation terminates due to a change of F (for example, due to a phase transition that transforms the solid into a fluid [7]). In the evolution shown, we are simply following the evolution of the anisotropy for 60 e-folds of inflation. For a longer duration of inflation, one finds that the fast decreasing mode of (4.37) has already decreased to negligible values during the entire last ~ 60 e-folds of inflation.

4.4.1 Comparison with Wald's isotropization theorem

Ref. [11] showed that a Bianchi geometry (with the possible exception of the type-IX case) undergoes a rapid isotropization under the influence of a cosmological constant plus a source that satisfies the dominant and strong energy conditions. It is instructive to understand how the theorem precisely works and why it does not apply to the present context. To do this, we first summarize the computation of [11], and we then discuss the specific case of anisotropic solid inflation.
In the case analyzed by [11], the energy momentum tensor acquires the form

$$ T_{\mu\nu} \quad = \quad -\Lambda M_p g_{\mu\nu} + T_{\mu\nu}^{\text{2nd source}} , \tag{4.39} $$

where the first term is the cosmological constant contribution, and the second term satisfies the dominant and strong energy conditions $\mathcal{D} \geq 0$ and $\mathcal{S} \geq 0$,

---

[x]The number of e-folds shown in the figure is $N = e^{\alpha - \alpha_{\text{in}}}$. It is accurate to use the "average" expansion rate as a measure of the expansion, since the anisotropy is extremely small, $\dot{\sigma} \ll \dot{\alpha}$.

where

$$
\begin{aligned}
\mathcal{D} &\equiv t^\mu t^\nu T_{\mu\nu}^{\text{2nd source}} \ , \\
\mathcal{S} &\equiv t^\mu t^\nu \left(T_{\mu\nu}^{\text{2nd source}} - \frac{T^{\text{2nd source}}}{2} g_{\mu\nu} \right) \ ,
\end{aligned}
\tag{4.40}
$$

and where t^μ is any time-like future-directed vector.

Ref. [11] contracted the Einstein equations with a normal vector n^μ, to obtain their equations (9) and (10). In the Bianchi-I geometry (4.29) and in our notation, these equations read, respectively,

$$
\begin{aligned}
K^2 - 3\Lambda - \frac{3}{2}\sigma^{\mu\nu}\sigma_{\mu\nu} - \frac{3\,\mathcal{D}}{M_p^2} &= 0 \ , \\
\frac{d}{dt}K - \Lambda + \frac{K^2}{3} + \sigma^{\mu\nu}\sigma_{\mu\nu} + \frac{\mathcal{S}}{M_P^2} &= 0 \ ,
\end{aligned}
\tag{4.41}
$$

where we have set $n^\mu = t^\mu = \{1,0,0,0\}$. In this expression, K and $\sigma_{\mu\nu}$ are, respectively, the trace and the trace-free part of the extrinsic curvature on surfaces orthogonal to n^μ. For us , $K = 3\dot\alpha$, and $\sigma^{\mu\nu}\sigma_{\mu\nu} = 6\dot\sigma^2$, which are, respectively, the isotropic and anisotropic Hubble rates in (4.29). As long as the dominant and strong energy condition hold, $\mathcal{D},\mathcal{S} \geq 0$, the two equations (4.41) imply [11]

$$
\mathcal{D},\mathcal{S} \geq 0 \ \Rightarrow \ K > \sqrt{3\Lambda} \ , \ \frac{1}{K^2 - 3\Lambda}\frac{dK}{dt} \leq -\frac{1}{3} \ .
\tag{4.42}
$$

The second relation can be then integrated and combined with the first one to show that $K \to \sqrt{3\Lambda}$ with exponential accuracy on a timescale $\sqrt{3/\Lambda}$ [11]. Inserting this result into the first of (4.41), we then see that $\sigma^{\mu\nu}\sigma_{\mu\nu} \to 0$ on the same timescale. We thus recover an (isotropic) de Sitter expansion driven by Λ [11]. The inequalities (4.42) play a crucial role for this result. We stress that they are a consequence of the dominant and strong energy conditions.

Let us now discuss solid inflation, for which the energy momentum is given in eq. (4.7). Strictly speaking, this is not the energy momentum tensor of a cosmological constant plus a second source; however, given that the model supports inflation, it still proves useful for the comparison with [11] to use this two component decomposition as an effective description. The form of (4.7) would suggest to identify the first term as the cosmological constant contribution. However, the function F is not constant (but rather slow roll evolving), and the proof in [11] would not apply. We therefore decompose eq. (4.7) as

$$
\begin{aligned}
T_{\mu\nu} &= g_{\mu\nu}F(t_0) + \left\{ g_{\mu\nu}[F(t) - F(t_0)] - 2\partial_\mu\phi^i\partial_\nu\phi^j \frac{\partial F}{\partial B^{ij}} \right\} \\
&\equiv -\Lambda M_p^2 g_{\mu\nu} + T_{\mu\nu}^{\text{2nd source}} \ ,
\end{aligned}
\tag{4.43}
$$

where $\Lambda \equiv -F(t_0)/M_p^2 > 0$, and where t_0 is a fixed time during inflation, say the starting time, at which the geometry is of the Bianchi-I type, and one is interested in whether the rapid isotropization takes place.

Inserting (4.43) into (4.40) we obtain

$$
\begin{aligned}
\mathcal{D} &= -F\left(t\right) + F\left(t_0\right) \ , \\
\mathcal{S} &= F\left(t\right) - F\left(t_0\right) - F_X\left(\frac{1}{a^2} + \frac{2}{b^2}\right) \ ,
\end{aligned}
\tag{4.44}
$$

and, using these expressions, we can readily verify the system (4.41) is equivalent to the three background equations (4.30) (we recall that only two of these equations are independent). We have already solved these equations in the first part of this Section, and we have obtained that the anisotropy is not erased on the timescale $\sqrt{3/\Lambda}$. The technical reason for this is that $\mathcal{D} < 0$ in this model (while instead $\mathcal{S} > 0$). This is due to the fact that F is negative and it decreases in magnitude during inflation. As a consequence, the two conditions (4.42) do not hold.

We have therefore shown that the total energy momentum tensor of solid inflation cannot be rewritten as the sum of a cosmological constant plus a second term that satisfies the dominant and strong energy conditions, which explains why Wald's theorem does not apply. One may worry that the failure of the dominant energy condition might be a signal of instability. This is not the case, since the split in (4.43) is only an effective description to be able to compare with the premise of Wald's theorem, but there is no instability associated with the full energy momentum tensor.

4.5   Scalar curvature perturbations on the anisotropic solution

We now compute the primordial perturbation $\hat{\zeta}$ on the anisotropic background obtained in the previous Section. As we shall see, the observed statistical isotropy of the CMB perturbations forces the background anisotropy to be small, $\sigma \ll 1$. Therefore, we can compute $\hat{\zeta}$ in a perturbative expansion around the FRW solution studied in Section 4.3. [xi] We perform the computation through the in-in formalism:

$$
\begin{aligned}
\left\langle \hat{\zeta}_{\vec{k}_1} \hat{\zeta}_{\vec{k}_2}\left(\tau\right) \right\rangle &= \sum_{N=0}^{\infty} (-i)^N \int^{\tau} d\tau_1 \ldots \int^{\tau_{N-1}} d\tau_N \\
&\quad \left\langle \left[\left[\ldots \left[\hat{\zeta}_{\vec{k}_1}^{(0)} \hat{\zeta}_{\vec{k}_2}^{(0)}\left(\tau\right), H_{\text{int}}\left(\tau_1\right)\right], \ldots\right], H_{\text{int}}\left(\tau_N\right)\right] \right\rangle
\end{aligned}
\tag{4.45}
$$

where $H_{\text{int}} = -\int d^3x \mathcal{L}_{\text{int}}$, and $\mathcal{L}_{\text{int}}$ is the quadratic lagrangian for the perturbations on the Bianchi background minus the quadratic lagrangian on a FRW

[xi]In this Section, $\hat{\zeta}$ (respectively $\hat{\zeta}^{(0)}$) denotes the curvature perturbation of the anisotropic background (resp. on the FRW background). The hat denotes the quantum operator for the curvature, expanded in terms of annihilation / creation operators and of the mode function ζ (resp. $\zeta^{(0)}$), see eq. (4.57). The FRW mode function $\zeta^{(0)}$ is given in (4.25), where it was denoted without the (0) suffix.

$$\begin{matrix} & & L_{LL} & & L_{LL} \ L_{LL} & & L_{LT} \ L_{LT} \\ \text{-------} & + & \text{----×----} & + & \text{---×--×---} & + & \text{---×$\sim$×---} & + & \dots \end{matrix}$$

Figure 4.2: Leading diagrams for $\langle \hat{\zeta}^2 \rangle$ on an anisotropic background. The first diagram is the FRW result, while the second diagram is the linear correction in the anisotropy. Only these two diagrams are computed in the main text. We disregard quadratic (the last two diagrams shown) and higher order corrections in the anisotropy.

background (we disregard terms that are higher order than quadratic in the perturbations inside $\mathcal{L}_{\text{int}}$). We note that each term in $\mathcal{L}_{\text{int}}$ can be written as an expansion series in the anisotropy σ, that, in general, starts at $\mathrm{O}(\sigma)$.

In the in-in formalism, perturbations are quantized in the interaction picture: this means that, in our computation, the FRW quantization of [7] applies. However, due to the anisotropy, the scalar/vector/tensor perturbations are no longer decoupled from each other in the full quadratic action, and this gives rise to additional terms in $\mathcal{L}_{\text{int}}$. Due to the residual SO(2) background isotropy of (4.29), one mode of π_T^i and one mode of h_{ij} remain decoupled from π_L at the quadratic level [10]. Therefore, $\mathcal{L}_{\text{int}}$ couples $\zeta^{(0)}$ with one mode of π_T^i and one mode of h_{ij}. Since $\mathcal{L}_{\text{int}}$ is quadratic in the fields, its terms can be diagrammatically visualized as the "mass insertions" L_{LL} (terms involving two scalar modes), L_{LT} (terms involving one scalar and one vector mode), L_{LH} (terms involving one scalar and one tensor mode), L_{TT}, L_{TH}, and L_{HH}. Figure (4.2) shows some of the leading order contributions to $\langle \hat{\zeta}^2 \rangle$ arising when these mass insertions are used in (4.45) (the variable N in (4.45) coincides with the number of mass insertions present in the diagram). In the Figure, dashed lines denote the scalar mode; curved line denotes the vector mode, and the crosses denote mass insertions.

It is clear from the Figure that the interactions between the scalar mode (L) and one of the other two modes (T or H) contribute to $\langle \hat{\zeta}^2 \rangle$ only at $\mathrm{O}(\sigma^2)$ or higher. Therefore, if L_{LL} provides the only $\mathrm{O}(\sigma)$ contribution to $\langle \hat{\zeta}^2 \rangle$, it is the dominant correction to the power spectrum of $\hat{\zeta}$ due to the anisotropy. We now compute this contribution. We do so in two Subsections. In Subsection 4.5.1 we compute the interaction hamiltonian. In Subsection 4.5.2 we insert the interaction hamiltonian in (4.45) and evaluate the correction of the power spectrum due to the anisotropy.

4.5.1 │ Computation of H_{int}

To obtain L_{LL}, we set to zero all the perturbations apart from the scalar one. For the three scalar fields, this means

$$\phi^i = x^i - 3i \int \frac{d^3k}{(2\pi)^{3/2}} \mathrm{e}^{i\vec{k}\cdot\vec{x}} \frac{k^i}{k^2} \hat{\zeta}\left(t, \vec{k}\right) \ , \tag{4.46}$$

where the relation (4.20) has been used.

We recall that we are working in the spatially flat gauge, so that the spatial part g_{ij} of the metric is given by (4.29). We instead introduce perturbations in $g_{00} = -1 - 2\Phi$, and $g_{0i} = \delta g_{0i}$, which need to be retained as they are nondynamical and are algebraically given in terms of $\hat{\zeta}$ and $\dot{\hat{\zeta}}$ (from the linearized Einstein equation, which is equivalent to extremizing the quadratic action of the perturbations with respect to them). We then evaluate the action up to second order in the perturbations, and integrate out the nondynamical modes in $\delta g_{0\mu}$. The solutions for Φ and δg_{0i} in terms of $\hat{\zeta}$ and $\dot{\hat{\zeta}}$ are rather lengthy and not illuminating, and so we do not explicitly report them here. We insert the solutions back in the quadratic action, which then becomes the action for the dynamical mode $\hat{\zeta}$ only. This is the standard procedure to obtain the quadratic action for the perturbations of any system. The resulting expression is formally of the type

$$
\begin{aligned}
S\left[\hat{\zeta}\right] &= \int dt d^3k \Bigg\{ f_{\text{kin}}\left[\alpha, \dot{\alpha}, \sigma, \dot{\sigma}\right] |\dot{\hat{\zeta}}|^2 + f_{\text{mas}}\left[\alpha, \dot{\alpha}, \sigma, \dot{\sigma}\right] |\hat{\zeta}|^2 \\
&\quad + \left(f_{\text{mix}}\left[\alpha, \dot{\alpha}, \sigma, \dot{\sigma}\right] \dot{\hat{\zeta}}^* \hat{\zeta} + \text{h.c.} \right) \Bigg\} ,
\end{aligned} \tag{4.47}
$$

where the three functions are functions of the background (we eliminate $\ddot{\alpha}$ and $\ddot{\sigma}$ from these expressions by the use of the background equations of motion (4.30); specifically, we enforce the background equations by expressing $\ddot{\alpha}, \ddot{\sigma}$ and F as a function of the other quantities. Thanks to this, we are sure that our expressions cannot be further simplified by the use of the background equations). The explicit expressions for these three functions (that we obtained by the use of Mathematica), are extremely lengthy, and not illuminating, and for this reason we do not report them here. We expand these expressions in the anisotropy parameter σ, and obtain an expansion of the action $S\left[\hat{\zeta}\right]$ in the anisotropy. We formally write the resulting expression as

$$
S\left[\hat{\zeta}\right] = \sum_{n=0}^{\infty} S^{(n)}\left[\hat{\zeta}\right] , \tag{4.48}
$$

where $S^{(n)}$ is of order n in the anisotropy. Namely, it is obtained by the $\text{O}\left(\sigma^n, \sigma^{n-1}\dot{\sigma}, \sigma^{n-2}\dot{\sigma}^2, \ldots, \dot{\sigma}^n\right)$ expressions for f_{kin}, f_{mix}, and f_{mas}. We verified that, as it must be, the zeroth-order action $S^{(0)}$ coincides with (4.19). According to the above discussion, we are only interested in the explicit expression for $S^{(1)}$, as this is the term that gives L_{LL} at first order in the anisotropy. Inside $S^{(0)} + S^{(1)}$, the following functional derivatives of F appear: $F_X, F_Y, F_Z, F_{XX}, F_{XY}, F_{XZ}$. These functions can be evaluated in the FRW background, as the three invariants X, Y, Z in the Bianchi geometry coincides with that in the FRW geometry up to $\text{O}\left(\sigma^2\right)$. We eliminate the mix term $\propto f_{\text{mix}}$ from this expression through an integration by parts. This introduces the three derivatives $\frac{d}{dt}F_X, \frac{d}{dt}F_Y$, and $\frac{d}{dt}F_Z$, which we evaluate through $\frac{d}{dt}F_i = \dot{X} F_{iX} \cong -6e^{-2\alpha}\dot{\alpha} F_{iX}$ (where $\cong$ indicates that the two expression coincide up to second order corrections in the anisotropy). Therefore, proceeding as just indicated, we obtain an expression for $S^{(1)}$ where

F only explicitly enters through its $F_X, F_Y, F_Z, F_{XX}, F_{XY}, F_{XZ}$ derivatives, evaluated on the FRW background. It is useful to rewrite these derivatives in terms of more immediate physical parameters, as the slow roll parameters and the sound speed. Using (4.13) and (4.14), we can write

$$
\begin{aligned}
F_X &= -\mathrm{e}^{2\alpha} M_p^2 \varepsilon \dot{\alpha}^2 \ , \\
F_{XX} &= \frac{1}{6}\mathrm{e}^{4\alpha} M_p^2 \varepsilon \left(2 - 2\varepsilon + \eta\right) \dot{\alpha}^2 \ , \\
F_Y + F_Z &= \frac{9}{2} M_p^2 \left(1 - c_T^2\right) \varepsilon \dot{\alpha}^2 \ .
\end{aligned}
\tag{4.49}
$$

The combination $F_Y - F_Z$ is not related to any background quantity defined above. In analogy with the last of (4.49) we define

$$
F_Y - F_Z \equiv \frac{9}{2} M_p^2 \mu \varepsilon \dot{\alpha}^2 \ .
\tag{4.50}
$$

where it is reasonable to assume that also μ is of order one, and slowly varying. Differentiating the last of (4.49) we obtain

$$
F_{XY} + F_{XZ} = \frac{3}{4}\mathrm{e}^{2\alpha} M_P^2 \varepsilon \left[2\varepsilon - \eta + c_T^2 \left(2s_T - 2\varepsilon + \eta\right)\right] \dot{\alpha}^2 \ ,
\tag{4.51}
$$

where, in analogy to [7], we have defined the slow roll quantity $s_T \equiv \frac{\dot{c}_T}{\dot{\alpha} c_T}$. Finally, we find that $F_{XY} - F_{XZ}$ does not enter in $S^{(1)}$. Using these expressions, the $\mathrm{O}(\sigma)$ action for $\hat{\zeta}$ acquires the form (4.47), with

$$
\begin{aligned}
f_{\mathrm{kin}}^{(1)} &= 18\mathrm{e}^{3\alpha} M_p^2 \varepsilon \dot{\alpha}^2 P_2\left(\cos\theta\right) \frac{2p^2 \left(c_T^2 - 1\right)\sigma + 3\varepsilon\dot{\alpha}\dot{\sigma}}{\left(p^2 + 3\varepsilon\dot{\alpha}^2\right)^2} \ , \\
f_{\mathrm{mas}}^{(1)} &= \frac{3\mathrm{e}^{3\alpha} M_p^2 \varepsilon \dot{\alpha}^2}{\left(p^2 + 3\varepsilon\dot{\alpha}^2\right)^3} P_2\left(\cos\theta\right) \left[c_6 p^6 + c_4 p^4 + c_2 p^2 + c_0\right] \ ,
\end{aligned}
\tag{4.52}
$$

with

$$
\begin{aligned}
c_6 &= 4\left[5 - 2c_T^2 \left(2 - 2s_T + 2\varepsilon - \eta\right) - \mu\right]\sigma \ , \\
c_4 &= 12\varepsilon \left[20 - 4\varepsilon + 2\eta - 2c_T^2 \left(11 - 4s_T + 2\varepsilon - \eta\right) - 3\mu\right]\dot{\alpha}^2\sigma \\
&\quad + 6\varepsilon \left[3 - 4c_T^2 - 2\varepsilon + \eta\right]\dot{\alpha}\dot{\sigma} \ , \\
c_2 &= 36\varepsilon^2 \left[16 - c_T^2 \left(21 - 6s_T + 4\varepsilon - 3\eta\right) - 3\mu\right]\dot{\alpha}^4\sigma \\
&\quad - 9\varepsilon^2 \left(2 + 12c_T^2 - 4\varepsilon + 3\eta\right)\dot{\alpha}^3\dot{\sigma} \ , \\
c_0 &= 108\varepsilon^3 \left[5 - c_T^2 \left(7 - 2s_T - \eta\right) - \mu\right]\dot{\alpha}^6\sigma \\
&\quad - 27\varepsilon^3 \left(4c_T^2 + \eta\right)\dot{\alpha}^5\dot{\sigma} \ .
\end{aligned}
\tag{4.53}
$$

In (4.52), $p \equiv k\mathrm{e}^{-\alpha}$ is the physical momentum of the mode, θ the angle between the direction of the momentum and the anisotropic direction $\hat{x}$, and P_2 is the Legendre polynomial of order two. Moreover, we recall that $f_{\mathrm{mix}} = 0$ thanks to

the integration by parts.

As we are interested in the perturbations around the slowly decreasing anisotropic solution obtained in the previous Section, we set $\dot{\sigma} \cong -\frac{4}{3}c_T^2 \varepsilon H \sigma$ (we recall that $H = \dot{\alpha}$). The expressions (4.52) then become

$$
\begin{aligned}
f_{\text{kin}}^{(1)} &\cong -36\mathrm{e}^{3\alpha} M_p^2 \varepsilon H^2 P_2 \left(\cos\theta\right) \sigma \frac{\left(1-c_T^2\right) p^2 + 2c_T^2 \varepsilon^2 H^2}{\left(p^2 + 3\varepsilon H^2\right)^2} \ , \\
f_{\text{mas}}^{(1)} &\cong \frac{12\mathrm{e}^{3\alpha} M_p^2 \varepsilon H^2 \sigma}{\left(p^2 + 3\varepsilon H^2\right)^3} P_2 \left(\cos\theta\right) \left[p^6 \left(5 - 4c_T^2 - \mu\right) \right. \\
&\quad + 3\varepsilon H^2 p^4 \left(20 - 22c_T^2 - 3\mu\right) + 9\varepsilon^2 H^4 p^2 \left(16 - 21c_T^2 - 3\mu\right) \\
&\quad \left. + 27\varepsilon^3 H^6 \left(5 - 7c_T^2 - \mu\right) \right] \ ,
\end{aligned}
\tag{4.54}
$$

where we have disregarded terms of $\mathrm{O}\left(\varepsilon, \eta, s_T\right)$ or higher when compared with $\mathrm{O}\left(1\right)$ terms. Finally, switching to conformal time, from the expression (4.47) we obtain the interaction hamiltonian

$$
\begin{aligned}
H_{\text{int}}^{(1)} \left(\tau\right) &= -\int d^3k \left[\mathrm{e}^{-\alpha} f_{\text{kin}}^{(1)} \hat{\zeta}_{-\vec{k}}^{(0)\prime} \left(\tau\right) \hat{\zeta}_{\vec{k}}^{(0)\prime} \left(\tau\right) \right. \\
&\quad \left. + \mathrm{e}^{\alpha} f_{\text{mas}}^{(1)} \hat{\zeta}_{-\vec{k}}^{(0)} \left(\tau\right) \hat{\zeta}_{\vec{k}}^{(0)} \left(\tau\right) \right] + \mathrm{O}\left(\sigma^2\right) \ .
\end{aligned}
\tag{4.55}
$$

4.5.2 | Evaluation of the power spectrum

We now insert (4.55) into (4.45) , to obtain

$$
\begin{aligned}
\left\langle \hat{\zeta}_{\vec{k}_1} \hat{\zeta}_{\vec{k}_2} \left(\tau\right) \right\rangle &= \left\langle \hat{\zeta}_{\vec{k}_1}^{(0)} \hat{\zeta}_{\vec{k}_2}^{(0)} \left(\tau\right) \right\rangle \\
&\quad -i \int^\tau d\tau_1 \left\langle \left[\hat{\zeta}_{\vec{k}_1}^{(0)} \hat{\zeta}_{\vec{k}_2}^{(0)} \left(\tau\right), H_{\text{int}}^{(1)} \left(\tau_1\right) \right] \right\rangle + \mathrm{O}\left(\sigma^2\right) \ .
\end{aligned}
\tag{4.56}
$$

To evaluate this expression, we decompose the quantum field $\hat{\zeta}_{\vec{k}}$ into

$$
\hat{\zeta}_{\vec{k}} \left(\tau\right) = \zeta_{\vec{k}} \left(\tau\right) a_{\vec{k}} + \zeta_{-\vec{k}}^* \left(\tau\right) a_{-\vec{k}}^\dagger \ , \quad \left[a_{\vec{k}}, a_{\vec{k}'} \right] = \delta^{(3)} \left(\vec{k} + \vec{k}'\right) \ ,
\tag{4.57}
$$

and identically for $\hat{\zeta}^{(0)}$.

The two point correlation function is related to the power spectrum by

$$
\left\langle \hat{\zeta}_{\vec{k}_1} \left(\tau\right) \hat{\zeta}_{\vec{k}_2} \left(\tau\right) \right\rangle \equiv 2\pi^2 \frac{\delta^{(3)} \left(\vec{k}_1 + \vec{k}_2\right)}{k_1^3} P_\zeta \left(\vec{k}_1\right) \ ,
\tag{4.58}
$$

and we finally define

$$P_\zeta\left(\vec{k}\right) = P_\zeta^{(0)}\left(k\right) + P_\zeta^{(1)}\left(\vec{k}\right) + \mathrm{O}\left(\sigma^2\right) , \tag{4.59}$$

corresponding, respectively, to the unperturbed FRW correlator and to the first order correction in σ. To leading order in slow roll, the FRW expression (4.27) gives

$$P_\zeta^{(0)}\left(\vec{k}\right) = \frac{k^3}{2\pi^2}\left|\zeta_k^{(0)}\right|^2 \simeq \frac{1}{8\pi^2 c_L^5}\frac{H^2}{M_p^2\varepsilon} , \quad -c_L k\tau \ll 1 . \tag{4.60}$$

For the first order correction, evaluating the commutator and the expectation value in (4.56) we obtain

$$
\begin{aligned}
P_\zeta^{(1)}\left(\vec{k}\right) &= \frac{2k^3}{\pi^2} \times \\
&\mathrm{Im}\left[\zeta_k^{(0)*2}\left(\tau\right)\int^\tau d\tau_1\left(\mathrm{e}^{-\alpha}f_{\mathrm{kin}}^{(1)}\zeta^{(0)\prime 2} + \mathrm{e}^{\alpha}f_{\mathrm{mas}}^{(1)}\zeta^{(0)2}\right)_{\tau_1,\vec{k}}\right] .
\end{aligned}
\tag{4.61}
$$

We inserted the solution (4.25)-(4.26) into this expression. We could not perform the time integration in an exact closed form, and we therefore divided the integral into the two regimes $-\infty < \tau_1 < -\mathrm{O}\left(\frac{1}{c_L k}\right)$, and $-\mathrm{O}\left(\frac{1}{c_L k}\right) < \tau_1 < \tau$. In the first regime, we used the sub-horizon limit of (4.25) for $\zeta\left(\tau_1\right)$ and its derivative, while in the second regime we used the super-horizon limit. For $\zeta\left(\tau\right)$ we instead use the super horizon limit of (4.25), given that we are interested in the super-horizon value for $P_\zeta^{(1)}$. Proceeding in this way, we obtain the estimate

$$\frac{P_\zeta^{(1)}\left(\vec{k}\right)}{P_\zeta^{(0)}\left(k\right)} = P_2\left(\cos\theta\right)\sigma\left[\left(1 + 24c_L^2 + 4\mu^2\right)\varepsilon N_{\mathrm{cmb}} + \mathrm{O}\left(1\right)\right] \tag{4.62}$$

where the first term in the square parenthesis is the contribution from the late time integration limit $\tau_1 \lesssim \tau$, while the second term is the contribution from τ_1 in the sub-horizon regime and at horizon crossing. The second contribution may be the dominant one, so we regard (4.62) as an estimate of $P_\zeta^{(1)}$, which we will use to set an order of magnitude upper bound on the anisotropy parameter σ. We recall that P_2 is the Legendre polynomial of order two, while θ is the angle between $\vec{k}$ and the anisotropic direction. The quantity σ, as well as the other quantities on the right hand side of (4.62) are the values assumed at horizon crossing.

Therefore our estimate for the power spectrum of ζ on super-horizon scales is

$$P_\zeta\left(\vec{k}\right) = \frac{1}{8\pi^2 c_L^5}\frac{H^2}{M_p^2\varepsilon}\left[1 + \mathrm{O}\left(1\right)\sigma P_2\left(\cos\theta\right)\right] . \tag{4.63}$$

Let us conclude this section with a few comments. First, from Eq. (4.63) we can read the anisotropic amplitude of the power-spectrum g_* in the parameteriza-

tion [8]

$$P_\zeta\left(\vec{k}\right) = P\left(k\right)\left[1 + g_* \cos^2\theta\right] . \qquad (4.64)$$

We find, in the phenomenologically allowed region $|g_*| \ll 1$, that $g_* = O(1)\,\sigma$. Different limits have been obtained on such a parameter, starting from the analysis of the WMAP7 data [33] that gives $g_* = 0.29 \pm 0.031$ [65]. Such a large effect has been clearly demonstrated to be due to beam asymmetries in WMAP9 data [64, 66, 14] and is not present in the Planck data [4]. On different scales (and marginalizing over the preferred direction) Large-Scale Structure data analysis constrain $-0.41 < g_* < 0.38$ at 95% C.L. [69] (the amplitude of the anisotropy may in general be scale dependent [8]). Therefore a 10% level anisotropy, $|g_*| = 0.1$ ((1%) level, $|g|_* = 0.01$) would correspond to an anisotropy parameter $\sigma \simeq 0.1$ (0.01).

As a second comment, notice that g_*, being determined by σ, is not simply proportional to the "anisotropic Hubble rate" $\Delta H/H = \dot{\sigma}/H$, as one might naively expect. Rather, since $\dot{\sigma} \propto c_T^2 \varepsilon H \sigma$ (see eq. (4.37)), g_* turns out to be

$$g_* = \mathrm{O}\left(\frac{\Delta H}{\varepsilon\,H}\right) \gg \mathrm{O}\left(\frac{\Delta H}{H}\right) \qquad (4.65)$$

This is analogous to what happens in the $f\left(\phi\right)F^2$ models [90, 61, 91].

As a third comment, we note that the final background anisotropy still present at the end of inflation may give rise to corrections to the variable ζ which are of $\mathrm{O}\left(\frac{\Delta H}{H}|_{\mathrm{end}}\right) = \mathrm{O}\left(\frac{\dot{\sigma}}{H}|_{\mathrm{end}}\right) = \mathrm{O}\left(\varepsilon_{\mathrm{end}}\sigma_{\mathrm{end}}\right)$, where the suffix "end" refers to the value assumed at the end of inflation. This, and - more in general - the dynamics of reheating after inflation, may generate corrections to the observed value of P_ζ. As discussed in [7], it is reasonable to assume that in this model inflation is terminated by a phase transition, during which the solid decays into conventional matter. Ref. [7] computed the perturbations of solid inflation on an isotropic background, showing that ζ is continuous at this transition. Therefore, any correction to g_* that emerges from these effects can be at most of $\mathrm{O}\left(\sigma_{\mathrm{end}}\right)$ which is parametrically much smaller than the $\mathrm{O}\left(\frac{\sigma}{\varepsilon}\right)$ value that we have studied and given in (4.65).

Finally, we note that, while the $f\left(\phi\right)F^2$ results in a negative g_* [90, 61, 91], in our case both signs of g_* are possible.

4.6 Conclusions

We showed that solid inflation supports prolonged anisotropic inflationary solutions. This constitutes a stable example based on standard gravity and scalar fields only that violates the conditions of the so called cosmic no-hair conjecture [11]. This result strengthens the analogy between solid inflation and the $f\left(\phi\right)F^2$ mechanism. It was already shown that both models exhibits a bispectrum with a nontrivial angular dependence in the squeezed limit. We have now shown that

this analogy also holds at the background level, since the $f(\phi) F^2$ mechanism also supports anisotropic inflation without instabilities. In this Section we discuss a few open questions on solid inflation. First of all, given the strong analogy between solid inflation and the $f(\phi) F^2$ mechanism, both at the background level and at the level of the bispectrum, it would be interesting to explore whether the models have other similarities, and, in particular, whether they can be formulated within a unique effective description. For instance, ref. [12] showed how the previously obtained results for the $f(\phi) F^2$ models can be understood in terms of symmetries of the vector field. It may be possible that their computations can be further extended to include solid inflation as well, perhaps developing an effective field theory of broken spatial translational and rotational symmetries during inflation (analogously to the effective field theory that identifies the cosmological perturbations with the goldstone bosons of the broken time translational invariance in the standard cases [129, 130]).

Possibly, the similarities between the two models will also include the infra-red sensitivity to anisotropic super-horizon modes that characterizes the $f(\phi) F^2$ model [62]. Assume that inflation starts from an isotropic configuration, for instance with a triad of orthogonal vectors of equal magnitude, and choose the function $f(\phi)$ to produce a frozen scale invariant spectrum of vector perturbations outside the horizon. Assume also that the total number of e-folds of inflation $N_{\rm tot}$ is greater than the number of e-folds $N_{\rm CMB} \simeq 60$ at which the CMB modes left the horizon. The modes of the vector fields that left the horizon in the first $\sim N_{\rm tot} - N_{\rm CMB}$ e-folds of inflation become classical at horizon exit and randomly add up with each other. This sum is not constant across the universe, but the nontrivial spatial-dependence takes place only on scales much greater than our current horizon, and therefore this nontrivial spatial dependence is unobservable. However, it is crucial to realize that the sum itself is *not unobservable*. The modes that leave the horizon in the final 60 e-folds see this sum as a classical homogeneous background quantity. This last statement is commonly accepted in the case of scalar fields (this is the origin of the coherent vev in the Affleck-Dine [154] and in the curvaton [155] mechanisms), but - as remarked in [62] - its validity has nothing to do with the spin of the field, but only with the property of the super-horizon modes. Any field (of any spin) that has a frozen spectrum of perturbations outside the horizon develops a coherent vev, that is locally observed as a homogeneous quantity. The only role played by the higher spin is that, differently from a scalar field, a homogeneous vector breaks isotropy locally.

The theory only provides a statistical prediction for this classical vector field $\vec{V}_{\rm IR}$: if we could observe many independent realizations of the first $N_{\rm tot} - N_{\rm CMB}$ e-folds of inflation, we would find a (nearly) gaussian distribution for $\vec{V}_{\rm IR}$ with zero mean and variance $\langle V_{\rm IR}^2 \rangle \propto N_{\rm tot} - N_{\rm CMB}$ [62]. However, we can observe only one realization, so we naturally expect to observe a vector with magnitude $|\vec{V}_{\rm obs}| \simeq \sqrt{\langle \vec{V}_{\rm IR}^2 \rangle}$. Even if classically one starts from an isotropic triad, there is no reason why the three infra-red sums of the different vectors should be equal to each other (each sums is the random addiction of quantum vectors,

and no gauge symmetry can enforce that the quantum fluctuation of each mode of one vector is identical to the quantum fluctuation of each mode of another vector), and the natural statistical expectation for the difference is also given by $\sqrt{\langle \vec{V}_{\mathrm{IR}}^2 \rangle}$. This unavoidably generates an anisotropy for the classical vector background, which in turns imprints a strong anisotropy to the power spectrum of the inflation through its direct $f(\phi) F^2$ coupling to the vector. This results in a natural expectation for the duration of inflation in all models that support a scale invariant vector field outside the horizon, and, in particular, for all models of anisotropic inflation, anisotropic curvaton, and inflationary magnetogenesis [62]. In the $f(\phi) F^2$ mechanism, the anisotropy exceeds the 1% level (10% level) if inflation lasted ~ 5 e-folds (~ 50 e-folds) more than the minimal amount required to produce the CMB modes [62].

It is possible that a similar problem also holds for solid inflation. This is not the anisotropy that we have studied in this work, as here we have assumed that the background is initially anisotropic, and we have followed the background evolution dictated by the classical equations of motion. However, there is no reason to expect that, even starting from an isotropic background, the three scalars of solid inflation will develop three identical power spectra. The difference will be encoded both in the longitudinal and in the vector modes of the three scalars' primordial perturbations. Such modes were studied in [7], where it was shown that their amplitudes is nearly frozen outside the horizon. It remains to be studied whether these modes can result in a sizable anisotropic IR background, and then imprint an anisotropic contribution to P_ζ, analogously to what happens in the $f(\phi) F^2$ model.

The discussion we have just presented is on whether an isotropic classical background can be destabilized by the random anisotropic addition of the super-horizon modes of the different fields. A different problem, strongly motivated by our results, is on whether solid inflation can lead to a isotropic and homogeneous background starting from generic initial conditions. We have shown here that solid inflation erases an initial anisotropy on a rather long timescale, $\Delta t = \mathrm{O}\left(\frac{1}{H\varepsilon}\right)$. We understood this in terms of the fact that the medium of solid inflation must be extremely insensitive to spatial deformations. It is natural to wonder whether an analogous inefficiency will also take place for an initially inhomogeneous background. This would question the validity of solid inflation as a solution of the homogeneity and isotropy problem, in contrast to more standard models of inflation [34].

Finally, an open question already pointed out in [7] is related to the physics of reheating. It was shown in [7] that the primordial perturbation ζ is constant if reheating occurs instantaneously. It is possible that this is no longer the case for a more prolonged duration (we would not expect that the qualitative features of the perturbations will be changed in this case). This would require entering in the details of the field theory described by solid inflation, and of how it is coupled to ordinary matter, which by itself would also be an interesting direction to explore.

5

PARITY VIOLATION IN THE CMB BISPECTRUM BY A ROLLING PSEUDOSCALAR

This chapter, based on [156], focuses on a pseudoscalar-vector model with distinctive signatures in the CMB bispectrum. In particular the vector sources both scalar and tensor metric perturbations but the latter, due to helicity conservation, have a larger amplitude and, moreover, exhibit parity violating signal that can open a window on the detection of such kind of tensor non-Gaussianity.

Contents

Cosmological parity violation may be a key indicator of UV theories of gravity and early Universe models, and has been well-studied from both theoretical and observational sides (e.g., refs. [157, 158, 159, 160, 161, 162, 163, 164, 165, 166, 167, 168, 56, 81, 169, 6, 170, 171, 135, 4]). Nowadays the investigation of the connections between the parity violation and tensor non-Gaussianity has attracted attention [172, 173, 174, 175, 176, 57]. Such non-Gaussianity imprints new types of distinguishable signatures in temperature and polarization bispectra of the cosmic microwave background (CMB), e.g., temperature auto-bispectrum in $\ell_1 + \ell_2 + \ell_3 = $ odd or B-mode auto-bispectrum in $\ell_1 + \ell_2 + \ell_3 = $ even [177, 174, 175]. Recently, ref. [6] has proposed an inflationary model where a rolling pseudoscalar, gravitationally coupled to the inflaton, amplifies the vacuum fluctuations of a $U(1)$ gauge field. This gauge field can add extra signals in power spectrum and bispectrum of curvature perturbations and of gravitational waves in addition to normal signals generated by the inflaton. The introduction of a second (pseudoscalar) field minimizes the amount of scalar perturbations and an interesting gravitational wave signal can be obtained without conflicting with the bounds on non-Gaussianity from the scalar perturbations. Resulting gravitational waves are chiral, can produce TB and EB correlations and parity-violating non-Gaussianities. Investigating these characteristic observables is a meaningful way to judge the validity of this model. More recently, ref. [57] has found that in this model the non-Gaussianity of gravitational waves is $\mathcal{O}(10^3)$ times than the curvature non-Gaussianity. This implies the existence of sizable CMB bispectrum unlike usual scalar-mode one. The authors have evaluated the magnitude of resultant temperature auto-bispectrum through an approximation based on flat-sky formalism, and have translated a current bound on the equilateral nonlinearity parameter into a rough bound on the pseudoscalar coupling. Their analysis is a reasonable way to evaluate the signals roughly. However, their flat-sky analysis may be no longer appropriate on large scales where the tensor mode is effective. As we will show, the tensor non-Gaussianity in this model breaks parity invariance asymmetrically and creates separate signals in both parity-even ($\ell_1 + \ell_2 + \ell_3 = $ even) and parity-odd ($\ell_1 + \ell_2 + \ell_3 = $ odd) spaces. It may be hard to evaluate such signatures precisely in the flat-sky formalism which is based on non-discrete ℓ space. Furthermore, we expect that inclusion of the polarization bispectra can improve detectability drastically since, in this case, the tensor mode is a major source of non-Gaussianity [178].

In this chapter, we present a concrete study of the temperature and polarization bispectra generated from a rolling pseudoscalar. Firstly, on the basis of a full-sky formalism with full radiation transfer dependence [179], we construct a general form for the CMB bispectra. The primordial tensor bispectrum is given by a nonseparable form between three wave numbers and it makes the computation of the CMB bispectra quite difficult. We solve this by replacing it with a reconstructed separable one. Through technical treatments of ℓ dependence in the full-sky

formulation, we confirm that resulting CMB bispectra do not vanish both in the parity-even and parity-odd ℓ spaces. Next, we estimate the detectability of the tensor non-Gaussianity for cases with the auto- and cross-bispectra between the temperature and E-mode anisotropies, and with the B-mode auto-bispectrum alone. In the analysis with the temperature and E-mode bispectra, we assume the existence of a contamination by the standard equilateral non-Gaussianity, while we show that it is a negligible effect. For both cases, we assume the *Planck* and the proposed PRISM experiments. Then, we show that considering the polarization information and both the parity-even and parity-odd signals improves the detectability. We also summarize the expected 1σ errors of a model parameter determined by a coupling constant and a rolling condition of the pseudoscalar field.

This chapter is organized as follow. In the next section, we review an inflationary model with a rolling pseudoscalar by following ref. [6]. In sec. 5.3, we compute the primordial tensor bispectrum and find its reconstructed form which is useful in CMB computation. In sec. 5.4, we produce a full-sky form for the CMB temperature and polarization bispectra and analyze their behaviors. section 5.5 presents Fisher matrix analysis for estimating the detectability of the tensor non-Gaussianity, and the final section is devoted to summary and discussion of our results.

5.2   Gauge field amplification by a rolling pseudoscalar

We consider a model where in addition to a standard inflationary sector, we have a (hidden) sector with a rolling pseudoscalar χ coupled to a $U(1)$ gauge field A_μ, whose Lagrangian is given by

$$\mathcal{L} = -\frac{1}{2}(\partial\phi)^2 - V(\phi) - \frac{1}{2}(\partial\chi)^2 - U(\chi) - \frac{1}{4}F_{\mu\nu}F^{\mu\nu} - \frac{\chi}{4f}F_{\mu\nu}\tilde{F}^{\mu\nu} \ , \quad (5.1)$$

where f is a coupling constant like an axion decay constant and $F_{\mu\nu} \equiv \partial_\mu A_\nu - \partial_\nu A_\mu$ is the field strength and $\tilde{F}_{\mu\nu}$ its dual [6, 57]. In this model, a successful slow-roll inflation occurs owing to an inflaton potential $V(\phi)$, and χ contributes to the generation of curvature and tensor perturbations through gravitational interaction with the gauge field. Such a scenario is different from the case in which a direct coupling between the inflaton and the gauge field is present [56]. In that case the coupling is much stronger than the gravitational one and scalar curvature fluctuations are sourced with much more efficiency than gravitational waves [6]. Observed power spectra of curvature and tensor perturbations will consist of both these gauge-field modes and considerable normal modes generated in the slow-roll regime, which are expressed as $\mathcal{P} \equiv \frac{H^2}{8\pi^2\varepsilon M_P^2}$ and $\mathcal{P}_h = 16\varepsilon\mathcal{P}$ with H, ε and $M_P \equiv 1/\sqrt{8\pi G}$ being the Hubble parameter, the slow-roll parameter for the inflaton and the reduced Planck mass, respectively. On the other hand, the gauge-field contributions can dominate over the bispectrum signals owing

to the slow-roll suppression of the normal-mode non-Gaussianities [6, 57]. This implies that we can obtain tight constraints on this model from CMB bispectrum analysis.

We shall analyze the dynamics of the gauge field in the Coulomb gauge $A_0 = 0$ and $\nabla \cdot \mathbf{A} = 0$. Then, equation of motion of the gauge field reads

$$\mathbf{A}'' - \nabla^2 \mathbf{A} - \frac{\chi'}{f} \nabla \times \mathbf{A} = 0 , \qquad (5.2)$$

where $' \equiv \partial/\partial\tau$ denotes conformal time derivative. To solve this, we move to a quantization process in Fourier space, reading

$$A_i(\tau, \mathbf{x}) = \int \frac{d^3\mathbf{k}}{(2\pi)^{3/2}} \sum_{\lambda=\pm 1} v_\lambda(\tau, \mathbf{k}) \varepsilon_i^{(\lambda)}(\mathbf{k}) e^{i\mathbf{k}\cdot\mathbf{x}} , \qquad (5.3)$$

$$v_\lambda(\tau, \mathbf{k}) = a_\lambda(\mathbf{k}) A_\lambda(\tau, \mathbf{k}) + a_\lambda^\dagger(-\mathbf{k}) A_\lambda^*(\tau, -\mathbf{k}) , \qquad (5.4)$$

where creation and annihilation operators satisfy

$$\left[a_\lambda(\mathbf{k}), a_{\lambda'}^\dagger(\mathbf{k}')\right] = \delta_{\lambda\lambda'}\delta^{(3)}(\mathbf{k} - \mathbf{k}') , \qquad (5.5)$$

and $\varepsilon_i^{(\pm 1)}$ is a divergenceless polarization vector (for details see appendix A.1).[i] Then assuming rolling condition like $\dot{\chi} \simeq$ const. leads to an explicit form of A_+:

$$A_+(\tau, k) \simeq \frac{1}{\sqrt{2k}} \left(-\frac{k\tau}{2\xi}\right)^{1/4} e^{\pi\xi - 2\sqrt{-2\xi k\tau}} , \qquad (5.7)$$

where $\xi \equiv \frac{\dot{\chi}}{2fH}$ with $\dot{} \equiv d/dt$ being physical time derivative, and $\xi > 0$ is assumed without loss of generality. We are interested in the situation where the gauge field may give observable effects on cosmological perturbations, namely $\xi \gtrsim \mathcal{O}(1)$. Then, this solution will perform well for all interesting scales. Note that A_+ is exponentially amplified as ξ becomes large, due to tachionic instability, while A_- has no amplification mechanism and is negligible in comparison to A_+ [56]. Owing to this chiral property, the tensor non-Gaussianity and resultant CMB bispectra break parity invariance and the signal can be distinguishable from the vacuum one since one gravity wave helicity is produced in a much stronger way than the other.

---

[i] We use the Fourier transform convention as

$$f(\mathbf{x}) = \int \frac{d^3\mathbf{k}}{(2\pi)^{3/2}} f(\mathbf{k}) e^{i\mathbf{k}\cdot\mathbf{x}} . \qquad (5.6)$$

The polarization vector $\varepsilon_i^{(\pm 1)}(\hat{\mathbf{k}})$ is equivalent to $\varepsilon_\pm^i(\mathbf{k})$ in refs. [56, 168, 6, 57].

5.3 | Parity-violating tensor non-Gaussianity

The produced gauge field quanta give rise to scalar and tensor modes, giving rise to non-standard power spectra and bispectra. Very interestingly, due to helicity conservation, the tensor non-Gaussianity has a larger amplitude in comparison with the scalar one that can be considered negligible [57]. In this section, we shall formulate such tensor non-Gaussianity to estimate its CMB signals in our convention. Then, we will confirm the consistency of our results with ref. [57].

5.3.1 | Primordial tensor bispectrum

The tensor metric perturbation, which is defined in $\delta g_{ij}^{(T)} = a^2 h_{ij}$ with a being the scale factor, obeys the Einstein equation:

$$h_{ij}'' + 2\frac{a'}{a}h_{ij}' - \nabla^2 h_{ij} = -\frac{2a^2}{M_P}(E_i E_j + B_i B_j)^{TT} , \tag{5.8}$$

where $\mathbf{E} = -\mathbf{A}'/a^2$ and $\mathbf{B} = \nabla \times \mathbf{A}/a^2$ are electric and magnetic parts of the gauge field, and TT denotes transverse and traceless elements. Here, the source term arises not from the $F\tilde{F}$ term but from the FF term in eq. (5.1). Parity-violating information of the gauge field is transmitted to the tensor metric perturbation through this source term. In Fourier space, a solution is given by the Green function G_k as [57]

$$h_{ij}(\tau, \mathbf{x}) = \int \frac{d^3\mathbf{k}}{(2\pi)^{3/2}} \sum_{\lambda = \pm 2} h_{\mathbf{k}}^{(\lambda)}(\tau) e_{ij}^{(\lambda)}(\hat{\mathbf{k}}) e^{i\mathbf{k}\cdot\mathbf{x}} , \tag{5.9}$$

$$h_{\mathbf{k}}^{(\lambda)}(\tau) = -\frac{2H^2}{M_P^2} \int d\tau' G_k(\tau, \tau')\tau'^2 \int \frac{d^3\mathbf{k}'}{(2\pi)^{3/2}} d^3\mathbf{k}'' \frac{1}{2} e_{ij}^{(-\lambda)}(\hat{\mathbf{k}})$$
$$\times [\mathcal{E}_i(\tau', \mathbf{k}')\mathcal{E}_j(\tau', \mathbf{k}'') + \mathcal{B}_i(\tau', \mathbf{k}')\mathcal{B}_j(\tau', \mathbf{k}'')] \, \delta(\mathbf{k}' + \mathbf{k}'' - \mathbf{k}), \tag{5.10}$$

where $e_{ij}^{(\pm 2)}$ is the transverse and traceless polarization tensor defined in appendix A.1[ii] and

$$G_k(\tau, \tau') = \frac{1}{k^3\tau'^2} \left[(1 + k^2\tau\tau')\sin k(\tau - \tau') + k(\tau' - \tau)\cos k(\tau - \tau') \right] \Theta(\tau - \tau') \tag{5.11}$$

$\mathcal{E}_i$ and $\mathcal{B}_i$ represent the dependence on E_i and B_i in Fourier space, namely

$$\mathcal{E}_i(\tau, \mathbf{k}) \equiv v_+'(\tau, \mathbf{k})\varepsilon_i^{(+)}(\mathbf{k}) , \tag{5.12}$$

$$\mathcal{B}_i(\tau, \mathbf{k}) \equiv kv_+(\tau, \mathbf{k})\varepsilon_i^{(+)}(\mathbf{k}) , \tag{5.13}$$

[ii]Our polarization tensor $e_{ij}^{(\pm 2)}(\hat{\mathbf{k}})$ is equal to $2\Pi_{\mp}^{ij}(\mathbf{k})$ in refs. [168, 57].

where we ignore A_- for its smallness. Then, the tensor bispectrum is formed by 6-point functions of $\mathcal{E}_i$ and $\mathcal{B}_i$. Computing it on superhorizon scales $(-k\tau \to 0)$ using the Wick's theorem and conventions of the polarization vector and tensor (appendix A.1), yields

$$
\begin{aligned}
\left\langle \prod_{n=1}^{3} h_{\mathbf{k_n}}^{(\lambda_n)} \right\rangle &= \left[\prod_{n=1}^{3} \int \frac{d^3 \mathbf{k_n'}}{(2\pi)^{3/2}} \right] \delta(\mathbf{k_1} - \mathbf{k_1'} + \mathbf{k_3'})\delta(\mathbf{k_2} - \mathbf{k_2'} + \mathbf{k_1'})\delta(\mathbf{k_3} - \mathbf{k_3'} + \mathbf{k_2'}) \\
&\quad \times \varepsilon_a^{(+)}(\hat{\mathbf{k_1'}})\varepsilon_d^{(-)}(\hat{\mathbf{k_1'}})\varepsilon_e^{(+)}(\hat{\mathbf{k_3'}})\varepsilon_b^{(-)}(\hat{\mathbf{k_3'}})\varepsilon_c^{(+)}(\hat{\mathbf{k_2'}})\varepsilon_f^{(-)}(\hat{\mathbf{k_2'}}) \\
&\quad \times \frac{1}{2}e_{ab}^{(-\lambda_1)}(\hat{\mathbf{k_1}})\frac{1}{2}e_{cd}^{(-\lambda_2)}(\hat{\mathbf{k_2}})\frac{1}{2}e_{ef}^{(-\lambda_3)}(\hat{\mathbf{k_3}})\mathcal{F}(k_1', k_2', k_3') \\
&\equiv (2\pi)^{-3/2} B_{\mathbf{k_1 k_2 k_3}}^{\lambda_1 \lambda_2 \lambda_3} \delta^{(3)}\left(\sum_{n=1}^{3} \mathbf{k_n}\right) ,
\end{aligned}
\tag{5.14}
$$

where

$$
\begin{aligned}
\mathcal{F}(k_1', k_2', k_3') &\equiv \left(-\frac{2H^2}{M_P^2}\right)^3 \left[\prod_{n=1}^{3} \lim_{-k_n\tau \to 0} \int_{-\infty}^{0} d\tau_n \tau_n^2 G_{k_n}(\tau, \tau_n) \right] \\
&\quad \times \mathcal{A}_h(\tau_1, k_1', k_3')\mathcal{A}_h(\tau_2, k_2', k_1')\mathcal{A}_h(\tau_3, k_3', k_2') ,
\end{aligned}
\tag{5.15}
$$

and $\mathcal{A}$ is given by

$$
\mathcal{A}_h(\tau, k, q) \equiv 2\left[A_+'(\tau, k)A_+'(\tau, q) + kq A_+(\tau, k)A_+(\tau, q) \right] .
\tag{5.16}
$$

We are interested in the bispectrum signatures for $\xi \gtrsim \mathcal{O}(1)$. In this condition, eq. (5.16) becomes

$$
\mathcal{A}_h(\tau, k, q) \simeq \left(\sqrt{-\frac{kq\tau}{2\xi}} - \sqrt{-\frac{2\xi}{\tau}} \right)[kq]^{1/4}e^{2\pi\xi}e^{-2\sqrt{-2\xi\tau}(\sqrt{k}+\sqrt{q})} ,
\tag{5.17}
$$

and hence $\mathcal{F}$ is analytically evaluated as [56]

$$
\mathcal{F}(k_1', k_2', k_3') \simeq \frac{\Gamma(7)^3}{3^3 2^{24}}\frac{H^6}{M_P^6}\frac{e^{6\pi\xi}}{\xi^9}\frac{(k_1' k_2' k_3')^{1/2}}{[(\sqrt{k_1'} + \sqrt{k_2'})(\sqrt{k_2'} + \sqrt{k_3'})(\sqrt{k_3'} + \sqrt{k_1'})]^7}
\tag{5.18}
$$

This form is equivalent to that found in [57]. From numerical evaluation, we confirm that this tensor bispectrum resembles closely the usual equilateral shape, and the bispectrum amplitude in the equilateral configuration $(k_1 = k_2 = k_3)$ can be expressed as

$$
\left\langle \prod_{n=1}^{3} h_{\mathbf{k_n}}^{(+2)} \right\rangle_{k_n \to k} \simeq 6 \times 10^{-10} \frac{H^6}{M_P^6}\frac{e^{6\pi\xi}}{\xi^9}\frac{\delta(\mathbf{k_1} + \mathbf{k_2} + \mathbf{k_3})}{k^6} .
\tag{5.19}
$$

This is in agreement with the result in ref. [57]. We also confirm the smallness of the other spin modes, reading $B^{+2+2+2} \sim 10^2 B^{+2+2-2} \sim 10^5 B^{+2-2-2} \sim 10^5 B^{-2-2-2}$, and hence we shall ignore these contributions in the rest of the chapter.

An exact form of the tensor bispectrum (5.14) has three convolutions with respect to $\mathbf{k_n'}$ due to the 6-point functions of $\mathcal{E}_i$ and $\mathcal{B}_i$. This implies that resultant CMB bispectrum has also three convolutions in ℓ space, which corresponds to the 1-loop computation [180, 175]. The numerical computation of such CMB bispectrum is quite hard due to the non-separability of the k integrals. Accordingly, we introduce an approximate separable form without convolutions, which is reconstructed from the exact bispectrum.

The radial function $\mathcal{F}$ has three poles, i.e., $k_1' = k_2' = 0$, $k_2' = k_3' = 0$ and $k_3' = k_1' = 0$, and contributions around these poles may dominate over total signals. Evaluating these contributions in the similar way as refs. [180, 175] yields

$$
\begin{aligned}
B^{+2+2+2}_{\mathbf{k_1 k_2 k_3}} \approx & \ (2\pi)^{-3} \frac{\Gamma(7)^3}{3^3 2^{27}} \frac{H^6}{M_P^6} \frac{e^{6\pi\xi}}{\xi^9} \delta^{(3)}\left(\sum_{n=1}^{3} \mathbf{k_n}\right) \frac{4\pi}{3} e_{ab}^{(-2)}(\hat{\mathbf{k_1}}) e_{bc}^{(-2)}(\hat{\mathbf{k_2}}) e_{ca}^{(-2)}(\hat{\mathbf{k_3}}) \\
& \times \frac{\ln\left(\frac{k_{\max}}{k_{\min}}\right)}{2^7} \left[\frac{\sqrt{k_1 k_2}}{(\sqrt{k_1} + \sqrt{k_2})^{14}} + \frac{\sqrt{k_2 k_3}}{(\sqrt{k_2} + \sqrt{k_3})^{14}} + \frac{\sqrt{k_3 k_1}}{(\sqrt{k_3} + \sqrt{k_1})^{14}} \right]
\end{aligned}
\tag{5.20}
$$

where we have used relationships between the polarization vector and tensor (appendix A.1) and

$$
\int \frac{k_1'^2 dk_1'}{(2\pi)^{9/2}} \mathcal{F}(k_1' \sim k_2' \ll k_3') = (2\pi)^{-9/2} \frac{\Gamma(7)^3}{3^3 2^{24}} \frac{H^6}{M_P^6} \frac{e^{6\pi\xi}}{\xi^9} \frac{\ln\left(\frac{k_{\max}}{k_{\min}}\right)}{2^7} \frac{\sqrt{k_2' k_3'}}{(\sqrt{k_2'} + \sqrt{k_3'})^{14}}
\tag{5.21}
$$

$$
\int d^2 \hat{\mathbf{k}}' \varepsilon_a^{(1)}(\hat{\mathbf{k}}') \varepsilon_b^{(-1)}(\hat{\mathbf{k}}') = \frac{4\pi}{3} \delta_{ab} .
\tag{5.22}
$$

This form produces an almost exact spin and angle dependence. However, since it is not separable with respect to k_n, we have to alter it to a separable form. Then, we shall replace the non-separable part with the usual equilateral template as

$$
B^{+2+2+2}_{\mathbf{k_1 k_2 k_3}} \approx N \mathcal{P}^3 X^3 B^{\mathrm{eq}}_{k_1 k_2 k_3} e_{ab}^{(-2)}(\hat{\mathbf{k_1}}) e_{bc}^{(-2)}(\hat{\mathbf{k_2}}) e_{ca}^{(-2)}(\hat{\mathbf{k_3}}) ,
\tag{5.23}
$$

$$
\begin{aligned}
B^{\mathrm{eq}}_{k_1 k_2 k_3} = & \ -\frac{1}{k_1^3 k_2^3} - \frac{1}{k_2^3 k_3^3} - \frac{1}{k_3^3 k_1^3} - \frac{2}{k_1^2 k_2^2 k_3^2} \\
& + \frac{1}{k_1 k_2^2 k_3^3} + \frac{1}{k_1 k_3^2 k_2^3} + \frac{1}{k_2 k_3^2 k_1^3} + \frac{1}{k_2 k_1^2 k_3^3} + \frac{1}{k_3 k_1^2 k_2^3} + \frac{1}{k_3 k_2^2 k_1^3}
\end{aligned}
\tag{5.24}
$$

where $\mathcal{P} = \frac{H^2}{8\pi^2 \varepsilon M_p^2}$ and

$$
X \equiv \varepsilon \frac{e^{2\pi\xi}}{\xi^3} .
\tag{5.25}
$$

To check the shape resemblance between exact (5.14) and reconstructed (5.23)

bispectra, we introduce the shape correlator defined as

$$r = \frac{B^{\mathrm{ex}} \cdot B^{\mathrm{rec}}}{\sqrt{(B^{\mathrm{ex}} \cdot B^{\mathrm{ex}})(B^{\mathrm{rec}} \cdot B^{\mathrm{rec}})}} \ , \tag{5.26}$$

where a scalar product is defined as

$$B \cdot B' \quad \equiv \quad \int_0^1 dx_2 \int_{1-x_2}^1 dx_3 (x_2 x_3)^4 B_{1,x_2,x_3} B'_{1,x_2,x_3} \ . \tag{5.27}$$

A numerical evaluation yields $r = 0.98$, which guarantees a consistency between the bispectra. Then, the normalization factor can be estimated as

$$N = \frac{B^{\mathrm{ex}} \cdot B^{\mathrm{rec}}(N=1)}{B^{\mathrm{rec}}(N=1) \cdot B^{\mathrm{rec}}(N=1)} = 4.3174 \times 10^{-3} \ . \tag{5.28}$$

In the next section, we adopt this reconstructed bispectrum in the computation of the CMB bispectra.

5.4 CMB temperature and polarization bispectra

In this section, let us analyze CMB signatures of the parity-violating tensor non-Gaussianity discussed in the previous section.

Tensor metric perturbations, which are generated during inflation and stretched beyond horizon, re-enter horizon around recombination and create both temperature and polarization anisotropies. Major signals in the temperature anisotropy appear on large scales ($\ell \lesssim 100$) due to the Integrated Sachs Wolfe (ISW) effect after recombination. On the other hand, the polarization anisotropies are generated through Thomson scattering at both recombination and reionization, and have peaks at corresponding scales, namely $\ell \sim 100$ and 10, respectively [181].

In general, the CMB anisotropies are quantified through a multipole expansion, i.e., $\frac{\Delta \mathcal{X}(\hat{\mathbf{n}})}{\mathcal{X}} = \sum_{\ell m} a_{\ell m}^{\mathcal{X}} Y_{\ell m}(\hat{\mathbf{n}})$. Here the superscript $\mathcal{X}$ denotes the temperature (I), E-mode (E) and B-mode (B) fields. Then, each multipole coefficient can be expressed as [179, 182]

$$a_{\ell m}^{\mathcal{X}} \quad = \quad 4\pi(-i)^\ell \int_0^\infty \frac{k^2 dk}{(2\pi)^{3/2}} \mathcal{T}_\ell^{\mathcal{X}}(k) \sum_{\lambda=\pm 2} \left(\frac{\lambda}{2}\right)^x \int d^2 \hat{\mathbf{k}} h_{\mathbf{k}}^{(\lambda)} {}_{-\lambda} Y_{\ell m}^*(\hat{\mathbf{k}}) \tag{5.29}$$

where x discriminates parities of three modes: $x = 0$ for $\mathcal{X} = I, E$ and $x = 1$ for $\mathcal{X} = B$, and $\mathcal{T}_\ell^{\mathcal{X}}$ is a radiation transfer function yielding the ℓ dependence as mentioned above. Accordingly, a formula for the CMB bispectra induced by the

tensor non-Gaussianity reads

$$\left\langle \prod_{n=1}^{3} a_{\ell_n m_n}^{\mathcal{X}_n} \right\rangle = \left[\prod_{n=1}^{3} 4\pi(-i)^{\ell_n} \int_0^\infty \frac{k_n^2 dk_n}{(2\pi)^{3/2}} \mathcal{T}_{\ell_n}^{\mathcal{X}_n}(k_n) \right]$$
$$\times (2\pi)^{-3/2} \left[\prod_{n=1}^{3} \int d^2 \hat{\mathbf{k}}_\mathbf{n} {}_{-2}Y_{\ell_n m_n}^*(\hat{\mathbf{k}}_\mathbf{n}) \right] B_{\mathbf{k_1 k_2 k_3}}^{+2+2+2} \delta^{(3)}\left(\sum_{n=1}^{3} \mathbf{k_n} \right) \tag{5.30}$$

Here we note that dependence on x disappears due to the $\lambda_n = +2$ polarizing nature of the tensor bispectrum. This equation involves integrals of angle-dependent parts in the tensor bispectrum (5.23) and the delta function as shown in appendix A.1. Dealing with these angular integrals by using Wigner symbols as in ref. [179], yields a reduced form

$$\left\langle \prod_{n=1}^{3} a_{\ell_n m_n}^{\mathcal{X}_n} \right\rangle = B_{\ell_1 \ell_2 \ell_3}^{\mathcal{X}_1 \mathcal{X}_2 \mathcal{X}_3} \begin{pmatrix} \ell_1 & \ell_2 & \ell_3 \\ m_1 & m_2 & m_3 \end{pmatrix}, \tag{5.31}$$

$$B_{\ell_1 \ell_2 \ell_3}^{\mathcal{X}_1 \mathcal{X}_2 \mathcal{X}_3} = -\frac{(8\pi)^{3/2}}{10} \sqrt{\frac{7}{3}} N \mathcal{P}^3 X^3 \left[\prod_{n=1}^{3} \sum_{L_n} (-1)^{\frac{L_n}{2}} (-i)^{\ell_n} I_{\ell_n L_n 2}^{2\,0-2} \right] \times$$

$$I_{L_1 L_2 L_3}^{0\,0\,0} \begin{Bmatrix} \ell_1 & \ell_2 & \ell_3 \\ L_1 & L_2 & L_3 \\ 2 & 2 & 2 \end{Bmatrix} \int_0^\infty r^2 dr \left[\prod_{n=1}^{3} \frac{2}{\pi} \int_0^\infty k_n^2 dk_n \mathcal{T}_{\ell_n}^{\mathcal{X}_n}(k_n) j_{L_n}(k_n r) \right] B_{k_1 k_2 k_3}^{\mathrm{eq}} \tag{5.32}$$

where

$$I_{l_1 l_2 l_3}^{s_1 s_2 s_3} \equiv \sqrt{\frac{(2l_1+1)(2l_2+1)(2l_3+1)}{4\pi}} \begin{pmatrix} l_1 & l_2 & l_3 \\ s_1 & s_2 & s_3 \end{pmatrix}. \tag{5.33}$$

Here, selection rules of the Wigner symbols allow L_n to run over $|\ell_n - 2| \leq L_n \leq \ell_n + 2$ under the restrictions: $L_1 + L_2 + L_3 = $ even and $|L_1 - L_2| \leq L_3 \leq L_1 + L_2$. On the other hand, concerning ℓ_n, we stress that there is no restriction except a triangle inequality $|\ell_1 - \ell_2| \leq \ell_3 \leq \ell_1 + \ell_2$. This implies that the CMB bispectra have nonzero values for both $\ell_1 + \ell_2 + \ell_3 = $ even and $\ell_1 + \ell_2 + \ell_3 = $ odd. Physically, this is a consequence of an asymmetric spin dependence of the tensor bispectrum, i.e., $|B^{\lambda_1 \lambda_2 \lambda_3}| \neq |B^{-\lambda_1 -\lambda_2 -\lambda_3}|$, and directly connected to the absence of x in eq. (5.30).

Figure 5.1 depicts reduced bispectra given by eq. (5.32) of the temperature, E-mode and B-mode anisotropies for $\ell_1 \approx \ell_2 \approx \ell_3$, which is defined as

$$b_{\ell_1 \ell_2 \ell_3}^{\mathcal{X}_1 \mathcal{X}_2 \mathcal{X}_3} = G_{\ell_1 \ell_2 \ell_3}^{-1} B_{\ell_1 \ell_2 \ell_3}^{\mathcal{X}_1 \mathcal{X}_2 \mathcal{X}_3}, \tag{5.34}$$

$$G_{\ell_1 \ell_2 \ell_3} \equiv \frac{1}{6} \left[\frac{2\sqrt{\ell_3(\ell_3+1)\ell_2(\ell_2+1)}}{\ell_1(\ell_1+1) - \ell_2(\ell_2+1) - \ell_3(\ell_3+1)} \sqrt{\frac{\prod_{n=1}^{3}(2\ell_n+1)}{4\pi}} \begin{pmatrix} \ell_1 & \ell_2 & \ell_3 \\ 0 & -1 & 1 \end{pmatrix} \right.$$
$$\left. +5 \text{ perms.} \right]. \tag{5.35}$$

Note that $G_{\ell_1 \ell_2 \ell_3} = I_{\ell_1 \ell_2 \ell_3}^{0\,0\,0}$ holds if $\ell_1 + \ell_2 + \ell_3 = $ even. In figure 5.1, the usual equilateral bispectra with $f_{\mathrm{NL}} = 150$ are also plotted, and it seems to be comparable in magnitude to the tensor bispectra with $X = 2.1 \times 10^5$ for $\ell \lesssim 100$.
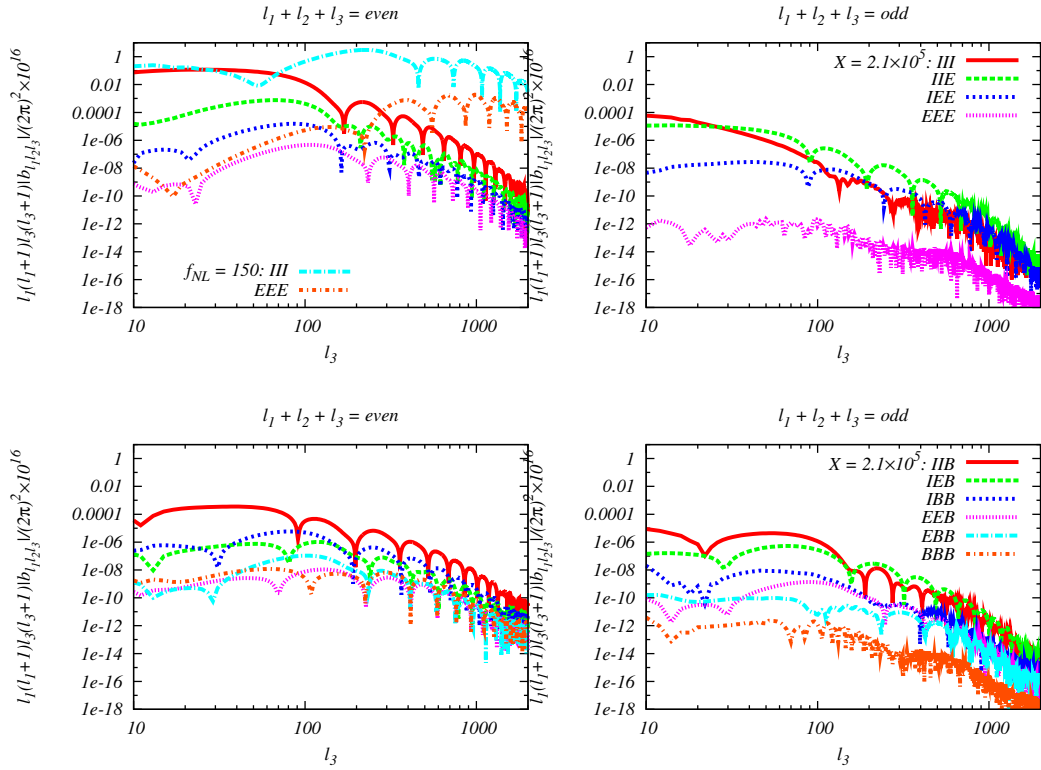
Figure 5.1: All possible CMB bispectra, i.e., $\langle III \rangle$, $\langle IIE \rangle$, $\langle IEE \rangle$ and $\langle EEE \rangle$ (top two panels), and $\langle IIB \rangle$, $\langle IEB \rangle$, $\langle IBB \rangle$, $\langle EEB \rangle$, $\langle EBB \rangle$ and $\langle BBB \rangle$ (bottom two panels), induced by the tensor non-Gaussianity with $X = 2.1 \times 10^5$ and $\mathcal{P} = 2.5 \times 10^{-9}$ for $\ell_1 + 2 = \ell_2 + 1 = \ell_3$. Left and right two panels describe the parity-even ($\ell_1 + \ell_2 + \ell_3 = $ even) and parity-odd ($\ell_1 + \ell_2 + \ell_3 = $ odd) components, respectively. For comparison, we also plot $\langle III \rangle$ and $\langle EEE \rangle$ from the equilateral non-Gaussianity with $f_{\rm NL} = 150$. Other cosmological parameters are fixed using the *Planck* results [2]. The parity-odd bispectra seem to oscillate rapidly since they hate symmetric signals as $\ell_1 \sim \ell_2 \sim \ell_3$.

This relation has also been confirmed in the flat-sky analysis [57]. In the tensor bispectra, we can see the characteristic signatures associated with the tensor-mode CMB fields as mentioned above, i.e., the ISW enhancement in temperature for $\ell \lesssim 100$ and a peak due to Thomson scattering in the polarization at $\ell \sim 100$. Generally, in the tensor mode, the temperature fluctuations are larger than the polarization ones, and E and B modes have almost same amplitudes [181]. Such a magnitude relationship seems to hold in this figure too. With a confirmation of both parity-even ($\ell_1 + \ell_2 + \ell_3 = $ even) and parity-odd ($\ell_1 + \ell_2 + \ell_3 = $ odd) signals in all types of the CMB bispectra, These support the validity of our computations.

While in the cross-bispectra the parity-odd signals are comparable in magnitude to the parity-even ones, the parity-odd auto-bispectra, i.e., $\langle III \rangle$, $\langle EEE \rangle$ and $\langle BBB \rangle$, are slightly smaller than the parity-even counterparts. This is because of antisymmetry of the parity-odd CMB bispectrum, which means that three fields forming the bispectrum cannot take the identical states each other, e.g., $B^{III}_{\ell\ell\ell} = B^{EEE}_{\ell\ell\ell} = 0$ [174, 175]. This suppression may slightly decrease the total signals from the parity-odd bispectra in comparison with the parity-even case,

as seen in the next section.

5.5 — Detectability analysis

To discuss detectability of the above bispectrum signals due to the tensor non-Gaussianity, in this section we evaluate error bars of X (5.25) using the Fisher matrix. We are then interested in $X \lesssim \mathcal{O}(10^5)$. In this region, gauge-field-induced curvature perturbations are negligible and therefore $\mathcal{P}$ will coincide with observed power spectrum of curvature perturbations [57]. Accordingly, we here adopt $\mathcal{P} = 2.5 \times 10^{-9}$. As instrumental noise information, we adopt the data expected from the *Planck* and the proposed PRISM experiments [183, 184]. Computational methodology for the Fisher forecast is based on ref. [178].

5.5.1 — Temperature and E-mode bispectra

Let us start from an estimation for the temperature and E-mode bispectra. In this case, we shall analyze under a contamination of the usual equilateral non-Gaussianity since its CMB bispectra are also amplified at $\ell_1 \sim \ell_2 \sim \ell_3$. The contamination by the equilateral non-Gaussianity appears only in the parity-even space ($\ell_1 + \ell_2 + \ell_3 =$ even). Then, each element of the Fisher matrix can be defined as

$$F_{ij} = \sum_{\substack{\mathcal{X}_1\mathcal{X}_2\mathcal{X}_3 \\ \mathcal{X}_1'\mathcal{X}_2'\mathcal{X}_3'}} \sum_{\ell_1 \leq \ell_2 \leq \ell_3 \leq \ell_{\max}} \frac{1}{\Delta_{\ell_1\ell_2\ell_3}} \tilde{B}_{i,\ell_1\ell_2\ell_3}^{\mathcal{X}_1'\mathcal{X}_2'\mathcal{X}_3'} \left[\prod_{n=1}^{3} (C^{-1})_{\ell_n}^{\mathcal{X}_n\mathcal{X}_n'} \right] \tilde{B}_{j,\ell_1\ell_2\ell_3}^{\mathcal{X}_1\mathcal{X}_2\mathcal{X}_3} \, , \quad (5.36)$$

where

$$\Delta_{\ell_1\ell_2\ell_3} = (-1)^{\ell_1+\ell_2+\ell_3}(1 + 2\delta_{\ell_1,\ell_2}\delta_{\ell_2,\ell_3}) + \delta_{\ell_1,\ell_2} + \delta_{\ell_2,\ell_3} + \delta_{\ell_3,\ell_1} \, , \quad (5.37)$$

and $\mathcal{X}_1\mathcal{X}_2\mathcal{X}_3$ or $\mathcal{X}_1'\mathcal{X}_2'\mathcal{X}_3'$ runs over 8 combinations: *III, IIE, IEI, EII, IEE, EIE, EEI* and *EEE*. Note that this formula is applicable to not only the parity-even space but also the parity-odd one ($\ell_1 + \ell_2 + \ell_3 =$ odd). The inverse matrix of the power spectrum reads

$$(C^{-1})_{\ell}^{\mathcal{X}\mathcal{X}'} \equiv \begin{pmatrix} C_{\ell}^{II} & C_{\ell}^{IE} \\ C_{\ell}^{EI} & C_{\ell}^{EE} \end{pmatrix}^{-1} \, , \quad (5.38)$$

where $C_{\ell}^{\mathcal{X}\mathcal{X}'}$ is the sum of the cosmic variance spectrum and the noise spectrum [178]. $\tilde{B}_i$ and $\tilde{B}_j$ consist of normalized CMB bispectra generated from the tensor non-Gaussianity ($\tilde{B}_p \equiv B_p/X^3$) and the equilateral curvature non-Gaussianity
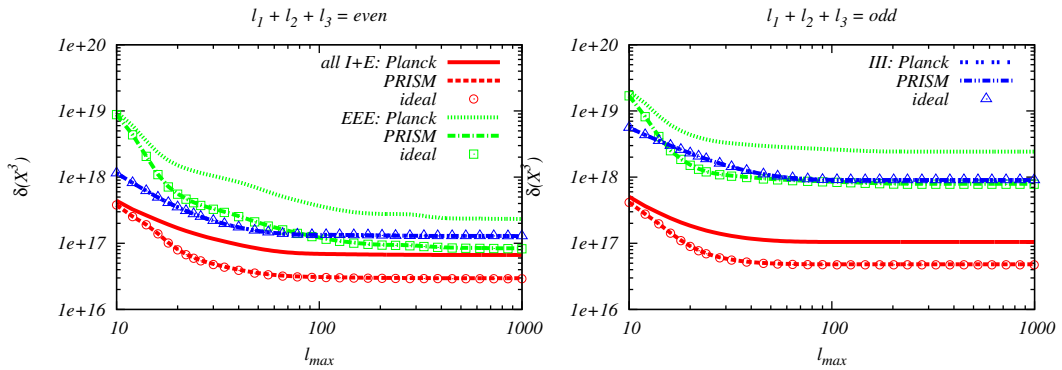
Figure 5.2: Expected 1σ errors of X^3 (5.40) obtained by using the parity-even (left panel) and parity-odd (right panel) signals in all types of the temperature and E-mode bispectra (red lines), the E-mode auto-bispectrum alone (green lines) and the temperature auto-bispectrum alone (blue lines). Here we assume the *Planck*, PRISM, and cosmic-variance-limited ideal experiments.

($\tilde{B}_e \equiv B_e/f_{\rm NL}$). If we set a 2-dimensional Fisher matrix as

$$
{}^{(2)}F \quad = \quad \begin{pmatrix} F_{pp} & F_{pe} \\ F_{ep} & F_{ee} \end{pmatrix} \ , \tag{5.39}
$$

the 1σ error bars are expressed as

$$
\left(\delta(X^3), \delta f_{\rm NL} \right) = \left(\sqrt{{}^{(2)}F_{11}^{-1}}, \sqrt{{}^{(2)}F_{22}^{-1}} \right) \ . \tag{5.40}
$$

Figure 5.2 depicts $\delta(X^3)$ as functions of $\ell_{\rm max}$ estimated from all combinations of the temperature and E-mode bispectra, the E-mode auto-bispectrum alone and the temperature auto-bispectrum alone, respectively. Here, we display results from the parity-even and parity-odd spaces separately. From this figure, we can notice that $\delta(X^3)$ saturates for $\ell_{\rm max} \gtrsim 100$ in every case. This is due to rapid decays of the tensor temperature and polarization bispectra for $\ell \gtrsim 100$ (see figure 5.1). Concerning features associated with parity, one can find that the error bars from the parity-odd signals are larger than those from the parity-even signals in the $\langle III \rangle$ and $\langle EEE \rangle$ cases. This is a consequence of the suppression of the auto-bispectra as mentioned in sec. 5.4. Regardless of it, owing to contributions of the 6 cross-bispectra, the errors estimated from all possible 8 bispectra are comparable to or slightly smaller than the parity-even counterparts.

Practical values of $\delta(X^3)$ at $\ell_{\rm max} = 1000$ are summarized in table 5.1. Interestingly, if using full set of the temperature and E-mode bispectra in both the parity-even and parity-odd spaces, $\delta(X^3)$ can be 80% reduced in comparison with the $\langle III \rangle$ analysis under the cosmic-variance-limited ideal experiment. This seems to be a common feature of the tensor non-Gaussianity [178]. Such a level of improvement cannot be attained in the scalar non-Gaussianity case, where $\delta f_{\rm NL}$ is only 50% reduction (see appendix A.2). This result shows the powerful of the polarization bispectra. In this table, we can notice that the parity-odd

	III	EEE	all $I+E$	BBB ($r=0.05$)	BBB ($r=5\times10^{-4}$)
Planck	127 (129)	232 (233)	56 (65)	17 (19)	2.1 (2.1)
PRISM	127 (129)	83 (84)	25 (30)	0.87 (1.0)	0.015 (0.017)
ideal	127 (129)	82 (83)	25 (29)	0.12 (0.20)	$1.2\ (2.0)\times10^{-4}$

Table 5.1: Expected 1σ errors of X^3 normalized by 10^{15} in the III, EEE, all $I+E$ cases ($\ell_{\max}=1000$) and the BBB case ($\ell_{\max}=500$) for each experiment. The tensor-to-scalar ratio r determines the amplitude of the B-mode cosmic variance spectrum. Here we summarize the results estimated from both the parity-even and parity-odd signals. In addition, for comparison, the errors from the parity-even signals alone are written in parentheses.

information also improves the errors if we use all types of the temperature and E-mode bispectra. These improvements yield $\delta(X^3)=5.6\times10^{16}$ (*Planck*) and 2.5×10^{16} (PRISM or ideal).

Finally, we shall mention the contamination of the usual equilateral non-Gaussianity. The correlation coefficient between the tensor temperature and E-mode bispectra in both the parity-even and parity-odd spaces and the parity-even equilateral ones reads

$$\frac{F_{pe}}{\sqrt{F_{pp}F_{ee}}}=0.036\ ,\tag{5.41}$$

which shows the lack of correlation, and hence they do not bias each other's error estimation. This is a consequence of the shape difference of the CMB fields between the scalar and tensor modes.

5.5.2 | B-mode bispectra

Here, let us consider error estimations including the B-mode information. Such bispectra correspond to 6 additional contributions: $\langle IIB \rangle$, $\langle IEB \rangle$, $\langle IBB \rangle$, $\langle EEB \rangle$, $\langle EBB \rangle$ and $\langle BBB \rangle$ and considering all these information will improve $\delta(X^3)$ drastically. However, this is a very complicated procedure and hence here we focus only on the $\langle BBB \rangle$ analysis. In this case, there is no contamination from the usual equilateral non-Gaussianity because of the absence of B-mode creation by the scalar mode. Therefore, we can estimate the error through 1-dimensional Fisher matrix as

$$F \equiv \sum_{\ell_1\leq\ell_2\leq\ell_3\leq\ell_{\max}} \frac{\left(\tilde{B}^{BBB}_{\ell_1\ell_2\ell_3}\right)^2}{\Delta_{\ell_1\ell_2\ell_3}\prod_{n=1}^{3}C^{BB}_{\ell_n}}\ ,\tag{5.42}$$

$$\delta(X^3) = F^{-1/2}\ ,\tag{5.43}$$

where $\tilde{B}\equiv B_p/X^3$. Here we take $\ell_{\max}\leq500$ since lensing B-mode contribution may behave as a bias on small scales [185, 186].
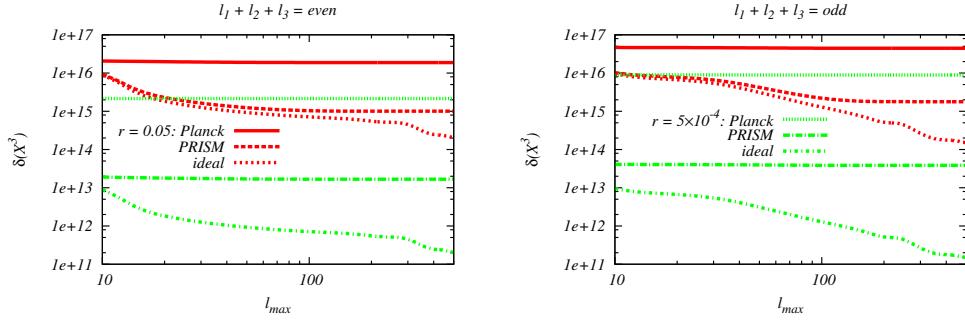
Figure 5.3: Expected 1σ errors of X^3 (5.43) estimated by using the parity-even (left panel) and parity-odd (right panel) signals in the B-mode auto-bispectrum. As the cosmic variance spectra, we adopt the B-mode power spectra with $r = 0.05$ (red lines) and 5×10^{-4} (green lines). Here we assume the *Planck*, PRISM, and cosmic-variance-limited ideal experiments.

Numerical results of $\delta(X^3)$ are described in figure 5.3. We also summarize the values at $\ell_{\max} = 500$ in table 5.1. As the cosmic variance spectra, we adopt the standard B-mode power spectra where corresponding tensor-to-scalar ratios are $r = 0.05$ and 5×10^{-4}. In the cosmic-variance-limited ideal experiment, the variance of the bispectrum is determined by r alone and hence we can find a simple relationship $\delta(X^3) = 1.1 \times 10^{16} r^{3/2}$ at $\ell_{\max} = 500$ using both the parity-even and parity-odd signals. $\langle BBB \rangle$ can improve the error more than $\langle EEE \rangle$ despite the same noise spectrum (see appendix in ref. [178]) because of smallness of the B-mode cosmic variance spectrum. While the improvements of the parity-odd signals are slightly weaker than the parity-even signals for low $\ell_{\max}$, interestingly, this situation seems to be reversed for high $\ell_{\max}$ if the instrumental noise is negligible. Owing to these signatures, $\delta(X^3)$ can reach the values comparable to or less than 10^{15} in the *Planck* or the proposed PRISM experiment.

5.6   Summary and discussion

A rolling pseudoscalar can induce large equilateral-type non-Gaussianity in the tensor perturbations via the dynamics of a chiral gauge field. Such non-Gaussianity violates parity invariance and imprints characteristic signatures in the CMB temperature and polarization bispectra.

In general, the parity-violating signatures in the non-Gaussianity appear in the complicated spin and angle dependence of resulting CMB bispectra. We dealt with these in the full-sky formalism and confirmed that all types of CMB temperature, E-mode and B-mode bispectra have nonzero signals for both $\ell_1 + \ell_2 + \ell_3 =$ even and $\ell_1 + \ell_2 + \ell_3 =$ odd. This property cannot be seen in the flat-sky analysis because of lack of the discreteness in ℓ space. Physically, this reflects the asymmetric spin dependence of the tensor non-Gaussianity, namely

$|B^{\lambda_1\lambda_2\lambda_3}| \neq |B^{-\lambda_1-\lambda_2-\lambda_3}|$. Numerical evaluations show that such CMB bispectra are amplified on large scales and take quite different shapes from the usual scalar equilateral bispectra due to the tensor-mode transfer functions. These mean that the existence of the usual equilateral bispectra does not bias the estimation of pseudoscalar signals.

We evaluated the detectability of these signals through the Fisher matrix analysis. Then, it was clarified that considering both the parity-even and parity-odd contributions improve the detectability more. The analysis of the temperature auto-bispectrum alone will detect a model parameter, defined in eq. (5.25), $X = 5.0 \times 10^5$ at 68% CL under the *Planck* or proposed PRISM experiment. Inclusion of the E-mode contributions and whole ℓ-space analysis potentially improve of 400% the detectability of the primordial tensor bispectrum ($\propto X^3$) with respect to the above temperature alone case. The corresponding 1σ values of X read 3.8×10^5 and 2.9×10^5 under the *Planck* and PRISM experiments, respectively. Moreover, we presented the power of the B-mode bispectra to reduce the error drastically. If the instrumental noise is negligible and the B-mode cosmic variance can be expressed by the tensor-to-scalar ratio r, we can write the 1σ error of X as $\delta X = 2.2 \times 10^5 \sqrt{r}$. In this sense, we will be able to observe X less than 10^4 if $r < 0.002$. In practice, the instrumental noises prevent δX from becoming smaller, and under $r = 0.05$ (5×10^{-4}), $X = 2.6$ $(1.3) \times 10^5$ and 9.5 $(2.5) \times 10^4$ will be possible to be detected in the *Planck* and PRISM experiments, respectively. The CMB bispectra seem to have the detectability of X comparable to or greater than the TB and EB correlations as shown in appendix A.3.

In this chapter, we focused on the CMB signatures originating from a rolling pseudoscalar. However, there also exist other sources which create the parity-violating tensor non-Gaussianities and imprint similar signatures in the CMB bispectra [174, 175]. To differentiate between these sources, a more comprehensive analysis considering each contamination will be required. Then, the correlations $\langle IIB \rangle$, $\langle IEB \rangle$, $\langle IBB \rangle$, $\langle EEB \rangle$, $\langle EBB \rangle$ and $\langle BBB \rangle$ may also be informative.

6

CONCLUSIONS AND OUTLOOK

This chapter concludes and discuss future developments of the thesis

Contents

6.1 Summary

The work presented in this thesis aimed at opening new window on the primordial universe in order to understand the content of this. The current era of precision cosmology is opening a window on the physics of the early universe and the results of the *Planck* mission [1, 2, 4, 128] have put stringent limits on the models that can describe the early universe. It seems that a single-field slow roll model of inflation is favoured, with the consequent isotropy and homogeneity of the distribution of the fluctuations and absence of non-Gaussianity. This seems to be confirmed by the analysis made in [15], where the effects of *Planck*'s asymmetric beams and Galactic foreground emission are removed, and a $g_* = 0.002 \pm 0.016$ ($68\%CL$) has been found. Up to now this provides the most stringent test of rotational symmetry. At same time *Planck* gives results that seems to confirm the presence of anomalies in the CMB as previously seen by WMAP. A cosmological explanation of these anomalies would suggest a possible (early) phase of anisotropic expansion sustained by an anisotropic source.

In chapter 1 we reviewed the standard Big Bang model and its success in explaining the evolution of the universe. At same time we showed that an inflationary phase has now become a cornerstone of the modern cosmology. In addition to solving the horizon and the flatness problems, inflation gives an elegant solution to the problem of primordial density perturbations that are the seeds for the temperature fluctuations in the CMB sky and for the growth of large scale structures.

In chapter 2 we firstly review all the primordial models that involve vector fields and then we give all the observational constraints related to the violation of symmetries in the early universe. We show that different models of vector inflation, even if can generate accelerated expansion and anisotropy in agreement with observations, they show problems of instability. The problem of stability and the difficulty in building models, starting from the conformal Maxwell Lagrangian, are also confirmed by an Hamiltonian analysis and by the study of the hyperbolicity of their equations of motion. However these problems, which today are still debated, can be overcomed by the introduction of models with varying gauge coupling. And this is the main topic of chapter 3, where, in addition to studying the first stable and free of ghost instabilities scalar-vector model $I(\phi)F^2$, we give answers related to consistency relations between observables in anisotropic inflationary models. This result gives rise to a model independent test of anisotropic inflation. We show that the anisotropy in the power spectrum is correlated with a characteristic and very likely detectable bispectrum

$$f_{\mathrm{NL}} \simeq 26 \, \frac{|g_*|_{\mathrm{CMB}}}{0.1} \tag{6.1}$$

We also find for the first time a non-trivial angular dependence in the shape of the bispectrum; presently there are no observational constraints on the angular

modulation of f_{NL}. With such increase in sensitivity of measurements reached by *Planck*, one expects that anisotropy in the spectrum and bispectrum will be discovered or constrained very tightly. In case of the discovery, with the magnitude and anisotropy of f_{NL} proposed above, it will be a smoking gun for a anisotropic field contribution to the primordial curvature perturbation.

In chapter 4 we have shown that a "solid" supports prolonged anisotropic inflationary solutions and this represents the first stable example based on standard gravity and scalar fields that violates the conditions of the cosmic no-hair conjecture. The symmetry pattern of this model is completely different from the standard ones that characterize all the models of inflation: in this case the time translations are unbroken and this has crucial consequences on the background dynamics and on the correlation functions. In particular we pointed out that the solid to drive inflation must be extremely insensitive to spatial deformations and this implies that the initial anisotropies, setted in the initial Bianchi I metric, are erased on a rather long timescale $\Delta t = \mathcal{O}\left(\frac{1}{H\varepsilon}\right)$. Of course, this gives a contribution to the amplitude of the power spectrum $g_* \simeq \mathcal{O}\left(1\right)\sigma$ where σ encodes the anisotropy, but put also problems on whether solid inflation can lead to isotropic and homogeneous background starting from generic initial conditions, so if it is a good inflationary model.

We have seen that anisotropic evolution (driven by anisotropic source) leaves observable effects on the correlation functions and in particular anisotropic contribution to the power spectrum and non-trivial angular dependence in the bispectrum (and in principle in all higher order correlation functions). Another usefull signature to distinguish type of fields and interactions populating the specific primordial inflationary phase is the parity violation. In chapter 5 we have shown that the coupling between a vector and a pseudoscalar field gives parity violating signatures in the tensor bispectrum. In particular the vector sources both scalar and tensor metric perturbations. Both kinds of perturbations are nongaussian, but, due to helicity conservation, the tensors have a larger amplitude and the pesudoscalar signal is not biased by the usual equilateral bispectra. We also evaluate the detectability of these signals through a Fisher matrix analysis and we show that considering both parity-even and parity-odd contributions improves the detectability of such signal, in particularthe use of E-mode improves of 400% the detectability with respect to an analysis in temperature and the B modes are even more powerful since it increase the signal-to-noise ratio by 3 orders of magnitude.
Statistical anisotropy, parity violation and non-Gaussianity can be mentioned among the best distinctive features for the early universe and certainly deserve further investigations, looking forward for a comparison with new and promising experimental data.

6.2 Outlook

Based on the findings of this thesis and my experience working in the covered areas these are my thoughts on the future development within the field of statistical anisotropy, parity violation and primordial non-Gaussianity.

6.2.1 Estimator for Anisotropic Bispectrum

The observational hint of statistical isotropy breaking, provided by different data analysis at level of the power spectrum and in higher-order correlation functions, suggests that, maybe, is promising to develop a novel formalism to construct an estimator for the bispectrum which can be used to constrain the parameters of many CMB anisotropic models. Many technical issues must be overcome in the construction and implementation of such estimators: the possibility to write the anisotropic bispectrum in a separable form in order to reduce the computational costs, a deep understanding of the anisotropic distribution of the noise in pixel space and the galactic masks that can cover the anisotropic signal and the detectability of that. A joint analysis power spectrum-bispectrum for this kind of models would be very promising since both must exhibit anisotropic signatures. Eventually such estimator could be also helpful as model independent test for the CMB "anomalies".

6.2.2 Effective Description for Anisotropic Model

It is known that symmetries play a fundamental role in costraining the properties of cosmological models [12]. Motivated by this, a good idea would be to develop in the future an "effective field theory" of broken spatial translational and rotational symmetries during inflation analogously to the effective field theory that identifies the cosmological perturbations with the goldstone boson of the broken time translational invariance in the standard case. As seen in [127] different models that sustain an anisotropic phase of expansion share many features at the background and correlation functions level. So the idea is to find a general framework to investigate these kind of models and to characterize the statistics only on the basis of symmetries.

A

APPENDIX

Contents:

A.1   Polarization vector and tensor

In this paper, we utilize a divergenceless polarization vector $\varepsilon_a^{(\pm 1)}$ and a transverse and traceless polarization tensor $e_{ab}^{(\pm 2)}$ satisfying [179]

$$
\begin{aligned}
\hat{k}^a \varepsilon_a^{(\lambda)}(\hat{\mathbf{k}}) &= 0 \;, \\
\eta^{abc} \hat{k}_a \varepsilon_b^{(\lambda)}(\hat{\mathbf{k}}) &= -\lambda i \varepsilon_c^{(\lambda)}(\hat{\mathbf{k}}) \;, \\
\varepsilon_a^{(\lambda)*}(\hat{\mathbf{k}}) &= \varepsilon_a^{(-\lambda)}(\hat{\mathbf{k}}) = \varepsilon_a^{(\lambda)}(-\hat{\mathbf{k}}) \;, \\
\varepsilon_a^{(\lambda)}(\hat{\mathbf{k}}) \varepsilon_a^{(\lambda')}(\hat{\mathbf{k}}) &= \delta_{\lambda,-\lambda'} \;,
\end{aligned} \tag{A.1}
$$

and

$$
\begin{aligned}
e_{ab}^{(\lambda)}(\hat{\mathbf{k}}) &\equiv \sqrt{2}\,\varepsilon_a^{(\frac{\lambda}{2})}(\hat{\mathbf{k}}) \varepsilon_b^{(\frac{\lambda}{2})}(\hat{\mathbf{k}}) \;, \\
e_{aa}^{(\lambda)}(\hat{\mathbf{k}}) &= \hat{k}_a e_{ab}^{(\lambda)}(\hat{\mathbf{k}}) = 0 \;, \\
e_{ab}^{(\lambda)*}(\hat{\mathbf{k}}) &= e_{ab}^{(-\lambda)}(\hat{\mathbf{k}}) = e_{ab}^{(\lambda)}(-\hat{\mathbf{k}}) \;, \\
e_{ab}^{(\lambda)}(\hat{\mathbf{k}}) e_{ab}^{(\lambda')}(\hat{\mathbf{k}}) &= 2\delta_{\lambda,-\lambda'} \;,
\end{aligned} \tag{A.2}
$$

where η^{abc} is a 3-dimensional antisymmetric tensor normalized by $\eta^{123} = 1$. An expression in ℓ space is convenient, reading

$$
e_{ab}^{(\lambda)}(\hat{\mathbf{k}}) = \frac{3}{\sqrt{2\pi}} \sum_{Mm_am_b} {}_{-\lambda}Y_{2M}^*(\hat{\mathbf{k}}) \alpha_a^{m_a} \alpha_b^{m_b} \begin{pmatrix} 2 & 1 & 1 \\ M & m_a & m_b \end{pmatrix} \;, \tag{A.3}
$$

with

$$
\alpha_a^m \alpha_a^{m'} = \frac{4\pi}{3}(-1)^m \delta_{m,-m'} \;, \quad \alpha_a^m \alpha_a^{m'*} = \frac{4\pi}{3}\delta_{m,m'} \;. \tag{A.4}
$$

Then, dealing with the Wigner symbols yields

$$
e_{ab}^{(-\lambda_1)}(\hat{\mathbf{k_1}}) e_{bc}^{(-\lambda_2)}(\hat{\mathbf{k_2}}) e_{ca}^{(-\lambda_3)}(\hat{\mathbf{k_3}}) = -\frac{(8\pi)^{3/2}}{10}\sqrt{\frac{7}{3}} \left[\prod_{n=1}^{3} \sum_{\mu_n} {}_{\lambda_n}Y_{2\mu_n}^*(\hat{\mathbf{k_n}}) \right] \begin{pmatrix} 2 & 2 & 2 \\ \mu_1 & \mu_2 & \mu_3 \end{pmatrix} \tag{A.5}
$$

With a multipole expansion of the delta function:

$$
\begin{aligned}
\delta^{(3)}\left(\sum_{n=1}^{3} \mathbf{k_n}\right) &= 8 \int_0^\infty r^2 dr \left[\prod_{n=1}^{3} \sum_{L_nM_n} (-1)^{\frac{L_n}{2}} j_{L_n}(k_n r) Y_{L_nM_n}^*(\hat{\mathbf{k_n}}) \right] \\
&\quad \times I_{L_1L_2L_3}^{0\ 0\ 0} \begin{pmatrix} L_1 & L_2 & L_3 \\ M_1 & M_2 & M_3 \end{pmatrix} \;,
\end{aligned} \tag{A.6}
$$

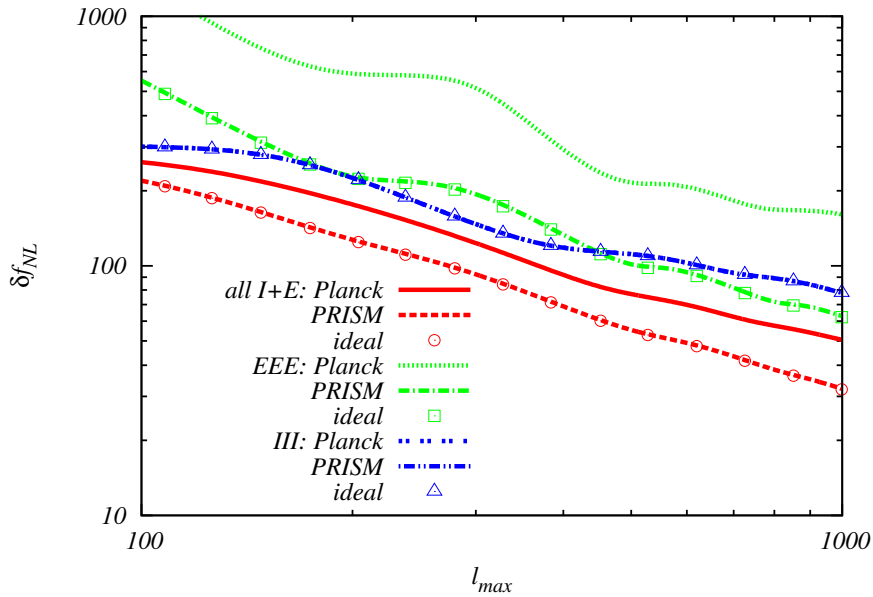this representation is applied to formulation of the CMB bispectrum in sec. 5.4.

Figure A.1: Expected 1σ errors of $f_{\rm NL}$ (5.40) estimated from all information of the temperature and E-mode bispectra (red lines), $\langle EEE \rangle$ (green lines) and $\langle III \rangle$ (blue lines) in the *Planck*, PRISM and ideal experiments.

A.2 Errors of the equilateral non-Gaussianity

In figure A.1, we plot 1σ errors of the equilateral nonlinearity parameter in the 2-dimensional Fisher matrix analysis with the parity-violating tensor non-Gaussianity. It is observed that the analysis with all types of the temperature and E-mode bispectra leads to 50% reduction of $\delta f_{\rm NL}$ in comparison with the analysis of $\langle III \rangle$ alone under the PRISM or ideal experiment. Thanks to uncorrelation with the tensor non-Gaussianity, $\delta f_{\rm NL}$ is in good agreement with $F_{ee}^{-1/2}$ of eq. (5.39).

A.3   TB and EB correlations

Here, we shall discuss the detectability of the parameter X from TB and EB power spectra (hereinafter noted as C_ℓ^{IB} and C_ℓ^{EB}, respectively). The TB or EB correlation is sourced by the difference between $\lambda = +2$ and -2 tensor power spectra, given as $\left\langle h_{\mathbf{k_1}}^{(+2)} h_{\mathbf{k_2}}^{(+2)} \right\rangle - \left\langle h_{\mathbf{k_1}}^{(-2)} h_{\mathbf{k_2}}^{(-2)} \right\rangle \equiv \Delta_h(k_1)\delta^{(2)}(\mathbf{k_1} + \mathbf{k_2})$, reading

$$C_\ell^{IB/EB} = \frac{2}{\pi} \int_0^\infty k^2 dk \mathcal{T}_\ell^{I/E}(k) \mathcal{T}_\ell^B(k) \Delta_h(k) . \tag{A.7}$$

In our case, gravitational waves are positively-polarized and hence Δ_h is dominated by the $+2$ power spectrum: [168]

$$\Delta_h(k) \approx 8.6 \times 10^{-7} \frac{H^4}{M_P^4} \frac{e^{4\pi\xi}}{\xi^6} k^{-3} \propto X^2 . \tag{A.8}$$

Concrete shapes of C_ℓ^{IB} and C_ℓ^{EB} can be seen in ref. [163].

Let us define a Fisher matrix for an error estimation of X^2 as [163]

$$F = \sum_{\ell=2}^{\ell_{\max}} \sum_{ij} \frac{\partial C_\ell^i}{\partial(X^2)} (Cov^{-1})_\ell^{ij} \frac{\partial C_\ell^j}{\partial(X^2)} , \tag{A.9}$$

where i or j runs over IB and EB, and a 2-dimensional covariance matrix is given by

$$Cov_\ell^{ij} = \frac{1}{2\ell+1} \begin{pmatrix} C_\ell^{II} C_\ell^{BB} & C_\ell^{IE} C_\ell^{BB} \\ C_\ell^{IE} C_\ell^{BB} & C_\ell^{EE} C_\ell^{BB} \end{pmatrix} . \tag{A.10}$$

Here, we have obeyed a null hypothesis of the cosmic variance and instrumental noise from the TB and EB correlations. Figure A.2 describes expected 1σ errors of X^2, which is calculated by $\delta(X^2) = F^{-1/2}$, under the presence of the B-mode cosmic variance spectrum with $r = 0.05$ and 5×10^{-4}. These results are compatible with the previous works [163]. We can also observe the rapid reduction of $\delta(X^2)$ for $\ell < 10$ thanks to large-scale information of the TB power spectrum, as discussed in ref. [163].

This figure indicates that $X = 1.8 \ (1.4) \times 10^5$ or $1.2 \ (0.54) \times 10^5$ will be detected at 68% CL in the *Planck* or PRISM experiment when $r = 0.05 \ (5 \times 10^{-4})$. These values are comparable to or somewhat smaller than the results from the temperature and E-mode bispectra, and slightly larger than those from the B-mode bispectrum analysis (see sec. 5.6). In the cosmic-variance-limited experiment, the 1σ error bar of X is determined by $r^{1/4}$, reading $\delta X \approx 2.1 \times 10^5 r^{1/4}$. Because of the difference of r dependence, the detectability of X may be weaker than the B-mode bispectrum case for smaller r as favored by current or future observations.
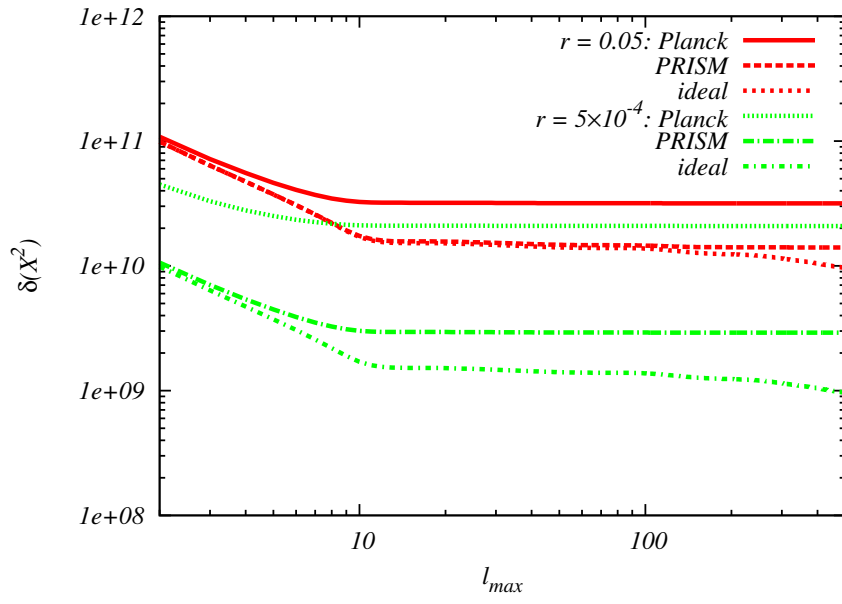
Figure A.2: Expected 1σ errors of X^2 estimated from the TB and EB correlations. Here we adopt the cosmic variance spectra and the noise spectra used in fig. 5.3.

Bibliography

[1] P.A.R. Ade et al. Planck 2013 Results. XXIV. Constraints on primordial non-Gaussianity. 2013.

[2] P.A.R. Ade et al. Planck 2013 results. XVI. Cosmological parameters. 2013.

[3] C.L. Bennett, R.S. Hill, G. Hinshaw, D. Larson, K.M. Smith, et al. Seven-Year Wilkinson Microwave Anisotropy Probe (WMAP) Observations: Are There Cosmic Microwave Background Anomalies? *Astrophys.J.Suppl.*, 192:17, 2011.

[4] P.A.R. Ade et al. Planck 2013 results. XXIII. Isotropy and statistics of the CMB. 2013.

[5] Masa-aki Watanabe, Sugumi Kanno, and Jiro Soda. Inflationary Universe with Anisotropic Hair. *Phys.Rev.Lett.*, 102:191302, 2009.

[6] Neil Barnaby, Jordan Moxon, Ryo Namba, Marco Peloso, Gary Shiu, et al. Gravity waves and non-Gaussian features from particle production in a sector gravitationally coupled to the inflaton. *Phys.Rev.*, D86:103508, 2012.

[7] Solomon Endlich, Alberto Nicolis, and Junpu Wang. Solid Inflation. *JCAP*, 1310:011, 2013.

[8] Lotty Ackerman, Sean M. Carroll, and Mark B. Wise. Imprints of a Primordial Preferred Direction on the Microwave Background. *Phys. Rev.*, D75:083502, 2007.

[9] Masa-aki Watanabe, Sugumi Kanno, and Jiro Soda. Imprints of anisotropic inflation on the cosmic microwave background. *Mon.Not.Roy.Astron.Soc.*, 412:L83–L87, 2011.

[10] A.E. Gumrukcuoglu, Carlo R. Contaldi, and Marco Peloso. Inflationary perturbations in anisotropic backgrounds and their imprint on the CMB. *JCAP*, 0711:005, 2007.

[11] Robert M. Wald. Asymptotic behavior of homogeneous cosmological models in the presence of a positive cosmological constant. *Phys.Rev.*, D28:2118–2120, 1983.

[12] M. Biagetti, A. Kehagias, E. Morgante, H. Perrier, and A. Riotto. Symmetries of Vector Perturbations during the de Sitter Epoch. *JCAP*, 1307:030, 2013.

[13] Marco Peloso and Massimo Pietroni. Ward identities and consistency relations for the large scale structure with multiple species. 2013.

[14] C.L. Bennett et al. Nine-Year Wilkinson Microwave Anisotropy Probe (WMAP) Observations: Final Maps and Results. *Astrophys.J.Suppl.*, 208:20, 2013.

[15] Jaiseung Kim and Eiichiro Komatsu. Limits on anisotropic inflation from the Planck data. *Phys.Rev.*, D88:101301, 2013.

[16] Craig J. Copi, Dragan Huterer, Dominik J. Schwarz, and Glenn D. Starkman. Large-scale alignments from WMAP and Planck. 2013.

[17] L.H. Ford. INFLATION DRIVEN BY A VECTOR FIELD. *Phys.Rev.*, D40:967, 1989.

[18] Alexey Golovnev, Viatcheslav Mukhanov, and Vitaly Vanchurin. Vector Inflation. *JCAP*, 0806:009, 2008.

[19] Sugumi Kanno, Masashi Kimura, Jiro Soda, and Shuichiro Yokoyama. Anisotropic Inflation from Vector Impurity. *JCAP*, 0808:034, 2008.

[20] Burak Himmetoglu, Carlo R. Contaldi, and Marco Peloso. Instability of anisotropic cosmological solutions supported by vector fields. *Phys.Rev.Lett.*, 102:111301, 2009.

[21] Gilles Esposito-Farese, Cyril Pitrou, and Jean-Philippe Uzan. Vector theories in cosmology. *Phys.Rev.*, D81:063519, 2010.

[22] Burak Himmetoglu, Carlo R. Contaldi, and Marco Peloso. Ghost instabilities of cosmological models with vector fields nonminimally coupled to the curvature. *Phys.Rev.*, D80:123530, 2009.

[23] Mindaugas Karciauskas and David H. Lyth. On the health of a vector field with $(RA^2)/6$ coupling to gravity. *JCAP*, 1011:023, 2010.

[24] Emanuela Dimastrogiovanni, Nicola Bartolo, Sabino Matarrese, and Antonio Riotto. Non-Gaussianity and Statistical Anisotropy from Vector Field Populated Inflationary Models. *Adv.Astron.*, 2010:752670, 2010.

[25] A. Maleknejad and M.M. Sheikh-Jabbari. Gauge-flation: Inflation From Non-Abelian Gauge Fields. *Phys.Lett.*, B723:224–228, 2013.

[26] Ryo Namba, Emanuela Dimastrogiovanni, and Marco Peloso. Gauge-flation confronted with Planck. *JCAP*, 1311:045, 2013.

[27] E. Kolb and M. Turner. *The Early Universe*. Westview Press, February 21, (1994).

[28] J.R. Bond, C.R. Contaldi, D. Pogosyan, B.S. Mason, S.T. Myers, et al. The cosmic microwave background and inflation, then and now. *AIP Conf.Proc.*, 646:15–33, 2003.

[29] P. Coles and F. Lucchin. *Cosmology: The Origin and Evolution of Cosmic Structure,*. John Wiley, 2002.

[30] R.M. Wald. *General Relativity*. The University of Chicago Press, (1984).

[31] Antonio Riotto. Inflation and the theory of cosmological perturbations. pages 317–413, 2002.

[32] C.L. Bennett, A. Banday, K.M. Gorski, G. Hinshaw, P. Jackson, et al. Four year COBE DMR cosmic microwave background observations: Maps and basic results. *Astrophys.J.*, 464:L1–L4, 1996.

[33] E. Komatsu et al. Seven-Year Wilkinson Microwave Anisotropy Probe (WMAP) Observations: Cosmological Interpretation. *Astrophys.J.Suppl.*, 192:18, 2011.

[34] Andrei D. Linde. Particle physics and inflationary cosmology. *Contemp.Concepts Phys.*, 5:1–362, 1990.

[35] Konstantinos Dimopoulos. Can a vector field be responsible for the curvature perturbation in the Universe? *Phys.Rev.*, D74:083502, 2006.

[36] A. Neronov and I. Vovk. Evidence for strong extragalactic magnetic fields from Fermi observations of TeV blazars. *Science*, 328:73–75, 2010.

[37] Dario Grasso and Hector R. Rubinstein. Magnetic fields in the early universe. *Phys.Rept.*, 348:163–266, 2001.

[38] Vittoria Demozzi, Viatcheslav Mukhanov, and Hector Rubinstein. Magnetic fields from inflation? *JCAP*, 0908:025, 2009.

[39] Camille Bonvin, Chiara Caprini, and Ruth Durrer. Magnetic fields from inflation: the transition to the radiation era. *Phys.Rev.*, D86:023519, 2012.

[40] Iain A. Brown. Primordial Magnetic Fields in Cosmology. 2006. Ph.D.Thesis.

[41] Takeshi Chiba. Initial Conditions for Vector Inflation. *JCAP*, 0808:004, 2008.

[42] Michael S. Turner and Lawrence M. Widrow. Inflation Produced, Large Scale Magnetic Fields. *Phys.Rev.*, D37:2743, 1988.

[43] Burak Himmetoglu, Carlo R. Contaldi, and Marco Peloso. Instability of the ACW model, and problems with massive vectors during inflation. *Phys.Rev.*, D79:063517, 2009.

[44] Shuichiro Yokoyama and Jiro Soda. Primordial statistical anisotropy generated at the end of inflation. *JCAP*, 0808:005, 2008. * Brief entry *.

[45] Nicola Bartolo, Emanuela Dimastrogiovanni, Sabino Matarrese, and Antonio Riotto. Anisotropic bispectrum of curvature perturbations from primordial non-Abelian vector fields. *JCAP*, 0910:015, 2009. * Brief entry *.

[46] Nicola Bartolo, Emanuela Dimastrogiovanni, Sabino Matarrese, and Antonio Riotto. Anisotropic Trispectrum of Curvature Perturbations Induced by Primordial Non-Abelian Vector Fields. *JCAP*, 0911:028, 2009.

[47] Emanuela Dimastrogiovanni. Cosmological correlation functions in scalar and vector inflationary models. 2010.

[48] Peter Adshead and Mark Wyman. Chromo-Natural Inflation: Natural inflation on a steep potential with classical non-Abelian gauge fields. *Phys.Rev.Lett.*, 108:261302, 2012.

[49] Emanuela Dimastrogiovanni, Matteo Fasiello, and Andrew J. Tolley. Low-Energy Effective Field Theory for Chromo-Natural Inflation. *JCAP*, 1302:046, 2013.

[50] Kei Yamamoto, Masa-aki Watanabe, and Jiro Soda. Inflation with Multi-Vector-Hair: The Fate of Anisotropy. *Class.Quant.Grav.*, 29:145008, 2012.

[51] Kei Yamamoto. Primordial Fluctuations from Inflation with a Triad of Background Gauge Fields. *Phys.Rev.*, D85:123504, 2012.

[52] Jihn E. Kim, Hans Peter Nilles, and Marco Peloso. Completing natural inflation. *JCAP*, 0501:005, 2005.

[53] S. Dimopoulos, S. Kachru, J. McGreevy, and Jay G. Wacker. N-flation. *JCAP*, 0808:003, 2008.

[54] Richard Easther and Liam McAllister. Random matrices and the spectrum of N-flation. *JCAP*, 0605:018, 2006.

[55] Nima Arkani-Hamed, Hsin-Chia Cheng, Paolo Creminelli, and Lisa Randall. Extra natural inflation. *Phys.Rev.Lett.*, 90:221302, 2003.

[56] Neil Barnaby, Ryo Namba, and Marco Peloso. Phenomenology of a Pseudo-Scalar Inflaton: Naturally Large Nongaussianity. *JCAP*, 1104:009, 2011.

[57] Jessica L. Cook and Lorenzo Sorbo. An inflationary model with large tensor and small scalar nongaussianities. 2013.

[58] Y. Choquet-Bruhat. *General Relativity and the Einstein Equations.* Oxford Oxford University Press.

[59] Jiro Soda. Statistical Anisotropy from Anisotropic Inflation. *Class.Quant.Grav.*, 29:083001, 2012.

[60] Burak Himmetoglu. Spectrum of Perturbations in Anisotropic Inflationary Universe with Vector Hair. *JCAP*, 1003:023, 2010.

[61] A.E. Gumrukcuoglu, Burak Himmetoglu, and Marco Peloso. Scalar-Scalar, Scalar-Tensor, and Tensor-Tensor Correlators from Anisotropic Inflation. *Phys.Rev.*, D81:063528, 2010.

[62] Nicola Bartolo, Sabino Matarrese, Marco Peloso, and Angelo Ricciardone. The anisotropic power spectrum and bispectrum in the $f(\phi)F^2$ mechanism. *Phys.Rev.*, D87:023504, 2013.

[63] Nicolaas E. Groeneboom and Hans Kristian Eriksen. Bayesian analysis of sparse anisotropic universe models and application to the 5-yr WMAP data. *Astrophys. J.*, 690:1807–1819, 2009.

[64] Duncan Hanson and Antony Lewis. Estimators for CMB Statistical Anisotropy. *Phys. Rev.*, D80:063004, 2009.

[65] Nicolaas E. Groeneboom, Lotty Ackerman, Ingunn Kathrine Wehus, and Hans Kristian Eriksen. Bayesian analysis of an anisotropic universe model: systematics and polarization. *Astrophys.J.*, 722:452–459, 2010.

[66] Duncan Hanson, Antony Lewis, and Anthony Challinor. Asymmetric Beams and CMB Statistical Anisotropy. *Phys. Rev.*, D81:103003, 2010.

[67] Anthony R. Pullen and Marc Kamionkowski. Cosmic Microwave Background Statistics for a Direction-Dependent Primordial Power Spectrum. *Phys.Rev.*, D76:103529, 2007.

[68] Yin-Zhe Ma, George Efstathiou, and Anthony Challinor. Testing a direction-dependent primordial power spectrum with observations of the Cosmic Microwave Background. *Phys.Rev.*, D83:083005, 2011.

[69] Anthony R. Pullen and Christopher M. Hirata. Non-detection of a statistically anisotropic power spectrum in large-scale structure. *JCAP*, 1005:027, 2010.

[70] A.E. Gumrukcuoglu, Carlo R. Contaldi, and Marco Peloso. CMB Anomalies from Relic Anisotropy. pages 1641–1646, 2006.

[71] A. Maleknejad and M.M. Sheikh-Jabbari. Revisiting Cosmic No-Hair Theorem for Inflationary Settings. *Phys.Rev.*, D85:123508, 2012.

[72] Mohamed M. Anber and Lorenzo Sorbo. Naturally inflating on steep potentials through electromagnetic dissipation. *Phys.Rev.*, D81:043534, 2010.

[73] Konstantinos Dimopoulos, George Lazarides, and Jacques M. Wagstaff. Eliminating the η-problem in SUGRA Hybrid Inflation with Vector Backreaction. *JCAP*, 1202:018, 2012.

[74] Razieh Emami, Hassan Firouzjahi, S.M. Sadegh Movahed, and Moslem Zarei. Anisotropic Inflation from Charged Scalar Fields. *JCAP*, 1102:005, 2011.

[75] Sugumi Kanno, Jiro Soda, and Masa-aki Watanabe. Anisotropic Power-law Inflation. *JCAP*, 1012:024, 2010.

[76] Keiju Murata and Jiro Soda. Anisotropic Inflation with Non-Abelian Gauge Kinetic Function. *JCAP*, 1106:037, 2011.

[77] Mikjel Thorsrud, David F. Mota, and Sigbjorn Hervik. Cosmology of a Scalar Field Coupled to Matter and an Isotropy-Violating Maxwell Field. *JHEP*, 1210:066, 2012.

[78] Konstantinos Dimopoulos, Mindaugas Karciauskas, and Jacques M. Wagstaff. Vector Curvaton with varying Kinetic Function. *Phys.Rev.*, D81:023522, 2010.

[79] Konstantinos Dimopoulos, Mindaugas Karciauskas, and Jacques M. Wagstaff. Vector Curvaton without Instabilities. *Phys.Lett.*, B683:298–301, 2010.

[80] Konstantinos Dimopoulos, Danielle Wills, and Ivonne Zavala. Statistical Anisotropy from Vector Curvaton in D-brane Inflation. *Nucl.Phys.*, B868:120–155, 2013.

[81] Konstantinos Dimopoulos and Mindaugas Karciauskas. Parity Violating Statistical Anisotropy. *JHEP*, 1206:040, 2012.

[82] Ryo Namba. Curvature Perturbations from a Massive Vector Curvaton. *Phys.Rev.*, D86:083518, 2012.

[83] Bharat Ratra. Cosmological 'seed' magnetic field from inflation. *Astrophys.J.*, 391:L1–L4, 1992.

[84] Massimo Giovannini. Electric-magnetic duality and the conditions of inflationary magnetogenesis. *JCAP*, 1004:003, 2010.

[85] Mindaugas Karciauskas, Konstantinos Dimopoulos, and David H. Lyth. Anisotropic non-Gaussianity from vector field perturbations. *Phys.Rev.*, D80:023509, 2009.

[86] Mindaugas Karciauskas. The Primordial Curvature Perturbation from Vector Fields of General non-Abelian Groups. 2011.

[87] Razieh Emami and Hassan Firouzjahi. Issues on Generating Primordial Anisotropies at the End of Inflation. *JCAP*, 1201:022, 2012.

[88] David H. Lyth and Mindaugas Karciauskas. Statistically anisotropic curvature perturbation generated during the waterfall. 2012.

[89] David H. Lyth and Mindaugas Karciauskas. Modulation of the waterfall by a gauge field. *JCAP*, 1301:031, 2013.

[90] Timothy R. Dulaney and Moira I. Gresham. Primordial Power Spectra from Anisotropic Inflation. *Phys.Rev.*, D81:103532, 2010.

[91] Masa-aki Watanabe, Sugumi Kanno, and Jiro Soda. The Nature of Primordial Fluctuations from Anisotropic Inflation. *Prog.Theor.Phys.*, 123:1041–1068, 2010. * Temporary entry *.

[92] Sigbjorn Hervik, David F. Mota, and Mikjel Thorsrud. Inflation with stable anisotropic hair: Is it cosmologically viable? *JHEP*, 1111:146, 2011.

[93] Neil Barnaby, Ryo Namba, and Marco Peloso. Observable non-gaussianity from gauge field production in slow roll inflation, and a challenging connection with magnetogenesis. *Phys.Rev.*, D85:123523, 2012.

[94] Jerome Martin and Jun'ichi Yokoyama. Generation of Large-Scale Magnetic Fields in Single-Field Inflation. *JCAP*, 0801:025, 2008.

[95] David Seery. Magnetogenesis and the primordial non-gaussianity. *JCAP*, 0908:018, 2009.

[96] Robert R. Caldwell, Leonardo Motta, and Marc Kamionkowski. Correlation of inflation-produced magnetic fields with scalar fluctuations. *Phys.Rev.*, D84:123525, 2011.

[97] Leonardo Motta and Robert R. Caldwell. Non-Gaussian features of primordial magnetic fields in power-law inflation. *Phys.Rev.*, D85:103532, 2012.

[98] Teruaki Suyama and Jun'ichi Yokoyama. Metric perturbation from inflationary magnetic field and generic bound on inflation models. *Phys.Rev.*, D86:023512, 2012.

[99] Rajeev Kumar Jain and Martin S. Sloth. Consistency relation for cosmic magnetic fields. *Phys.Rev.*, D86:123528, 2012.

[100] Maresuke Shiraishi, Shohei Saga, and Shuichiro Yokoyama. CMB power spectra induced by primordial cross-bispectra between metric perturbations and vector fields. *JCAP*, 1211:046, 2012.

[101] Andrei D. Linde. Inflationary Cosmology. *Lect.Notes Phys.*, 738:1–54, 2008.

[102] Sugumi Kanno, Jiro Soda, and Masa-aki Watanabe. Cosmological Magnetic Fields from Inflation and Backreaction. *JCAP*, 0912:009, 2009.

[103] Tomohiro Fujita and Shinji Mukohyama. Universal upper limit on inflation energy scale from cosmic magnetic field. *JCAP*, 1210:034, 2012.

[104] Thiago S. Pereira, Cyril Pitrou, and Jean-Philippe Uzan. Theory of cosmological perturbations in an anisotropic universe. *JCAP*, 0709:006, 2007.

[105] Cyril Pitrou, Thiago S. Pereira, and Jean-Philippe Uzan. Predictions from an anisotropic inflationary era. *JCAP*, 0804:004, 2008.

[106] Konstantinos Dimopoulos, Mindaugas Karciauskas, David H. Lyth, and Yeinzon Rodriguez. Statistical anisotropy of the curvature perturbation from vector field perturbations. *JCAP*, 0905:013, 2009.

[107] Cesar A. Valenzuela-Toledo, Yeinzon Rodriguez, and David H. Lyth. Non-gaussianity at tree- and one-loop levels from vector field perturbations. *Phys.Rev.*, D80:103519, 2009.

[108] Cesar A. Valenzuela-Toledo and Yeinzon Rodriguez. Non-gaussianity from the trispectrum and vector field perturbations. *Phys.Lett.*, B685:120–127, 2010.

[109] Cesar A. Valenzuela-Toledo, Yeinzon Rodriguez, and Juan P. Beltran Almeida. Feynman-like Rules for Calculating n-Point Correlators of the Primordial Curvature Perturbation. *JCAP*, 1110:020, 2011.

[110] Anindya Dey and Sonia Paban. Non-Gaussianities in the Cosmological Perturbation Spectrum due to Primordial Anisotropy. *JCAP*, 1204:039, 2012.

[111] Juan P. Beltran Almeida, Yeinzon Rodriguez, and Cesar A. Valenzuela-Toledo. The Suyama-Yamaguchi consistency relation in the presence of vector fields. *Mod.Phys.Lett.*, A28:1350012, 2013.

[112] Anindya Dey, Ely Kovetz, and Sonia Paban. Non-Gaussianities in the Cosmological Perturbation Spectrum due to Primordial Anisotropy II. *JCAP*, 1210:055, 2012.

[113] N. Bartolo, S. Matarrese, M. Pietroni, A. Riotto, and D. Seery. On the Physical Significance of Infra-red Corrections to Inflationary Observables. *JCAP*, 0801:015, 2008.

[114] Gia Dvali, Andrei Gruzinov, and Matias Zaldarriaga. A new mechanism for generating density perturbations from inflation. *Phys.Rev.*, D69:023505, 2004.

[115] Lev Kofman. Probing string theory with modulated cosmological fluctuations. 2003.

[116] Francis Bernardeau, Lev Kofman, and Jean-Philippe Uzan. Modulated fluctuations from hybrid inflation. *Phys.Rev.*, D70:083004, 2004.

[117] Sabino Matarrese and Antonio Riotto. Large - scale curvature perturbations with spatial and time variations of the inflaton decay rate. *JCAP*, 0308:007, 2003.

[118] Christian Armendariz-Picon. Could dark energy be vector-like? *JCAP*, 0407:007, 2004.

[119] Cristiano Germani and Alex Kehagias. P-nflation: generating cosmic Inflation with p-forms. *JCAP*, 0903:028, 2009.

[120] Tsutomu Kobayashi and Shuichiro Yokoyama. Gravitational waves from p-form inflation. *JCAP*, 0905:004, 2009.

[121] Tomi S. Koivisto, David F. Mota, and Cyril Pitrou. Inflation from N-Forms and its stability. *JHEP*, 0909:092, 2009.

[122] Cristiano Germani and Alex Kehagias. Scalar perturbations in p-nflation: the 3-form case. *JCAP*, 0911:005, 2009.

[123] Tomi S. Koivisto and Nelson J. Nunes. Inflation and dark energy from three-forms. *Phys.Rev.*, D80:103509, 2009.

[124] Antonio De Felice, Khamphee Karwan, and Pitayuth Wongjun. Stability of the 3-form field during inflation. *Phys.Rev.*, D85:123545, 2012.

[125] Federico R. Urban and Tomi S. Koivisto. Perturbations and non-Gaussianities in three-form inflationary magnetogenesis. *JCAP*, 1209:025, 2012.

[126] David J. Mulryne, Johannes Noller, and Nelson J. Nunes. Three-form inflation and non-Gaussianity. *JCAP*, 1212:016, 2012.

[127] Nicola Bartolo, Sabino Matarrese, Marco Peloso, and Angelo Ricciardone. Anisotropy in solid inflation. *JCAP*, 1308:022, 2013.

[128] P.A.R. Ade et al. Planck 2013 results. XXII. Constraints on inflation. 2013.

[129] Clifford Cheung, Paolo Creminelli, A. Liam Fitzpatrick, Jared Kaplan, and Leonardo Senatore. The Effective Field Theory of Inflation. *JHEP*, 03:014, 2008.

[130] Steven Weinberg. Effective Field Theory for Inflation. *Phys. Rev.*, D77:123541, 2008.

[131] Enrico Pajer and Marco Peloso. A review of Axion Inflation in the era of Planck. *Class.Quant.Grav.*, 30:214002, 2013.

[132] C.B. Collins and S.W. Hawking. Why is the Universe isotropic? *Astrophys.J.*, 180:317–334, 1973.

[133] C. Armendariz-Picon. Creating Statistically Anisotropic and Inhomogeneous Perturbations. *JCAP*, 0709:014, 2007.

[134] Andrei Gruzinov. Elastic inflation. *Phys.Rev.*, D70:063518, 2004.

[135] Maresuke Shiraishi, Eiichiro Komatsu, Marco Peloso, and Neil Barnaby. Signatures of anisotropic sources in the squeezed-limit bispectrum of the cosmic microwave background. *JCAP*, 1305:002, 2013.

[136] Daniel Babich, Paolo Creminelli, and Matias Zaldarriaga. The shape of non-Gaussianities. *JCAP*, 0408:009, 2004.

[137] Antony Lewis. The real shape of non-Gaussianities. *JCAP*, 1110:026, 2011.

[138] Hiroyuki Funakoshi and Kei Yamamoto. Primordial bispectrum from inflation with background gauge fields. *Class.Quant.Grav.*, 30:135002, 2013.

[139] Ali Akbar Abolhasani, Razieh Emami, Javad T. Firouzjaee, and Hassan Firouzjahi. δN formalism in anisotropic inflation and large anisotropic bispectrum and trispectrum. *JCAP*, 1308:016, 2013.

[140] Tomohiro Fujita and Shuichiro Yokoyama. Higher order statistics of curvature perturbations in IFF model and its Planck constraints. *JCAP*, 1309:009, 2013.

[141] David H. Lyth and Mindaugas Karciauskas. The statistically anisotropic curvature perturbation generated by $f(\phi)^2 F^2$. *JCAP*, 1305:011, 2013.

[142] A. Maleknejad, M.M. Sheikh-Jabbari, and J. Soda. Gauge Fields and Inflation. *Phys.Rept.*, 528:161–261, 2013.

[143] Ricardo J.Z. Ferreira, Rajeev Kumar Jain, and Martin S. Sloth. Inflationary magnetogenesis without the strong coupling problem. *JCAP*, 1310:004, 2013.

[144] S. Matarrese. On the Classical and Quantum Irrotational Motions of a Relativistic Perfect Fluid. 1. Classical Theory. *Proc.Roy.Soc.Lond.*, A401:53–66, 1985.

[145] Frederico Arroja and Misao Sasaki. A note on the equivalence of a barotropic perfect fluid with a K-essence scalar field. *Phys.Rev.*, D81:107301, 2010.

[146] Xingang Chen, Hassan Firouzjahi, Mohammad Hossein Namjoo, and Misao Sasaki. Fluid Inflation. *JCAP*, 1309:012, 2013.

[147] Elisabetta Di Grezia, Giampiero Esposito, Agostino Funel, Gianpiero Mangano, and Gennaro Miele. Space-time noncommutativity and antisymmetric tensor dynamics in the early universe. *Phys.Rev.*, D68:105012, 2003.

[148] Junko Ohashi, Jiro Soda, and Shinji Tsujikawa. Anisotropic Non-Gaussianity from a Two-Form Field. *Phys.Rev.*, D87:083520, 2013.

[149] Guillermo Ballesteros and Brando Bellazzini. Effective perfect fluids in cosmology. *JCAP*, 1304:001, 2013.

[150] James M. Bardeen. Gauge Invariant Cosmological Perturbations. *Phys.Rev.*, D22:1882–1905, 1980.

[151] H. A. Feldman V. F. Mukhanov and R. H. Brandenberger. Theory of cosmological perturbations. Part 1. Classical perturbations. Part 2. Quantum theory of perturbations. Part 3. Extensions. *Phys. Rept.*, 215(203), 1992.

[152] Richard L. Arnowitt, Stanley Deser, and Charles W. Misner. The Dynamics of general relativity. *Gen.Rel.Grav.*, 40:1997–2027, 2008.

[153] Karim A. Malik and David Wands. Cosmological perturbations. *Phys.Rept.*, 475:1–51, 2009.

[154] I. Affleck and M. Dine. A New Mechanism for Baryogenesis. *Nucl. Phys. B*, 249(361), 1985.

[155] David H. Lyth and David Wands. Generating the curvature perturbation without an inflaton. *Phys.Lett.*, B524:5–14, 2002.

[156] Maresuke Shiraishi, Angelo Ricciardone, and Shohei Saga. Parity violation in the CMB bispectrum by a rolling pseudoscalar. *JCAP*, 1311:051, 2013.

[157] Arthur Lue, Li-Min Wang, and Marc Kamionkowski. Cosmological signature of new parity violating interactions. *Phys.Rev.Lett.*, 83:1506–1509, 1999.

[158] Stephon Alexander and Jerome Martin. Birefringent gravitational waves and the consistency check of inflation. *Phys.Rev.*, D71:063526, 2005.

[159] David H. Lyth, Carlos Quimbay, and Yeinzon Rodriguez. Leptogenesis and tensor polarisation from a gravitational Chern-Simons term. *JHEP*, 0503:016, 2005.

[160] Shun Saito, Kiyotomo Ichiki, and Atsushi Taruya. Probing polarization states of primordial gravitational waves with CMB anisotropies. *JCAP*, 0709:002, 2007.

[161] Masaki Satoh, Sugumi Kanno, and Jiro Soda. Circular Polarization of Primordial Gravitational Waves in String-inspired Inflationary Cosmology. *Phys.Rev.*, D77:023526, 2008.

[162] Tomohiro Takahashi and Jiro Soda. Chiral Primordial Gravitational Waves from a Lifshitz Point. *Phys.Rev.Lett.*, 102:231301, 2009.

[163] Vera Gluscevic and Marc Kamionkowski. Testing Parity-Violating Mechanisms with Cosmic Microwave Background Experiments. *Phys. Rev.*, D81:123529, 2010.

[164] A. Gruppuso, F. Finelli, P. Natoli, F. Paci, P. Cabella, et al. New constraints on Parity Symmetry from a re-analysis of the WMAP-7 low resolution power spectra. *Mon.Not.Roy.Astron.Soc.*, 411:1445–1452, 2011.

[165] Neil Barnaby and Marco Peloso. Large Nongaussianity in Axion Inflation. *Phys.Rev.Lett.*, 106:181301, 2011.

[166] Tomi S. Koivisto and David F. Mota. CMB statistics in noncommutative inflation. *JHEP*, 1102:061, 2011.

[167] N.E. Groeneboom, M. Axelsson, D.F. Mota, and T. Koivisto. Imprints of a hemispherical power asymmetry in the seven-year WMAP data due to non-commutativity of space-time. 2010.

[168] Lorenzo Sorbo. Parity violation in the Cosmic Microwave Background from a pseudoscalar inflaton. *JCAP*, 1106:003, 2011.

[169] Vera Gluscevic, Duncan Hanson, Marc Kamionkowski, and Christopher M. Hirata. First CMB Constraints on Direction-Dependent Cosmological Birefringence from WMAP-7. *Phys.Rev.*, D86:103529, 2012.

[170] J. Grain, M. Tristram, and R. Stompor. CMB EB and TB cross-spectrum estimation via pseudo-spectrum techniques. *Phys.Rev.*, D86:076005, 2012.

[171] Anzhong Wang, Qiang Wu, Wen Zhao, and Tao Zhu. Polarizing primordial gravitational waves by parity violation. 2012.

[172] Juan M. Maldacena and Guilherme L. Pimentel. On graviton non-Gaussianities during inflation. *JHEP*, 1109:045, 2011.

[173] Jiro Soda, Hideo Kodama, and Masato Nozawa. Parity Violation in Graviton Non-gaussianity. *JHEP*, 1108:067, 2011.

[174] Maresuke Shiraishi, Daisuke Nitta, and Shuichiro Yokoyama. Parity Violation of Gravitons in the CMB Bispectrum. *Prog.Theor.Phys.*, 126:937–959, 2011.

[175] Maresuke Shiraishi. Parity violation of primordial magnetic fields in the CMB bispectrum. *JCAP*, 1206:015, 2012.

[176] Tao Zhu, Wen Zhao, Yongqing Huang, Anzhong Wang, and Qiang Wu. Effects of parity violation on non-gaussianity of primordial gravitational waves in Hořava-Lifshitz gravity. 2013.

[177] Marc Kamionkowski and Tarun Souradeep. The Odd-Parity CMB Bispectrum. *Phys. Rev.*, D83:027301, 2011.

[178] Maresuke Shiraishi. Polarization bispectrum for measuring primordial magnetic fields. 2013.

[179] Maresuke Shiraishi, Daisuke Nitta, Shuichiro Yokoyama, Kiyotomo Ichiki, and Keitaro Takahashi. CMB Bispectrum from Primordial Scalar, Vector and Tensor non-Gaussianities. *Prog. Theor. Phys.*, 125:795–813, 2011.

[180] Maresuke Shiraishi, Daisuke Nitta, Shuichiro Yokoyama, and Kiyotomo Ichiki. Optimal limits on primordial magnetic fields from CMB temperature bispectrum of passive modes. *JCAP*, 1203:041, 2012.

[181] Jonathan R. Pritchard and Marc Kamionkowski. Cosmic microwave background fluctuations from gravitational waves: An analytic approach. *Annals Phys.*, 318:2–36, 2005.

[182] Maresuke Shiraishi, Daisuke Nitta, Shuichiro Yokoyama, Kiyotomo Ichiki, and Keitaro Takahashi. Analytic formulae of the CMB bispectra generated from non-Gaussianity in the tensor and vector perturbations. *Phys.Rev.*, D82:103505, 2010.

[183] Planck: The scientific programme. 2006.

[184] Philippe Andre et al. PRISM (Polarized Radiation Imaging and Spectroscopy Mission): A White Paper on the Ultimate Polarimetric Spectro-Imaging of the Microwave and Far-Infrared Sky. 2013.

[185] Antony Lewis, Anthony Challinor, and Duncan Hanson. The shape of the CMB lensing bispectrum. *JCAP*, 1103:018, 2011.

[186] D. Hanson et al. Detection of B-mode Polarization in the Cosmic Microwave Background with Data from the South Pole Telescope. 2013.